STRESSES ARISING DURING GROWTH OF OXIDES ON METALS

Submitted for the Degree of

Doctor of Philosophy

in the University of London

by

Allan James Breen

Department of Metallurgy,
Royal School of Mines,
Imperial College of Science
and Technology,
London S.W.7.

October 1967.

ABSTRACT

This investigation is concerned with the stresses that arise during the anodic oxidation of aluminium and zirconium.

Stresses in anodic alumina have been shown to depend on hydration phenomena. Hydration causes compressive stresses by increasing the volume of the oxide, tensile stresses arise when water is eliminated from hydrated oxide films by anodic polarisation. The dehydration is accomplished by a deprotonation in which anhydrous oxide is formed by the consumption of the hydrate as each mobile aluminium ion displaces three protons from the latter.

In accordance with the Pilling-Bedworth volume ratio concept anodic zirconia, which grows by anion migration only, develops compressive stresses which are of the same magnitude as the compressive strength of the bulk oxide, suggesting that growth proceeds at the fracture stress by a crack-heal mechanism.

At low current densities the compressive stress in anodic oxides which accompanies the applied voltage is caused by electrostatic pressure.

Page

SECTION I. INTRODUCTION 9

SECTION II. PREVIOUS WORK 12

Part 1. Growth of Oxides During Corrosion 13

a. Theories to Explain Transition from Protective to Non-Protective Oxidation Kinetics .. 13

Part 2. Mechanical Properties of Oxides 20

a. Stresses in Oxides 20

b. Stresses in Anodic Oxide Films 23

c. Plasticity of Oxides 26

Part 3. Anodic Oxide Films 34

a. The Mechanism of Growth 34

i. High Field Conduction 34

ii. The Oxidation Reaction 36

iii. Current Efficiency During Anodising .. 36

iv. Temperature Rise During Anodising .. 37

v. Field Induced Stresses 39

vi. Dominant Ion Migration 39

b. The Structure of Anodic Oxide Films 42

i. Anodic Alumina 42

ii. Anodic Zirconia 45

Part 4. Conclusions from Previous Work 45

Page

SECTION III. EXPERIMENTAL PROCEDURE 49

Part 1. Preparation of Anodic Oxide Films 50

a. Materials and Surface Preparations 50

i. Aluminium 50

ii. Zirconium 50

iii. Zircaloy 2 51

iv. Foil Dimensions 51

b. The Anodising Technique and Growth Rate Measurements 52

Part 2. Measurement of Growth Stresses 54

a. Method 54

b. The Convention for the Sign of Stress 54

c. Calculation of Stress - Biaxial Analysis .. 55

d. The Effect of Specimen Geometry 57

e. Reliability of Stress Measurement 58

f. Stress Location by Oxide Removal 58

Part 3. Measurement of Oxide Thickness by Spectrophotometry 59

Part 4. Measurement of Electrical Properties of Oxides 61

a. Impedance Measurements 61

b. Voltage Measurements 62

c. Measurement of Current Transients 62

Page

SECTION IV. RESULTS 63

Part 1. Growth Stresses in Anodic Alumina 64

a. The Effect of Voltage 64

b. The Effect of Growth Rate on Stress 64

c. The Effect of pH on Stress 65

d. Location of Stress Gradients 65

Part 2. The Influence of Hydration Phenomena on Stress in Oxides 67

a. Immersion of Anodised Aluminium in Alkaline K_2CrO_4 67

b. Hydration of Anodic Alumina by Boiling in Water 68

c. The Effects of Cathodic Polarisation on Anodic Alumina 68

d. The Effects of Cathodic Polarisation on Anodic Zirconia 69

Part 3. The Removal of Hydrating Species from Oxides by Anodic Polarisation 69

a. The Effect of Anodic Polarisation on Alumina Previously Immersed in Alkaline K_2CrO_4 .. 69

b. The Effect of Anodic Polarisation on Alumina After Cathodic Polarisation 70

Page

c. The Dehydration of Alumina Hydrates Formed by Boiling Anodic Films in Water 71

d. The Effect of Anodic Polarisation on Zirconia After Cathodic Polarisation 72

e. The Effect on Stress of Anodic Polarisation of Hydrated/Protonated Oxides 73

Part 4. Growth Stresses in Anodic Zirconia 74

a. The Effect of Growth Rate and Electrolyte on the Stresses in Zirconia 74

b. Stresses Arising During Anodising of Zircaloy 2 74

Part 5. The Resistance of Anodic Zirconia Films .. 75

Part 6. Measurement of Anodic Oxide Thickness and Current Efficiency 75

Part 7. Field Induced Stresses During Anodising .. 76

SECTION V. DISCUSSION OF RESULTS 79

Introduction to Discussion 80

Part 1. Growth Stresses in Anodic Alumina 81

a. Possible Causes of Tensile Stresses 81

b. The Effect of Hydration on Stress 85

c. The Dehydration of Hydrated Alumina by Anodic Polarisation and its Effect on Stress 88

Page

d. A Mechanism to Explain Stresses in Anodic Alumina 99

Part 2. The Effect of Cathodically Polarising Anodic Oxides 104

a. Proton Gradients in Anodic Zirconia 105

b. Anodic Alumina - Electro-osmosis or Protonation? 107

Part 3. Growth Stresses in Anodic Zirconia 112

a. Tensile Stresses in Anodic Zirconia 112

b. Compressive Stresses in Anodic Zirconia .. 114

c. The Effect of Alloying Zirconium 115

Part 4. Field Induced Stresses During Anodising .. 116

SECTION VI. CONCLUSIONS 120

PROPOSALS FOR FUTURE WORK 124

ACKNOWLEDGEMENTS 125

REFERENCES 126

TABLES 135

FIGURES 143

SECTION I

INTRODUCTION

THE RELEVANCE OF MECHANICAL PROPERTIES OF OXIDES TO CORROSION OF METALS

Most metals are thermodynamically unstable with respect to their environments and are of practical use only when the corrosion product - usually the oxide - forms a protective layer which separates the reactants. Further oxidation occurs by transport of oxygen and/or metal through this kinetic barrier and usually diffusion of one of these two species becomes the rate controlling step in the reaction. To give protection the oxide must itself be stable; its efficiency as a barrier depends on its diffusion characteristics, its electrical conductivity and its thickness.

Metals forming protective oxides show at least two different types of behaviour, a period of protective kinetics when the corrosion rate diminishes with increase in oxide thickness is followed, after a certain time, by a non-protective period when the rate remains constant, although thickening of the oxide continues. Oxidation becomes a serious problem when the protective thickness is small and allows non-protective oxidation to consume the underlying metal at a constant, appreciable rate. It has been suggested[1, 2, 10, 14] that the mechanical properties of oxides, particularly stresses arising during growth and lack of plasticity are important in limiting the protective thickness of oxides.

Briefly the theory can be stated in the following way. As the oxide thickens a point is reached where the internal stress is equal to the fracture strength and it deforms by extensive cracking or blistering[3]. The average thickness of the uncracked part of the oxide is the protective thickness and this determines the subsequent rate of oxidation. If the oxide can be made better able to withstand stresses through increasing its plasticity or strength by suitable alloying of the metal, then a greater protective thickness may be obtained, resulting in lower corrosion rates. Thus, the main interest in investigating the mechanical properties of oxides lies in gaining an understanding of the factors which influence the thickness at which kinetic transition occurs and thereby improving corrosion resistance of materials in service. This investigation is particularly directed to studying the growth stresses in oxides, but has in mind the broader field of mechanical breakdown and corrosion resistance.

Aluminium and zirconium were chosen for this work because of their use in nuclear reactors. Alloys based on aluminium and zirconium are used as "cans" to protect uranium fuel elements from water coolant. Also, aluminium, when anodised, is widely used as a decorative material for building purposes.

SECTION II

PREVIOUS WORK

Part 1. Growth of Oxides During Corrosion

a. Theories to Explain Transition from Protective to Non-Protective Oxidation Kinetics

A typical curve of oxide thickness versus time for the oxidation of a metal is shown in Figure 1. The first inflection in the curve represents the transition from protective to non-protective kinetics. Often the linear rate may increase; this second inflection is sometimes referred to as breakaway.

A number of theories have been put forward to explain the transition from protective to non-protective corrosion of metals. Some of these are listed below:

1. Mechanical breakdown - at a critical oxide thickness internal growth stresses can cause extensive cracking.
2. Strain induced recrystallisation or fragmentation.
3. Grain boundary growth and pustule formation leading to rapid penetration of metal.
4. Plasticity change - the oxide may lose its plasticity as it changes from an anion deficient to a stoichiometric oxide.
5. In aqueous and steam oxidation two additional mechanisms can operate because of the presence of water.
   i. Hydrogen damage.
   ii. Oxide dissolution.

With the exception of oxide dissolution and electrical damage by hydrogen all of these theories are concerned with the mechanical

properties of the oxide. The most concrete evidence to support this mechanical approach to transition is supplied by optical and electron-optical studies which reveal the presence of cracks in the non-protective oxide layer. Such evidence is plentiful in the literature.

Cathcart et al.[4] have systematically studied the corrosion of tantalum in pure oxygen between 470°C and 530°C. The oxide was initially protective but became non-protective during later oxidation. The non-protective oxide layer contained microscopic "blister-like cracks" visible in the electron microscope. Since both portions of the oxide were crystalline it was concluded that an observed increase in oxidation rate was related to cracking of the film. Niobium was shown to have similar kinetics, the transition from parabolic to linear growth being accompanied by crack formation[5, 6]. For both niobium and tantalum oxidation proceeded by anion migration which produced oxide about 100-200% greater in volume than the metal consumed in forming it. This large increase in volume caused stresses which led to cracks in the overlying oxide layer. An attempt was subsequently made[7] to show whether the transition from protective to non-protective kinetics was accompanied by a change in the growth stresses by measuring the bending of a tantalum coupon oxidised in 1 atm. O_2 at 500°C. However, the bending was caused mainly by oxygen dissolution in the substrate, which masked the oxide stress and no correlation was found.

Qualitatively, however, a stress gradient could be inferred in the oxide because several films were observed to peel off the substrate.

Similar data have been obtained for the oxidation kinetics of pure uranium in carbon dioxide. In the temperature range 350°C to 650°C the oxides formed are several hundred microns thick and cracks in the non-protective layer, have been shown metallographically[8]. Oxides formed at temperatures up to 900°C on β uranium are extensively cracked and oxidation is believed to be controlled by a thin layer of UO_2 through which oxygen ions migrate[9]. Between 750°C and 900°C oxidation is very rapid due to self heating of the uranium, but between 900°C and 1000°C the oxidation is more uniform and the oxide is more compact and relatively crack-free. This change in the state of the oxide on γU is attributed to increased plasticity of the UO_2 which enables it to deform rather than crack. The kinetics of uranium oxidation have been studied at cathodic potentials in aqueous solutions below 100°C by measurement of intensity of reflected light[10]. Initially a parabolic rate law was followed which was succeeded by a linear law. Under some circumstances a linear-linear transition ("breakaway") was also observed. The change to non-protective kinetics was attributed to cracks in the non-protective film and by alloying uranium with 5 wt.% and 10 wt.% Zr the corrosion rate

was changed in a way which was interpreted as arising from an increase in the protective oxide thickness.

Interpretations of the protective kinetics of zirconium oxidation are varied; parabolic, logarithmic and cubic laws have been cited by different workers. However, there is undoubtedly a transition after a given time (depending on temperature) to non-protective growth and this has been the subject of extensive investigation. At 300°C in steam the non-protective oxide on zirconium is white and non-adherent. At the critical breakaway thickness stresses build up and can cause cracking in the oxide film[11]. Diffusion through the oxide grain boundaries is more rapid than through the grains and results in thickening of the oxide at grain boundaries. Oxygen ion movement can produce uneven growth below the oxide[12] which causes cracking at the grain boundaries. Zircaloy 2 has a greater protective thickness on these grounds[11] because diffusion through its oxide is faster than through the oxide of the pure metal and the resulting growth which is more uniform leads to less stress build up. Heavy pustules of oxide have been seen to develop on Van Arkel zirconium in steam at 500 psi and 500°C[13]. Local breakdown of the oxide nucleated from grain boundaries, twins, slip bands and grooves left from etching out hydride platelets in the substrate is thought to cause these pustules which appear white under polarised light and are considered to contain numerous

microcracks. The overall corrosion rate is controlled by the protective oxide thickness which in turn is effected by a balance between growth of the oxide and "degradation", a process causing cracking or pores in the oxide and which is related to stress accumulation in the film.

A slightly different explanation for transition has been put forward as a result of X-ray line broadening measurements of oxides on single crystals of zirconium oxidised in water at 360°C[14]. The pre-transition oxide was black, monocrystalline and highly strained whereas the post-transition oxide was polycrystalline, although highly oriented, and relatively strain free. It was concluded that the change in kinetics was related to a strain induced recrystallisation or fragmentation, accompanying the change from protective to non-protective oxides.

It has been suggested[15] that the corrosion transition in Zircaloy 2 occurs when the oxide loses its plasticity on changing from a non-stoichiometric to a stoichiometric oxide. Some support for this idea was found by hardness tests on the two types of oxide. Although the hardness values were similar the indentations in the non-stoichiometric oxide were crack free whereas those in the stoichiometric oxide were surrounded by cracks.

Pure aluminium at 100°C in water has been reported to corrode

parabolically[16] but after a certain time the process becomes logarithmic[16, 17]. In high temperature water a period of uniform corrosion is succeeded by severe intergranular attack of the metal. Crystallisation of the corrosion product adjacent to the metal and internal strain in the oxide causing cracking have been cited as possible causes of the change in mechanism. Examination of the inner and outer interfaces of the oxide by X-ray and electron optical methods[18], however, revealed (a) that the inner layer was still amorphous, the outer layer being boehmite, (b) that no cracks were visible. A mechanism involving continuous rupture and healing has been put forward for the logarithmic kinetics of aluminium[17]. This may explain the absence of visible cracks.

Draley and Ruther[19] postulated that hydrogen produced by the reaction of metal with water causes reduced corrosion resistance. Three effects have been suggested.

1. Diffusion of hydrogen into the metal producing embrittlement and evolution as a gas in cavities causes rupture of the metal.
2. The formation of gaseous hydrogen causing rupture of the barrier layer and increased corrosion.
3. The formation of a metal hydride reducing the adhesion of (and perhaps recrystallising) the barrier layer would reduce the protective nature of the latter.

Hydrogen introduced by cathodic polarisation has also been shown seriously to reduce the electrical resistance of oxides thereby leading to increased corrosion[20].

On the basis of hydrogen theories the beneficial effects of anodic polarisation and deleterious effects of cathodic polarisation can be explained. The beneficial effects of such additions as nickel to aluminium (or to the corroding solution) which provides active sites for hydrogen combination (preventing hydrogen absorption into the metal) or hydrogen evolution outside the barrier oxide layer, are further evidence. Below 350°C Al-1% Ni contains no hydrogen[19].

It has been suggested[19] that widespread cracking of the oxide caused by hydrogen may control the corrosion rate and cause the transition from protective to non-protective behaviour. Sites of breakdown were considered to be above hydride particles which reacted with water, forming hydrogen. Bubbles of the evolved gas would exert enormous pressures which could rupture the film. However, it has not always been possible to verify the presence of hydride after corrosion tests; Burkart[26] suggested that the hydride dissolved in uranium eventually precipitating UH_3 in the metal. The failure to correlate breakdown with hydrogen damage has led to the approach that internal stresses cause cracking of the oxide. Hence the present work is concerned with the mechanical properties of oxides, especially

stresses arising during their growth on metals.

Part 2. Mechanical Properties of Oxides

a. Stresses in Oxides

As a result of their investigation into the high temperature oxidation of metals Pilling and Bedworth[22] divided base metals into two categories. Their criterion for protective or non-protective corrosion behaviour was based on the ratio of volume of oxide and the volume of metal from which it was formed.

$$\text{Pilling-Bedworth Constant} = \frac{\text{Molecular Volume of Oxide}}{\text{Formula Volume of Metal}}$$

Oxygen was presumed to be the only migrant ion during growth. Metals having a ratio greater than unity formed compact, continuous oxides which gave protection during oxidation, whereas those with a value less than unity - with one exception - formed discontinuous, cellular layers which permitted a linear oxidation rate to continue. In the latter case the oxide assumed a cellular structure to retain adherence with the rapidly receding metal surface. This relative volume concept formed the basis of many subsequent attempts to explain the nature and magnitude of residual stresses in oxides.

The existence of stresses in oxides was shown by Evans[23]. Nickel oxide films formed at high temperature in oxygen were

mounted on vaseline-coated glass and the metal substrate removed by anodic ~~reduction~~ dissolution. Thick films were observed to wrinkle suggesting a uniform stress distribution "due to misfit between the volumes of metal and oxide". Curling of thin films, however, was interpreted as showing that a stress gradient was caused by inheritance of stress from the basis metal. Compressive stresses were attributed to the fact that nickel oxide occupied 1.6 times the volume of metal consumed in producing it.

Further corroboration for the volume ratio principle came from Dankov and Churaev[24] who observed the curvature of thin mica strips coated on one side with the metal to be oxidised. From the curvature during oxidation it was found that iron and nickel which have Pilling-Bedworth ratios greater than unity grew oxides under compression whereas magnesium (ratio = 0.82) formed an oxide under tension.

The growth of oxides on zirconium produces large dimensional changes in specimens which were directional depending on their shape and size[25]. Such dimensional changes were considered to have been caused by stresses in the oxide. A thin uranium foil wound in a spiral has been shown to uncoil after oxidation in moist air at 70°C[26]. The foil was oxidised on both surfaces. When the oxide at the convex side fractured, the uncompensated compressive stresses in the oxide on the concave side stretched

the foil. In the same work films of UO_2 were observed to curl on uranium plates. Uranium-niobium alloy wires extend 1-2% during oxidation indicating compressive stresses in uranium oxide[27].

Attempts have been made to explain stresses in U-Nb alloys[27] in terms of lattice mismatch theories. These were based on the theory of oriented overgrowths[28] in which the energy of a string of atoms deposited as a monolayer was calculated as a function of misfit between substrate and deposit. It was found that elastic misfit strains less than 9% would be stable, those from 9-14% would be metastable, but misfits greater than 14% could not be absorbed by elastic strain. These misfits were "accommodated by loss of coherence by the formation of dislocations between the monolayer and substrate".

However, little success has been obtained in relating lattice mismatch to breakdown of oxides on alloys.

A complication in the stress situation for high temperature oxidation has been shown by measuring the curvature of tantalum foils in oxygen at 500°C[7]. Overall compressive deflections were found but these were shown (by chemical thinning) to be in the metal not the oxide. Oxygen dissolved in the metal was the main source of stress, and a model relating the stress gradient to the oxygen concentration gradient was shown to explain the effects. Stresses in the oxide were also present and sometimes

caused the oxide film to curl away from the substrate.

Recently the oxidation of copper has been studied at various oxygen pressures in the temperature range $220^{o}C$-$400^{o}C$[29]. Stresses about 1.7×10^{5} psi (compressive and tensile) were measured. Epitaxy, vacancy formation within the metal, oxygen penetration through a porous layer and the transformation of CuO to Cu_2O successively altered growth stresses. Epitaxy has been cited as the cause of anisotropic strain in thin films (up to 500 Å) of Cu_2O grown on a (110) face of a copper single crystal[30]. The strain distribution measured from X-ray line broadening has been rationalised in terms of an array of dislocations in the plane of the film. The dislocation density was calculated to be about $10^{11}/cm.^{2}$.

b. Stresses in Anodic Oxide Films

Stresses in anodic oxides were noticed as early as 1930[31] when wrinkling of anodic films on iron was observed.

A quantitative measurement of stresses was obtained by Bradshaw and Clarke[32] from the deflection of aluminium foil anodised in sulphuric acid. A tensile stress of 0.42 tsi (64 $kg/cm.^{2}$) was measured after growth, during which aluminium dissolved in the electrolyte and a porous oxide was produced. However, after boiling in water to seal the pores the oxide

stress was closer to that predicted from consideration of the volume ratio (1.6 tsi or 245 kg/cm.^{2} compressive). The authors comment that the 28% volume expansion accompanying oxide formation should give rise to compressive stresses but dissolution considerably modifies this consideration.

Bradhurst[33] found stresses in compact barrier layer anodic films on aluminium anodised in ammonium borate solutions in which little dissolution occurred. At low current densities, stresses were compressive, but faster growth rates favoured tensile stresses. Further measurements also suggested that the electrolyte and its pH were other variables. The change in sign of stress with growth rate, he suggests, is caused by an increase in cationic conduction with increase in ionic current density[34]. This idea of balanced ionic fluxes affecting stress development is really an extension of the volume ratio principle and has been proposed[35] to explain the formation of stress-free inner layers of magnetite on iron which has a Pilling-Bedworth ratio of two. Sufficient iron dissolves in the environment for the oxide formed to occupy the space originally occupied by the metal.

It has also been suggested[33] that plasticity can be induced in alumina films even at room temperatures by the application of an electric field. Since the ionic fluxes in anodising are similar in magnitude to those during oxidation at

high temperatures, one might reasonably expect a diffusion assisted deformation mechanism to operate, despite the low thermal activation. Wires of aluminium had greater strength when covered by an anodic film than when only a thin air-formed film was present. Under tensile load the anodised aluminium wires stretched when small anodic currents were passed. Elongation of the wire occurred by the movement of dislocations which were permitted to escape from pile-ups in the metal at the metal-oxide interface by plastic deformation of the oxide layer. It was deduced that the high electric fields encountered in growing anodic films would cause relaxation and lowering of internal growth stresses by plastic deformation.

Stresses in the oxides of a series of metals Ta, Nb, Al, Zr and Ti were measured by Vermilyea[36]. Films were grown at constant current density in a borate electrolyte. Surface preparation was found to influence the development of stress which was generally tensile except in ZrO_2 which was tensile at low thicknesses, but highly compressive during later stages of growth. All the oxides studied had Pilling-Bedworth ratios greater than unity and, according to this criterion, should have formed in a state of compression. The tensile stresses were explained by the following theory:

Under the influence of the applied field protons migrate out of a hydrated oxide leaving it in a state of tension.

Greater tensile stresses produced at higher formation rates result from increased water trapping.

The results[33, 36] emphasise that the simple volume ratio principle in some instances is inadequate for predicting the magnitude or even the sign of stresses in oxides and, though it may often be important, other factors concerning the mechanism of growth, especially cation migration, the environment and the condition of the metal surface must be considered when formulating a theory for stress development.

c. Plasticity of Oxides

Plasticity is important in high temperature oxidation because it influences the integrity of the oxide which in turn determines the rate of oxidation. The more plastic an oxide is, the more it is able to relieve, without cracking, the area and other geometrical constraints imposed upon it by the substrate during growth. Increased plasticity is desirable (a) to increase the critical thickness at which oxides of uranium, tantalum, niobium and zirconium develop cracks and become non-protective, (b) to prevent void formation and loss of oxide adherence caused by wrinkling or metal ion migration, and (c) to enable the oxide to resist spalling during cooling as the metal contracts more than the oxide and imposes additional compressive stresses.

In some instances improvements in corrosion resistance have been seen to result from increased plasticity and considerable attention has been paid to high temperature deformation of bulk oxides, and oxide scales.

Usually increased temperature results in more rapid oxidation but this is not inevitably so. For example, below 900°C in CO_2 uranium forms a duplex oxide consisting of a thin layer of UO_2 (which is believed to control the oxidation rate) and a thick overlying layer which is extensively cracked and is non-protective. Between 900°C and 1000°C the rate actually decreases because the outer oxide formed at these temperatures is crack-free and therefore more protective. Temperature induced plasticity of uranium is considered to be responsible for the uncracked film[8].

The deformation mechanism of sintered uranium has been investigated at various temperatures by employing bend tests[37]. Exactly what atomic mechanism was responsible for deformation was not known, but plasticity was a function of the non-stoichiometry of the oxide. $UO_{2.06}$ and $UO_{2.16}$ could be plastically deformed at about 800°C but the stoichiometric oxide, $UO_{2.00}$ became plastic only above 1600°C. The increased oxygen:uranium ratio lowered the lattice binding energy as shown by the Young's modulus and it was suggested that the strength of a dislocation in a non-stoichiometric lattice might be five times lower than in the

stoichiometric material.

Similar conclusions have been drawn for the beneficial effect of non-stoichiometry on the plasticity of zirconia[15]. In this case the oxide was anion-deficient, and was considered more plastic because hardness indentations made at 23°C were crack free whereas the stoichiometric oxide, although giving the same hardness reading, contained indentations surrounded by cracks. Doping monoclinic zirconia with iron, nickel or chromium increased plasticity but yttrium slightly reduced it. Above 200°C calcia-stabilised cubic zirconia was found to be more plastic than the monoclinic form indicating that crystallographic structure influences deformability. Tensile tests on 72μ thick oxide films (on the substrate) showed that considerable plasticity occurred at 500°C but not at room temperature.

The plasticity of Cu_2O has been shown to modify the oxidation of high-purity Cu by increasing the activation energy for the diffusion of Cu^+ ions through Cu_2O[38]. Large compressive growth stresses are present in the oxide. At low oxidation temperatures where the oxide behaviour is elastic, these compressive stresses cause extrusion of CuO whiskers whose formation is accompanied by injection of vacancies into the CuO layer. Anion vacancies tend to migrate towards the oxide/gas interface under the influence of the chemical potential gradients present

during oxidation. The cation vacancies migrate to the Cu_2O/CuO boundary and are injected into the Cu_2O layer. This cation vacancy excess over the thermal equilibrium number eases the diffusion of Cu^+ through the Cu_2O, the rate controlling process. Below 700°C where the oxide is elastic and whiskers form, the activation energy is 20 kcal/mole. Above 700°C Cu_2O deforms plastically and relieves the stresses which are therefore never high enough to cause CuO whisker extrusion. Vacancies must be supplied by thermal activation alone and the activation energy for growth is consequently higher, 40 kcal/mole.

In contrast to its role in the oxidation of copper, oxide plasticity has the opposite effect on the growth rate of scales on iron after long exposures[39]. Cavities form by the condensation of cation vacancies left by outward migration of metal ions. These pores act as barriers to ionic migration and thus reduce the effective area over which oxidation can occur. The continued existence of such pores is only possible when the oxide is not able to deform and collapse on to the receding metal interface by force of adhesion or pressure of the oxidising atmosphere. Mackenzie and Birchenall[40] have demonstrated cavity formation by completely oxidising iron in pure oxygen at 800°C-850°C. When sectioned the resulting wüstite specimens contained a cavity of the same size as the original sample. If iron was oxidised in a hydrogen-water vapour atmosphere so that magnetite

and hermatite formation was prevented, the cavities disappeared. Creep bend tests on the three oxides at 800°C-1000°C showed that wüstite was more plastic than the other two oxides and it was concluded that plasticity was a function of the number of systems available for slip and hence depended on crystallographic structure.

The cavity was formed only in the presence of the higher oxides, magnetite and hermatite which, it was thought, conferred rigidity to the wüstite, preventing its collapse.

The cation vacancies left at the metal/oxide interface by metal ions entering the oxide have a bearing on oxide adhesion and stress build up in the oxide. Tylecote[41, 42] discusses adherence of oxides during oxidation. Unless the cation vacancies diffuse into the metal substrate, the void must be filled by oxygen diffusion, forming oxide internally or by the oxide shrinking in on the substrate. Otherwise, poor adhesion will result. It is concluded that good adhesion is only possible during oxidation if there is plasticity of the oxide and/or a balance between cationic and anionic migration.

A mechanism for the adhesion of low temperature oxides forming by cationic conduction has been proposed[43] which implies that metal ion migration produces a stress-free oxide. The theory is based on the assumptions that only those metal atoms which lie at lattice steps on the substrate surface enter the oxide and that oxide is formed at the oxide/atmosphere

interface. Metal atoms which lie at lattice steps have a number of nearest neighbour bonds only two-thirds of that of atoms which lie in the centre of a close-packed plane, and are therefore more easily removed. The lattice step is a region of misfit similar to an edge dislocation in a crystal (Figure 2). Removal of metal atoms constitutes the climb of the dislocation along the oxide/metal interface. The cation vacancies are destroyed by the atom in the extra layer of the dislocation entering the oxide. Since the oxide forms at an outside interface no stresses are considered to develop in it. Vermilyea appears to suggest that no deformation of the oxide occurs. This is not strictly true; somehow the oxide must move into space formerly occupied by metal. The mechanism, it seems, requires an oxide which will bend slightly and unbend - if not plastically then elastically - to accommodate the lattice step as it progresses along the interface.

The plasticity (deformability) of anodic films is of interest not only for practical reasons because they are used in electrical windings and capacitors, but also because some of the fundamental mechanisms which govern their behaviour may be common to high temperature oxidation and corrosion films.

At room temperature, anodic and corrosion films of aluminium are brittle; porous films formed in sulphuric acid when tested on wires develop cracks at about 1% strain and the crack density increases with greater strain[44]. Similar strain values prior

to cracking have been obtained for barrier type anodic films of alumina by bend tests on oxide covered strips[45]. The surprisingly large strain in anodic alumina prior to cracking has also been shown by testing in tension an oxide separated from its substrate[45]. The stress-strain curve for a 1500Å thick film showed approximately the same breaking strain as mentioned above but the ultimate tensile strength was about five times greater than that of the bulk oxide. Also the Young's modulus was 4.8×10^5 kg/cm.^{2} compared with 3.6×10^6 kg/cm.^{2} and the breaking strain was about 1-3% compared with 0.07% for the bulk oxide. The high strength may have been caused by a size effect being operative. Enormous increases in tensile strength have been noted[46] for electrodeposited films of silver below about 1μ critical thickness. Using Griffith's equation[47] one can calculate the appropriate size of the stress-raising defect to be of the order of 100Å, which suggests that it is not the thickness of the oxide which limits the crack size, but some other defect, a crystallite say, whose size or population varies with thickness. Bradhurst's results for anodic films emphasise nonetheless that extrapolation from bulk oxide properties to predict the probable behaviour of thin oxide films may be misleading.

The deformation of anodic films of tantalum, zirconium and aluminium has been investigated[48] by the technique of measuring the

amount of "bare" surface created by straining an anodised wire. The "bare" surface was covered by a thin oxide (maintained at 15-20Å with an applied potential) and electrons tunnelled through it to reduce ions in a ferro-ferri cyanide solution. Values of the percentage bare area created by the inability of the oxide to deform were calculated from the ratio of the current passed at a given strain to that passed by an oxide 15-20Å thick of similar total area. It was concluded that anodic ZrO_2 showed some ductility but that anodic Al_2O_3 showed none. However, anodic Ta_2O_5 had great ductility and deformed as much as 50%. This was confirmed by optical measurements of the reduction in oxide thickness caused by straining. The property of Ta_2O_5 which bestows this great deformability is not known but this result seems well worth pursuing further since ductile ceramics are rare and of considerable practical importance.

Although brittle under normal conditions alumina films have been shown to be ductile in the presence of an ionic flux[33, 49]. The strenghening of an aluminium wire under load by the presence of an anodic oxide disappeared when small anodic currents were passed through the oxide. The wire elongated. Deformation of the oxide during passage of an ionic flux allows dislocations within the metal but trapped at the metal/oxide interface, to escape and the wire stretches under the applied

load. The deformation increased with increasing current and the behaviour was found to be consistent with a mechanism, resembling Herring-Nabarro creep, in which the rate of deformation was controlled by the field induced flux. This mechanism has immediate relevance not only to stress relief during growth of anodic films but also to corrosion product oxides and is an example of a basic mechanism investigated using anodic oxides which finds an application to corrosion in other conditions.

Part 3. Anodic Oxide Films

a. The Mechanism of Growth

Since stresses in oxides are dependent on the growth mechanism general features of anodic oxidation, especially those which may influence stress development, are reviewed.

i. High Field Conduction

The metals aluminium, zirconium, niobium and tantalum can form compact anodic oxide films when they are made the anodes in a suitable electrolytic cell. The anodic current passed through the oxide sets up a high electrostatic field of about 10^6-10^7 volt/cm. This field, together with the chemical activity gradients which produce natural oxide films, acts as a driving force to assist

metal and oxygen ion migration and accelerates oxide growth. Anodising is thus a process of high field conduction complicated by transfer phenomena at the metal/oxide and oxide/electrolyte interfaces. Ohm's law does not apply to conduction at these high field strengths; the field F and ionic current i are exponentially related by an expression of the general form

$$i = \alpha \exp(\beta F) \qquad (1)$$

This is the high field conduction equation and the considerable investigations and theories on high field conduction are reviewed by Young[50]. α and β are constants which depend on oxide parameters and temperature.

Two modes of anodising are used (a) constant voltage, where the current decays as the oxide barrier thickness increases, and (b) constant current, where ideally, the voltage rises linearly with time as the oxide thickens uniformly at a constant rate. At a certain voltage called the spark voltage, the rate of voltage rise decreases and violent arcing through the oxide occurs. After a little further growth the maximum voltage is reached. The maximum voltage attainable before dielectric breakdown occurs can be raised by increasing the resistivity of the growth electrolyte[51] but the exact cause of dielectric breakdown has not yet been established.

ii. The Oxidation Reaction

The anodising reaction is due to the replacement of hydrogen from water by the metal. For example, the reaction of aluminium can be represented by the following equations, depending on whether aluminium reacts with water or hydroxyl ions.

$$2Al^{3+} + 3H_2O = Al_2O_3 + 6H^+$$

$$2Al^{3+} + 3OH^- = Al_2O_3 + 3H^+$$

Too much energy would be required to displace oxygen from electrolyte anions such as BO_3^{3-}, SO_2^{2-}. Electrolyte anions are incorporated into anodic films but not in sufficient quantities to affect their electrical or mechanical properties[52]. However, the electrolyte serves at least two purposes,

a. It reduces the resistance of the solution so that most of the cell voltage is applied across the oxide, and
b. It exerts a buffering action to reduce local acidity caused by protons produced in the above reaction.

iii. Current Efficiency During Anodising

Rarely does all the anodic current passed through the oxide result in oxide growth. Inefficiency can be caused by oxygen evolution and by field assisted dissolution of Al^{3+} ions from the

oxide[34, 52]. Above the oxygen evolution potential electrons (or positive holes) conducted mainly through flaws in the oxide cause oxygen to be formed[50].

$$4OH^- = O_2 + 2H_2O + 4\epsilon$$

iv. Temperature Rise During Anodising

The passage of an anodic current through a highly resistant oxide such as those on aluminium, zirconium or tantalum involves the production of considerable heat. At 1.0 mA/cm.^{2} and a field of 5 x 10^6 volt/cm. the power dissipation per unit volume of oxide is 5 kW/cm.^{3}.

Power dissipation/Unit volume = Field x Current density

In comparison with this the heat from the exothermic formation of oxide is negligible. If all this heat were retained in the oxide it would become extremely hot. Most of the heat is lost to the electrolyte and the substrate but the undesirable possibility of temperature rises occurring during growth exists and growth rates at which temperature rises are negligible must be used for stress measurements. Vermilyea[53] and Young[54] have estimated the temperature rise of an oxide during anodising by considering how the heat is lost to the surroundings.

Young[54] has treated the oxide as a constant heat source at the metal/solution interface. The oxide is so thin that its heat capacity and heat transfer resistance are negligible; thus its temperature does not rise above that of the metal and solution at the interfaces. Heat is transported away by conduction through the metal and convection in the electrolyte. The calculations showed that the temperature rise depended on the size and shape of the specimen but was about $1^{o}C$ at 1.0 $mA/cm.^{2}$ and 50 v and $10^{o}C$ at 10 $mA/cm.^{2}$ and 50 v[50]. Vermilyea's treatment considered the heat to be lost at a constant rate only to the metal substrate. The estimated temperature rise was about $4^{o}C$ after 4 seconds growth at 20-30 $mA/cm.^{2}$. Both workers are of the opinion that only at higher growth rates than several $mA/cm.^{2}$ does the temperature rise become noticeable and it is then manifested by an apparent change in relationship between field and current.

The temperature rise during anodising has been determined over a wide range of current densities from changes in the a.c. resistance of thin aluminium wires[55]. After growth to 250 volts at 1.0 $mA/cm.^{2}$ the maximum temperature of the wire, the hottest part of the anodising system, was always very much less than $5^{o}C$.

v. Field Induced Stresses

During stress measurements on anodic films an additional deflection, which is always compressive, accompanies the application of the anodic growth field. The high electric fields (10^6-10^7 volt/cm.) in anodising are expected to exert a compressive stress P, normal to the surface of the dielectric oxide. This would give rise to a component νP (ν = Poisson's Ratio of the oxide) parallel to the oxide surface, causing an additional deflection whilst the forming field is applied.

Vermilyea[36] considered that the difference between the field on and the zero field deflections was too large to be caused solely by electrostatic pressure. Poisson's ratio was assumed to be 0.2. Furthermore he stated that the stress was not proportional to the square of the field, as it should be if electrostatic pressure were involved, and concluded that while electrostatic pressure undoubtedly played some role, it was not the only factor responsible for the observed effects.

vi. Dominant Ion Migration

The volume ratio principle of Pilling and Bedworth which has been cited as an important factor in producing stress in oxides, assumed that oxygen ions were the only mobile species during growth. Evidence exists to show that this condition is not always applicable; frequently metal ions also migrate,

resulting perhaps in a stress free oxide[35, 43, 56].

Changes in topography of aluminium oxides grown in boric acid and borax electrolytes have been seen[50 p. 214] to occur at both the metal/oxide and oxide/electrolyte interfaces. Metal ion movement must have contributed to the changes in topography at the oxide/electrolyte interface since almost negligible oxide dissolution occurs in these solutions.

The interfaces of anodic films formed in 1% citric acid + 1% ammonium citrate on single crystals of aluminium have been studied by an unusual technique[57]. After anodised samples had been heated to 600°C for 15 minutes and cooled in air, vacancies condensed to form pits beneath the oxide. The oxide over the pits was removed with a cellulose nitrate replica and examined by electron microscopy. The topography of the surface was revealed by a shadowing technique. A double pit experiment was performed by reheating a sample to 600°C for 15 minutes. During this anneal further oxidation by the air occurred and thickening (revealed by shadowing) was seen at both oxide interfaces. Crystallites formed at the oxide/metal interface and amorphous oxide at the air/oxide interface. Hence it was deduced that crystallites grow by anion migration and amorphous oxide is a product of metal movement.

Lewis and Plumb[58] investigated the relative ionic mobility in anodic alumina films grown in ammonium tartrate. A radioactive

layer was formed by polarising the sample for 30 seconds at 15 volts in 0.1% H_2SO_4 containing S^{35}. By growing duplex oxides in which the tagged oxide was applied before or after the barrier tartrate layer and then dissolving the oxide away in 5% H_3PO_4-2% CrO_3 solution, it was concluded that the oxide applied first was last to be removed. Hence metal ion migration must have occurred for oxide to be formed at the oxide/solution interface. Quantitative measurements of the metal transport number were not made because of the possibility of non-uniform thinning by the dissolving solution. However, it was generally concluded that growth occurred mainly by cation diffusion.

Quantitative measurements of metal transport during anodising have been made by Davies et al.[34, 59, 60, 61] on a range of metals using Xe^{125} as a radiotracer and measuring the depth of the marker layer after growth by β-ray spectroscopy. Only oxygen transport occurred during the growth of ZrO_2 and HfO_2. Both ionic species were mobile in the oxidation of tantalum, niobium and tungsten[61]; the transport number of each of these metals was approximately 0.3. Aluminium anodised in 3% aqueous ammonium citrate showed a significant trend[61] in which the metal transport number increased with the total current density. However, in a non-aqueous borate solution where negligible dissolution occurred this trend was not evident, the cation transport number being 0.56 ± 0.04 (Table 1).

The amount of aluminium which must pass outwards during oxidation so that zero volume change occurs, has been calculated by Field and Holmes[56]. For the anodic oxide of density 3.1 g./cm.^{3} to exactly occupy the volume of the metal consumed, 40% of the aluminium must migrate outwards. On the basis of this zero volume change criterion, one might reasonably expect stresses in alumina to be low since this calculated transport number of aluminium lies in the range of values measured by Davies et al. (Table 1).

b. The Structure of Anodic Oxide Films

i. Anodic Alumina

Aluminium forms anodic oxide films having two distinct morphologies depending on the solvent action of the growth electrolyte. In highly dissolving media[62] a duplex film is formed which consists of a thin barrier layer adjacent to the metal, overlaid by a non-resistant porous oxide which contains some water[63]. Porous films can be grown several microns thick. In electrolytes where dissolution is small an insulating barrier type film is produced, the thickness of which is related to the applied voltage by the growth field (12-15 Å/V depending on growth current density).

Barrier alumina films are generally regarded as being

amorphous in structure since they give only diffuse X-ray and electron diffraction patterns[64]. They may not be completely amorphous; crystallite sizes less than ≈10Å[64] would produce this effect. Wilsdorf[65] regarded the amorphous oxide as a random arrangement of structural units of $(Al_2O_3)_2$. Oxides thicker than ≈1500Å have been observed to develop crystallites[64]. Similar crystallites have been observed in alumina grown at high temperatures in oxygen[57]. Two theories for crystal formation are (a) oxygen mobility produces crystalline oxide in the space formerly occupied by the metal[57] and (b) electrocrystallisation occurs[66]. These crystalline areas give sharp electron diffraction patterns and are considered to have a spinel structure γ'-Al_2O_3. The generally amorphous nature of anodic alumina precludes epitaxy as a cause of stresses during growth.

Barrier anodic Al_2O_3 films have a high electrical resistivity which rapidly diminishes in the presence of water. Analysis has shown[68] that no water is present in the oxide after growth except at low current densities where the anodic field is low and protons can enter the oxide attracting hydroxyl ions in as well, producing a heavily hydrated layer approximately 50-100Å thick at the oxide/electrolyte interface[69]. This hydration was detected by impedance measurements made during oxide thinning. Further work[70-72] shows a region of low resistivity at the metal/oxide interface which is considered to be due to electrons trapped at O^{--}

vacancies in a region of non-stoichiometry near the interface between metal and oxide. Separating the outer hydrated layer and non-stoichiometric layer is stoichiometric anhydrous alumina.

Infra-red spectrophotometric analysis has been used to study the molecular structure of alumina and it has been suggested that the barrier film is a trihydrate[73-75]. However, the barrier film studied was formed in orthoboric acid at 100°C. Boiling anodic barrier films in water results in extensive hydration so it is expected that growth in a boiling solution would produce a hydrated oxide. This result therefore may not contribute to the understanding of the nature of barrier films formed at room temperature.

Oxides are generally considered to grow at the interfaces. The nature of the oxide/electrolyte interface should be dependent on the processes, such as adsorption, occurring in this region. A model (Figure 3) has been postulated for the barrier oxide/electrolyte interface for alumina produced in H_2SO_4[76]. It involves the presence of a space charge of protons produced by the reaction of Al^{3+} ions with water or hydroxyl ions. Reactions of barrier films with water and adsorption and sealing properties are also discussed in terms of this model.

ii. Anodic Zirconia

The structure of anodic zirconia seems to be in some doubt. Early electron diffraction work[78] concluded that the oxide was amorphous, containing crystallites of the cubic modification. However, it has recently been suggested that the oxide is entirely crystalline and of the cubic modification[79]. This view agrees with the idea that metal ion migration produces amorphous oxides, oxygen migration produces crystalline oxides. Anion migration is the diffusion mechanism in anodic zirconia.

Hydration of zirconia has not been reported but protons which lower the electrical resistivity of the oxide can penetrate the film under cathodic polarisation[20].

Part 4. Conclusions from Previous Work

Considerable evidence supports the contention that transition in oxidation kinetics is caused by cracking of the oxide. Two factors control the integrity of a number of oxides:

a. Stresses arising during the growth of oxides on metals, and

b. Lack of oxide plasticity.

The presence of stresses has been inferred from deformation of the substrate by the oxide, but in no instance has a one-to-one correlation between stress and transition been obtained.

The factors which determine the magnitude and sign of growth

stresses in oxides are not fully understood. This situation has arisen because of the complexity of the oxidation mechanism in which several of the parameters which affect stresses often vary simultaneously. Oxygen dissolution in the metal and epitaxial effects both of which cause stresses at interfaces, will not be considered here because epitaxial stresses decrease to zero within the first 400-500Å of oxide and oxygen dissolution only occurs at high temperatures, while the present work will be found to be concerned with stresses in relatively thick films formed at temperatures below 100°C.

The volume ratio principle still forms the basis for qualitatively predicting the sign of stress when oxygen ions are the only mobile species during growth. Oxides with volume ratios greater than unity, e.g. Nb_2O_5, UO_2, and which grow by anion migration, form in compression in accordance with the volume criterion. The situation is less well defined when metal ions also contribute to growth; several consequences could follow from increased metal ion migration. Oxide forming at the outer oxide interface is under no constraint from the metal and should form free from stress[43]. Metal ion migration introduces a complication, however, which has not been satisfactorily resolved. In the case where both species are mobile and the volume of oxide formed by anion migration may be less than the volume of the cation vacancies left behind by outgoing metal

atoms, a void could conceivably be formed and adhesion lost. Birchenall's experiment[40] with iron during which a void was formed equal in volume to the original metal specimen, is convincing evidence that this can happen. In most cases oxides retain contact with the metal even if a balance between anion/cation conduction possibly does not operate; cation vacancies may collapse and form dislocation loops in the metal[80] or in high temperature oxidation the oxide may be sufficiently plastic to collapse on to the metal. Alternatively, a mechanism similar to Vermilyea's[43] may enable the oxide to maintain adhesion or the oxide may form in tension[45]. The influence of the dominant ionic species and of oxide plasticity on stresses still remains obscure.

Anodic alumina shows interesting features which are of practical and theoretical importance. The growth stresses are sensitive functions of the growth rate; at low current densities the oxide forms in compression but at higher current densities it is in tension. This implies that at a certain growth rate an oxide under zero stress can be produced. Tensile stresses in alumina, which has a volume ratio greater than unity, are of theoretical interest because their occurrence cannot be explained simply in terms of the volume ratio.

Two suggestions have been put forward to explain this failure of the volume ratio criterion.

a. Increased cationic conduction relieves the volume constraint and produces cation vacancies at the metal/oxide interface which collapse to form dislocations.

b. Each incremental layer of the anodic film forms first as a hydrated intermediate from which the protons are subsequently removed by the high growth field.

From the previous work it appears that three factors may influence growth stresses in alumina.

a. Oxide plasticity induced by the ionic growth flux.

b. Increasing cationic conduction with increasing growth rate.

c. Hydration-deprotonation phenomena.

The properties of anodic alumina mentioned above suggest that further investigation into stresses in anodic films would be fruitful. This work has two aims therefore; to elucidate the mechanism producing a stress-free oxide, in order to see if it is applicable to high temperature oxidation, and to determine the roles of dominant ion migration and/or hydration phenomena as causes of stresses, in particular the occurrence of tensile stress, where the volume ratio is greater than unity.

The anodic growth technique offers the advantages that oxides of reproducible thickness can be produced at growth rates which can be varied independent of temperature. Also a low temperature system can be used to measure stresses.

SECTION III

EXPERIMENTAL PROCEDURE

Part 1. Preparation of Anodic Oxide Films

a. Materials and Surface Preparations

The metals used in this investigation had the following analyses and were prepared as given below.

i. Aluminium

99.99% purity "Star" foil 0.010 cm. thick. Prior to any treatment the aluminium was annealed at 350°C in air to relieve any residual stresses caused by rolling during fabrication. The metal surface was prepared for anodising by etching for ten minutes in 10 w/o KOH to remove most of the oxide already on the surface, it was then dipped in 50 parts HNO_3/50 parts H_2O and washed in distilled water.

ii. Zirconium

99.8% purity foil 0.010 cm. thick. Stresses were relieved by annealing at 700°C in a sealed silica glass tube evacuated to 5×10^{-5} mm. Hg. The surface was chemically etched for ten seconds in 5:4:1 H_2O:HNO_3:HF and rinsed in distilled water. The analysis of I.M.I. billet Z8395 from which the foil was prepared was:

Element	ppm	Element	ppm
Al	30	Sn	<100
Cu	15-20	Ti	20-30
Hf	65-70	N	20-55
Fe	500-600	H	10-45
O	950-1300	Nb	-

iii. Zircaloy 2

This was supplied by I.M.I. and was about 0.05 cm. thick. After vacuum annealing at 700°C for an hour the thickness was reduced to about 0.010 cm. by dissolving the metal in 5:4:1 H_2O:HNO_3:HF. The thinning was found to be fairly uniform after checking the thickness with a micrometer.

Zircaloy 2 is an alloy of zirconium containing the following elements:

Sn 1.3-1.6% Fe 0.07-0.20% Cr 0.05-0.16%

Ni 0.03-0.08% N 0.006%

iv. Foil Dimensions

The foil specimens used for deflection experiments were of a standard size, i.e. 10 cm. x 0.5 cm. x 0.010 cm. A micrometer was used to measure the average thickness of each foil.

b. The Anodising Technique and Growth Rate Measurements

Oxides were grown at constant current densities in the range 0.1 to 10 $mA/cm.^2$, in order to study the effects of growth rate on stress development. The temperature of the growth electrolyte was not strictly controlled but was always in the range 18°C to 21°C. A current source (type C091) provided growth at constant current to a pre-set voltage after which growth proceeded at constant voltage and the current fell to a low "leakage" value. To calculate stresses during growth it is necessary to know the oxide thickness during growth.

Since the linear relationship between voltage and oxide thickness, the Å/V ratio, varies with the current density and electrolyte type, the growth Å/V ratio for each particular anodising condition was measured optically. Growth Å/V ratios were measured by curtailing growth at the pre-set voltage and eliminating growth to leakage.

The growth electrolytes for aluminium were aqueous solutions of 15 g/l boric acid or 10 g/l citric acid, the pH being adjusted by suitable additions of NH_4OH. Zirconium was anodised in pH = 9.0 (boric acid + NH_4OH), 0.1 N, 0.2 N and 0.5N H_2SO_4 or 10 w/o KOH. All solutions were prepared using distilled water and Analar reagents.

Providing no oxide or metal dissolution occurs during growth and the anodic film is non-porous, the ionic growth current can be

calculated from Faraday's laws and the growth rate dV/dt. Presence of water or components of the electrolyte in the oxide is ignored.

For unit area of metal the volume of oxide is equal numerically to its thickness b. Volume = 1.0 x b.

The useful increment in charge dQ producing incremental thickness db of oxide $Me_x O_y$ is

$$dQ = \left(\frac{2yF\rho}{M} \right) db$$

where ρ = oxide density.

M = oxide molecular weight.

F = Faraday's constant 96,500 coulombs/equivalent.

Oxide thickness b is linearly related to the voltage v by the $\mathring{A}/V$ ratio.

$$\therefore \quad db = \left(\frac{\mathring{A}}{V} \right) dv.$$

Ionic current $$i_{ionic} = \frac{dQ}{dt}$$

Hence $$i_{ionic} = \left(\frac{2yF\rho}{M} \right)\left(\frac{\mathring{A}}{V} \right)\left(\frac{dv}{dt} \right) \qquad (2)$$

In cases where the growth rate dV/dt is not constant, the $\mathring{A}/V$ relation is not valid and the thickness at each particular

voltage must be measured to obtain the current efficiency.

Part 2. Measurement of Growth Stresses

a. Method

Stresses were determined by measuring the horizontal deflection of the lower end of a thin metal foil held rigidly at the top and insulated so that oxidation occurred only on one side (Figure 4). The foils were insulated with cellulose lacquer applied as an aerosol. A travelling microscope with Vernier eyepiece reading to 0.004 mm. was used to follow the movement of the foil. Zero field deflections were measured at each required voltage by switching off the current source. Although the oxide growth was consequently intermittent, little change was apparent between the growth rate dV/dt of oxides grown intermittently in this fashion and those grown continuously.

b. The Convention for the Sign of Stress

By convention an oxide is said to be in tension when it would contract if removed from its metal base and in compression when it would expand when released. Lateral stresses deform the substrate to the shape of part of a spherical surface. The

oxide is on the concave surface of the sphere when tensile stresses are present in the oxide, on the convex surface when compressive stresses operate (Figure 5).

c. Calculation of Stress - Biaxial Analysis

A modified version of Stoney's formula[81] was used to calculate stress from the horizontal deflection Z. The modified analysis considers the deposit to cause biaxial deformation of the substrate instead of uniaxial bending.

Stoney's formula[81] derived for a foil under uniaxial stress caused by an overlying deposit is

$$\text{stress} = \frac{Ed^2}{6rt} \qquad (3)$$

where E = Young's modulus of the metal substrate.

d = thickness of substrate foil.

t = oxide thickness.

r = radius of curvature = $l^2/2Z$

l = length of foil.

For this approximation to hold $t \ll d$ and the substrate must not be deformed beyond its elastic limit.

As the oxide is capable of giving rise to a stress in the longitudinal direction of the foil, it will in the general case

have a similar component at right angles to this and parallel to the surface of the foil[82]. Thus a biaxial stress system operates which bends the foil into the shape of a sphere.

Hooke's Law of Elasticity in three dimensions is

$$\varepsilon_x = \frac{1}{E} \{ \sigma_x - \nu (\sigma_y + \sigma_Z) \}$$

$$\varepsilon_y = \frac{1}{E} \{ \sigma_y - \nu (\sigma_Z + \sigma_x) \}$$

$$\varepsilon_Z = \frac{1}{E} \{ \sigma_Z - \nu (\sigma_x + \sigma_y) \}$$

where ε = strain.

σ = stress.

ν = Poisson's ratio of the substrate.

The oxide can exert no stress on the metal perpendicular to its surface $\therefore \sigma_y = 0$.

For biaxial stresses $\sigma_x = \sigma_Z$

Hence

$$\varepsilon_x = \frac{\sigma_x}{E} \{ 1 - \nu \}$$

$$\sigma_x = \left(\frac{E}{1 - \nu} \right) \varepsilon_x$$

The simple beam formula $\sigma = E \left(\frac{y}{r} \right)$ where y = distance from neutral axis, must be adjusted to

$$\sigma = \left(\frac{E}{1-\nu}\right)\left(\frac{y}{r}\right)$$

A derivation similar to Stoney's but including the biaxial deformation term $\left(\frac{1}{1-\nu}\right)$ leads to the expression

$$\text{stress} = \left(\frac{1}{1-\nu}\right)\left(\frac{Ed^2Z}{3l^2t}\right) \qquad (4)$$

d. The Effect of Specimen Geometry

The deformation of oxide-covered metals has been reported to be dependent on their geometry[7, 26]. To ensure that the stress measurements in the present work were not influenced by the breadth b of the foil, a parameter which is not specified in the above analysis, deflection measurements were made on zirconium foils of various breadths. For length/breadth ratios greater than 10:1 the deflection was independent of the breadth. Below this limit, deflections were low, possibly because of distortion of the specimens. The specimens in this work have $l/b = 20:1$, i.e. in the range where deflection is independent of the breadth.

e. Reliability of Stress Measurement

The bending foil method is suitable for measuring stresses because the errors that can arise from approximations made in the stress analysis above are negligible in the case of barrier anodic films. The oxide is so thin that oxidation makes a negligible change in the substrate thickness and d can be correctly assumed to be a constant. Stress relaxation which occurs during bending is simply caused by bending the oxide and insulation layer[83]. Both are so thin that they add negligibly to the thickness of the foil and the stress necessary to deform them is minute.

The elastic moduli used for calculating stresses are given in Table 2.

f. Stress Location by Oxide Removal

In the Stoney analysis the stresses causing bending during oxide growth are assumed to be uniformly distributed across the oxide. To determine the stress distribution in the oxide, the deflections of anodised aluminium foils were observed during uniform, chemical thinning of the oxide in 5% H_3PO_4/3% CrO_3 solution which dissolves Al_2O_3 but not the metal[84].

Part 3. Measurement of Oxide Thickness by Spectrophotometry

To calculate growth stresses in oxides it is necessary to know the oxide thickness for each deflection of the anodised foil. A measure of oxide thickness can be obtained by multiplying the applied anodic voltage by an Å/V ratio obtained from the literature. However, Å/V ratios are sensitive functions of the current density[68] and electrolyte[85], and it was therefore necessary to measure the oxide thickness for the exact growth conditions used for stress measurement.

A number of methods are available for determining the thickness of anodic films, e.g. weight gain, coulometry, capacity, optical interference, resistance or spectrophotometry. None of these methods is absolute because auxiliary data must be available to supplement them; weight gain experiments require density measurements and assume the oxide's composition, capacity measurements require dielectric constants measured at the same frequency, etc.

The spectrophotometric method was chosen to measure the thickness of oxides on aluminium, zirconium and Zircaloy 2 because of its established precision[86] and convenience. The intensity of light reflected from the oxide on the metal was recorded over the ultra-violet range from 185-400 mμ wavelength on a Perkin-Elmer (model 450) spectrophotometer. Intensity versus wavelength plots were charted automatically. The wavelength

of each reflectivity minimum was noted and the film thickness read from a chart of wavelength of reflectivity minima versus thickness calibrated by determining the refractive index of alumina[86]. A similar procedure was followed with anodised zirconium and Zircaloy 2.

For the case of reflection from oxide on the metal the relationship between oxide thickness and wavelength of interference minima is given by[87]

$$2\eta t\cos\phi' + f(\lambda) = (m - \tfrac{1}{2})\lambda \qquad (5)$$

where η = refractive index of oxide.

ϕ' = angle of refraction for angle of incidence ϕ.

t = oxide film thickness.

$f(\lambda)$ = difference between phase changes at the air-oxide and oxide metal interfaces.

λ = wavelength.

m = integer, the order of interference.

For 45° angle of incidence used in this work $\cos\phi' = 0.95$.

Voltage/wavelength of minima plots may be transposed to oxide thickness/wavelength calibration charts from the relation

$$2\eta\,\Delta t = \lambda$$

obtained by assuming $f(\lambda)$ remains constant. Δt is the incremental thickness corresponding to ΔV the difference in voltage between two adjacent orders of reflection at constant wavelength λ.

The refractive indices of the oxides used to determine the calibration curves were taken as:

Anodic Al_2O_3	$\eta = 1.655$	at 5460Å[86]
Anodic ZrO_2	$\eta = 2.05$	at 5000Å[85]

The oxide film on Zircaloy 2 was assumed to have the same refractive index as anodic zirconia.

Part 4. Measurement of Electrical Properties of Oxides

a. Impedance Measurements

The resistance and capacity of anodic films were measured on a Wayne-Kerr A.C. bridge, generally at a fixed frequency of 1592 c/s. Readings were taken with the specimens (anodised flags 8 $cm.^2$ in area) immersed in the growth electrolyte or in a thinning solution at rest potential. A large cylindrical gauze cathode of stainless steel was used as the counter-electrode in the measurement cell. The impedance of the other various elements in the cell circuit (Figure 6) were negligible in

comparison with that of the oxide (Co & Ro) at the measurement frequency. The analogue circuit for the oxide was then assumed to be a resistance Ro and capacitance Co, in parallel.

b. Voltage Measurements

During anodising at constant current the rates of voltage rise were measured from the voltmeter on the current generator using a stop-watch or recorded automatically.

Rest potentials of metal electrodes were measured versus a standard calomel electrode using a high impedance valve voltmeter.

c. Measurement of Current Transients

The current transient during the anodic polarisation at constant voltage of a hydrated alumina film was measured with a Tektronix Cathode Ray Oscilloscope and recorded photographically (Figure 6a). The oscilloscope time-base was triggered by the applied transient, and the current was computed from the differential X-Y voltage across a known resistor.

SECTION IV

RESULTS

Part 1. Growth Stresses in Anodic Alumina

a. The Effect of Voltage

Figure 7 shows the tensile deflection of an aluminium foil anodised at 1.0 mA/cm.^{2}. At any given voltage (oxide thickness) the deflection is always more compressive when the growth field is applied than when no field exists across the oxide. The zero field deflection gives a measure of the growth stress in the oxide, the property which is of main interest in this investigation. The difference in deflection is caused by the applied voltage and is due wholly or partly to electrostatic pressure.

b. The Effect of Growth Rate on Stress

Stresses arising during the anodising of aluminium were studied as a function of the growth rate by varying the anodic growth current. The zero field deflections of aluminium foils anodised in pH = 9.0 ammonium borate (Figure 8) and pH = 6.0 ammonium citrate(Figure 9) vary with growth rate in accordance with previous observations[33]. Stress is a sensitive function of the growth rate; below a certain current density the average stress in the oxide is compressive but tensile at higher current densities (Figure 10). In most instances the deflection varied linearly with voltage (oxide thickness).

The influence of the growth rate on stress is also demonstrated by Figure 11b which shows the deflection of a duplex oxide, the first part of which was grown at a low current density and the second part at a faster rate. Growth at constant formation voltage to a low "leakage" current, invariably caused the zero field deflection to become compressive.

c. The Effect of pH on Stress

The pH of the growth electrolyte has a marked effect on the stresses in anodic alumina. Duplex films grown at the same total current density in ammonium citrate of either pH = 6 or 9, behave as shown in Figure 11a.

Quite different behaviour from that of the barrier films above is manifested (Figure 12) by aluminium anodised in pH = 10 ammonium citrate.

d. Location of Stress Gradients

Observing the deflection of anodised aluminium foils during the removal of the oxide by chemical thinning may reveal stress gradients in the specimen. The oxide thickness d was measured capacitatively and calculated from the expression:

$$C = \frac{kA}{4\pi d} \qquad (6)$$

where k = dielectric constant of the oxide.

C = capacity.

A = area of oxide.

Oxide films grown to 40V and less were considered to thin uniformly since 1/C versus time of thinning was very nearly linear (Figure 13). Thicker oxides lost their impedance quicker suggesting that dissolution was less uniform.

The deflection measurements show that the stresses do actually exist within the oxide, although even after prolonged immersion (Figures 14 and 15) the deflection (in the three specimens studied) remained compressive, suggesting that a compressively stressed layer still remains.

Growth at low current densities results in a layer ≈50-100Å thick at the outer oxide surface, in which there is a highly compressive stress (Figure 14).

Part 2. The Influence of Hydration Phenomena on Stress in Oxides

a. Immersion of Anodised Aluminium in Alkaline K_2CrO_4

An anodic alumina film rapidly lost its impedance during immersion for 3-4 hours in pH = 9.0 N/10 K_2CrO_4 (Figure 16a). After exposure to the atmosphere for ten days a portion of the reciprocal capacity was recovered. To throw some light on the cause of this reversible process the potential of a "bare" aluminium electrode was measured in similar solutions of K_2CrO_4 (Figure 16b). By using a "bare" surface it was intended that the metal should simply function as an electrical contact to measure the potential of a thin alumina film in the K_2CrO_4. The electrode potential was below $E_{HA} = 0$ during most of the immersion (Figure 16b), i.e. in the hydrogen evolution range.

Foils of aluminium anodised on one side to 100V deflected as shown in Figure 17 showing strong compressive stress in the oxide when immersed in N/10 K_2CrO_4. The greater the pH, the more compressive the stress was at any given time. Despite some oxide dissolution occurring simultaneously, log (deflection) versus log(time) plots (Figure 18), from which the exponent (n) in the equation $Z = kt^n$ may be deduced, are almost linear with gradients quite close to 0.5.

b. Hydration of Anodic Alumina by Boiling in Water

Boiling in water is a standard method for sealing porous alumina films. When barrier anodic alumina is treated in this way a hydrated oxide, containing boehmite is produced[16, 90, 91].

In boiling water, whose pH is adjusted to 8.0 by additions of NH_4OH, the barrier film is rapidly penetrated. The barrier voltage of a 50V anodic film was reduced to zero within two minutes. During this period the electrical resistance and reciprocal capacity also decreased (Figure 19), but from two minutes onwards they increased again. This effect is due to the formation of a corrosion product above the original anodic film[91].

Hydration in water at about $90^{o}C$ caused an anodised foil of aluminium to deflect compressively (Figure 20b)in a similar way to those immersed in alkaline K_2CrO_4.

c. The Effects of Cathodic Polarisation on Anodic Alumina

Cathodic polarisation of anodic alumina films in the hydrogen evolution region reduces the reciprocal capacity just as do immersion in K_2CrO_4 and hydration by boiling. Figure 23 shows 1/C versus time at -0.25 mA/cm.^{2}.

An anodic film which was thick enough to give large, measurable deflections required a high cathodic current density

≈7 mA/cm.^{2} for penetration. Despite some inconsistency due to hydrogen bubble evolution, anodised aluminium foils developed compressive stresses (Figure 24)like the hydrated specimens.

d. The Effects of Cathodic Polarisation on Anodic Zirconia

Cathodic polarisation of anodic zirconia films causes a decrease in the electrical resistance and reciprocal capacity, (Figure 23). The impedance is recovered on polarising at potentials anodic of E_{HA} = 0 or leaving open to the atmosphere. No change in deflection was observed when a zirconium foil bearing a 100V film was cathodised for several hours.

Part 3. The Removal of Hydrating Species from Oxides by Anodic Polarisation

a. The Effect of Anodic Polarisation on Alumina Previously Immersed in Alkaline K_2CrO_4

When an anodic current (1.0 mA/cm.^{2}) is passed through an alumina film which has been previously immersed in K_2CrO_4, the voltage rises steadily with time as, first, the effects of hydration are removed and then normal oxide growth prevails (Figure 25). From estimates of the rate of thinning in this

solution[92], the voltage at which the normal growth rate begins is about the value appropriate to the thickness of oxide remaining on the metal. Leaving a specimen in the atmosphere removed the first stage in the voltage/time behaviour.

b. The Effect of Anodic Polarisation on Alumina after Cathodic Polarisation

Alumina films cathodically polarised for various times show behaviour during reanodising slightly different from that shown by those immersed in K_2CrO_4. The time (and therefore anodic charge) necessary to restore the original growth voltage V_f was increased the greater the period of cathodic polarisation but the growth rate dV/dt above V_f (22 volts/min.) was higher than the normal growth rate (18 volt/min.) (Figure 26).

A 40 volt anodic film which was cathodically polarised for two hours at -0.25 mA/cm.^{2} showed a 7 µg./cm.^{2} weight gain even after two days drying. Thereafter this increase remained constant. After nine days the reciprocal capacity was 10%-20% greater but the resistance was only a quarter of that of the original 40 volt film.

Reanodising a portion of the above sample resulted in a complicated voltage/time curve (Figure 27). Growth began at the original formation voltage then proceeded at 30 volt/min. for

some time before increasing to 40 volt/min. Growth at the normal growth rate occurred at about 200 volts. The growth efficiencies before this stage was reached, were apparently 128%, followed by 143%, assuming that 28 volt/min. is the growth rate at 100% efficiency. (Calculated from Faraday's Law.)

c. The Dehydration of Alumina Hydrates Formed by Boiling Anodic Films in Water

The voltage/time response of hydrated films during reanodising depends on the time of hydration (Figure 28). Hydrates formed in less than two minutes boiling in pH = 8.0 water begin the second anodising at the voltage which corresponds to that part of the barrier film which remains unpenetrated (Figure 19). Initially dV/dt = 21 volt/min., a little higher than normal, but decreases after about two minutes.

The 50 volt film hydrated for two minutes is of interest because, before normal growth rate occurs at about 150 volts, there are two distinct periods of growth. These have apparent growth (dehydration) rates of 32-34 volts/min. and 45-48 volts/min. These are equivalent to growth efficiencies of 120-130% and 160-170%.

Anodic films boiled for fifteen minutes and longer show a third stage (Figure 28) similar to the first stage of 32-34 volts/min.

before dielectric breakdown accompanied by sparking occurs.

Similar three stage reanodising behaviour is obtained from the corrosion films formed by boiling "bare" aluminium in water for half an hour (Figure 30).

The voltage/time behaviour during reanodising is unaffected by the dissolving power of the growth electrolyte. After anodising in the presence of a hydrated oxide 1/C of the barrier layer is slightly lower at a given voltage than that of the normal barrier film (Figure 32).

d. The Effect of Anodic Polarisation on Zirconia after Cathodic Polarisation

Reanodising at constant current density expels the protons which have been introduced into zirconia films by cathodic polarisation. The barrier voltage rises at a rate which is inversely proportional to the concentration of protons in the oxide (Figure 31). At the voltage corresponding to the thickness of the anodic film, dV/dt decreases sharply for a short period before growth of new oxide occurs at the normal rate.

e. The Effect on Stress of Anodic Polarisation of Hydrated/ Protonated Oxides

Applying a constant anodic voltage to a hydrated alumina film (formed by boiling in water) causes a recovery of the reciprocal capacity and a large tensile deflection, (Figure 20a and b). Immediately this voltage was applied a large current surge occurred (Figure 21). A similar deflection resulted from the passage of an anodic current (1.0 mA/cm.^{2}) through a 150V alumina film which had previously been cathodically polarised; the large deflection (indicating compressive stress) caused by the cathodic treatment was almost entirely reversed by reanodising (Figure 24). From these results it appears that tension in alumina can arise through a form of electrical dehydration of the oxide.

Zirconia behaves in an entirely different way from alumina. Even prolonged boiling in water (fairly neutral pH) does not affect its impedance, suggesting that hydration, at 100°C and below, does not readily occur. Neither the introduction of protons during the cathodic evolution of hydrogen at the oxide surface, nor their removal by subsequent anodising, has any apparent effect on the deflection of anodised zirconium foils.

Part 4. Growth Stresses in Anodic Zirconia

a. The Effect of Growth Rate and Electrolyte on the Stresses in Zirconia

The deflection behaviour of zirconium foils during anodising is quite different from that of foils of aluminium. At lower voltages than 10-20 volts, small deflections indicative of tensile stresses occur, but as the oxide becomes thicker the overall stress becomes compressive - even at high current densities (Figure 36). It appears from Figure 37 that the stresses are dependent on the nature of the electrolyte. In fact the difference between deflections in KOH and those in H_2SO_4 are largely due to changes in the $\mathring{A}/V$ ratio with the varying growth conditions. The effect of growth rate and electrolyte are summarised in Figure 38; stress is not a function of the growth rate but is influenced slightly by the nature of the electrolyte.

b. Stresses Arising During Anodising of Zircaloy 2

The deflections of two foils of Zircaloy 2 anodised at 1.0 $mA/cm.^2$ in pH = 9 ammonium borate are shown in Figure 39. One specimen developed slightly lower stresses than pure zirconium but the other showed little difference. It appears that alloying of the metal has no significant effect on stresses developed during anodising.

Part 5. The Resistance of Anodic Zirconia Films

The resistance of anodic zirconia films is a function of the growth current density (Figure 41). At extremely low growth rates the resistance at a given oxide thickness (measured spectrophotometrically) decreases noticeably. This behaviour is similar to the effect of low growth rates on anodic alumina, where hydration of the outer oxide layers[69] was thought to be responsible.

Alloying zirconium to form Zircaloy 2 also affects the resistance of the anodic film (Figure 42). The resistance, at a given thickness of oxide grown on Zircaloy 2 is lower than that of an equivalent film produced on 99.8% pure zirconium.

Part 6. Measurement of Anodic Oxide Thickness and Current Efficiency

The intensity of light reflected from anodised metal surfaces shows interference minima which occur at particular wavelengths, depending on the oxide thickness. Typical traces recorded on the spectrophotometer from anodised aluminium, zirconium, and Zircaloy 2 are shown in Figure 43. The thickness of each anodic film was determined from calibration charts (Figures 44 and 45).

Current efficiencies calculated from the growth rate, dV/dt (Figures 46 and 47) and the $\text{Å}/\text{V}$ ratio (see Section III, Part 2) are summarised in Table 3. The efficiency of anodising

aluminium and zirconium increases with current density, reaching a limiting value which is less than 100%.

The unitary growth ($\frac{1}{i} \cdot \frac{dV}{dt}$) of alumina, an indication of the current efficiency, varies with the pH of the electrolyte (Figure 48). In ammonium citrate in the range from pH = 2.0 to pH = 9.0 the growth rate increases but above pH = 9.0, where dissolution of the oxide becomes appreciable[93], dV/dt decreases sharply. Similar behaviour in the alkaline region is shown in ammonium borate solution. In the acid region, growth in borate appears to be prevented possibly owing to the poor buffering qualities of the electrolyte. Polarisation curves (Figure 49) of anodised aluminium electrodes in alkaline Na_2SO_4 solutions show an anodic saturation current which increases exponentially with pH in a similar manner to the corrosion rate of aluminium (Figure 50).

Part 7: Field Induced Stresses During Anodising

A deflection of an anodised foil corresponding to compression in the oxide accompanies the application of an anodic electric field across the oxide. Figures 51 and 56 show how this difference in deflection varies with applied voltage during the anodising of zirconium and aluminium respectively. Three stages are shown, the phenomenon appears to show hysteresis.

As the film grows at constant current density the deflection increases linearly with voltage (stage A) until the formation voltage V_f is attained. Voltage V_f is maintained constant for about an hour until the current falls to a low "leakage" value (<0.1 mA/cm.^{2}) at which growth proceeds only very slowly (stage B). During this period the oxide thickness increases by about 10-20% and the deflection decreases with the logarithm of the current (Figure 54). Decreasing the voltage from V_f to zero causes the deflection to follow a lower, non-linear path (stage C).

The total stress acting at the surface of a dielectric which is subject to a normal electric field comprises two components[94]. Within the body of the dielectric a pressure p is caused by the alignment of atomic dipoles with the applied field.

$$p = \frac{k_o (k - 1) E^2}{2} \qquad (7)$$

where $k_o = \left(\frac{10^{-9}}{36\pi}\right)$ = permittivity of free space.
(meters^{-2} sec.$^{-2}$) MKS units.

k = dielectric constant of oxide.

E = applied field = voltage/thickness of dielectric.

In addition to this uniform pressure acting throughout the dielectric there is another stress, F_s, due to the transition layers which exists at the surface of a dielectric, where the

polarisation charges reside (Figure 55). During anodising the space charge boundary layers, being opposite in sign, attract each other and compress the oxide normal to its surface.

$$F_s = \frac{k_o (k - 1)^2 E^2}{2} \qquad (8)$$

The total stress on the surface is the sum of the surface stress F_s and the pressure, p, in the bulk of the oxide[94].

$$F_T = \frac{k_o k (k - 1) E^2}{2} \qquad (9)$$

Values of this electrostatic stress calculated by the above equation are shown in Table 4.

The field induced deflection during decreasing voltage on films already grown to various formation voltages is plotted versus the square of the applied voltage (Figures 52 and 57). Over a large range of voltage the deflection Z varies linearly with the square of the voltage. Around V_f, however, the deflection increases and is related to a higher power of the voltage.

SECTION V

DISCUSSION OF RESULTS

Introduction to Discussion

This discussion considers the origin of stresses in anodic alumina and zirconia with particular reference, in the case of alumina, to the effects of hydration and dehydration. A model for the dehydration process has been developed which suggests that this occurs by a chemical reaction between the hydrated oxide and aluminium ions. By applying an anodic current to a hydrated oxide, the water content can be progressively reduced. The general form of the reaction is as follows:

$$5Al(OH)_3 + Al \rightarrow 3Al_2O(OH)_4 + 3H^+ + 3e^-$$

$$(Al_2O_3.3H_2O) \qquad (Al_2O_3.2H_2O)$$

$$2Al_2O(OH)_4 + Al \rightarrow 5AlO(OH) + 3H^+ + 3e^-$$

$$(Al_2O_3.H_2O)$$

$$3AlO(OH) + Al \rightarrow 2Al_2O_3 + 3H^+ + 3e^-$$

This process can be described as a dehydration since water (or hydroxyl ions) are eliminated from the oxide. However, it does not involve the removal of water but is strictly a deprotonation, for in each step one aluminium ion displaces three protons from a compound containing hydrogen and oxygen.

Each of the intermediate compounds is chemically equivalent to a hydrated alumina.

In the following discussion the effects observed in this work (and other work in the field) are considered in terms of hydration and the dehydration model outlined above.

Part 1. Growth Stresses in Anodic Alumina

a. Possible Causes of Tensile Stresses

An important feature of anodic alumina is that it can grow in a state of tension - despite having a volume ratio greater than unity. In this condition the oxide, if grown on a rigid substrate, is stretched parallel to the surface so that it covers the area of contact with the latter. This development of tensile stresses must be dependent in some way on the mechanism of growth. Several properties of anodic oxidation could be responsible for a decrease in the volume or the area of contact of the oxide.

i. Cationic Conduction: Sufficient aluminium may pass out through the oxide during growth, relieving the volume constraint and possibly resulting in an unstressed oxide or one with tensile stresses.

ii. Electrostatic Effect: If the oxide does form stress free during anodic growth the removal of the electric field with

its highly compressive stress may result in tension.

iii. Temperature: The passage of current through the oxide may cause the temperature to rise. When growth is stopped the oxide will shrink due to cooling.

iv. Deprotonation: The oxide may form first as a hydrated intermediate which is subsequently deprotonated by the anodic field.

Preliminary evidence suggests that mechanisms (ii) and (iii) are unlikely to be significant. Stresses are tensile even during growth (Figure 7) so there must be some cause of tension other than temperature or electrostatic effects. In anodic zirconia, growth stresses are highly compressive and independent of the current density (Figure 38). It seems reasonable to assume that since stress in zirconia is not dependent on either of these two factors (both of which would vary with current density) even up to 6.0 mA/cm.^{2}, they can also be discounted with regard to alumina grown under similar conditions.

Cation transport numbers measured experimentally during the growth of anodic alumina[61] are greater than that calculated to be necessary for zero volume change[56]. In the high temperature oxidation of copper, which occurs by cation movement only[38], the production of vacancies has been cited as a cause of tensile stress in the underlying metal layers[29]. Dislocations and loops formed near the surface of initially unstrained single

crystals of zinc and cadmium have been seen after several weeks exposure to the air[80]. This was attributed to oxide growth by metal ion diffusion which caused the injection of cation vacancies into the metal. From these observations it appears that cation migration can cause tension in the metal but as yet no mechanism has been put forward to explain how cation conduction could lead to tensile stresses which are actually in the oxide, not in the metal. In the case of anodic alumina films showing an overall tensile stress (Figure 14), the stress gradients, revealed by chemical thinning, suggest that the oxide consists of two layers, the inner part being compressive while the outer one is tensile. As far as could be ascertained, there was no tensile stress in the oxide adjacent to the metal. Thus, the source of tension is located at, or near, the outer growth interface, a favourable position for dehydration to occur.

The possibility of hydration phenomena affecting stresses in alumina is not unlikely since the properties of barrier anodic films are extremely sensitive to water. They absorb water vapour to an extent depending on relative humidity[95], the electrical resistance and breakdown voltage decrease with increasing relative humidity[51]. One tenth of the sorption is a rapid process occupying a few minutes, the remainder, a slow process, requires a day for completion. A hysteresis is shown

by the slow process but not by the initial sorption. Although barrier films are usually regarded as being non-porous, it has been suggested that they are perforated by numerous small holes which can be penetrated by water[96]. Physical adsorption of water in these microfissures would not show hysteresis. The hysteresis associated with the second sorption may be due to chemical combination with water to form a hydrate since the oxide layer in contact with the electrolyte during anodising has been reported to be the monohydrate $Al_2O_3.H_2O$[97]. Investigations into anodic films by deuterium[98] or tritium[99] marker techniques and impedance measurements[69, 70-72] suggest that the outer oxide layer is hydrated.

In view of the acknowledged susceptibility of anodic alumina to water and the fact that aluminium forms hydrated oxides when immersed in water below 80°C[100], it is perhaps remarkable that anodic films are mainly anhydrous[68] despite formation in aqueous environments. To explain this, the following scheme for the anodising of aluminium[101, 102] implies that a dehydration process occurs.

$$Al + 3OH^- \rightarrow Al(OH)_3 + 3e^-$$

$$Al(OH)_3 \rightarrow AlO(OH) \rightarrow Al_2O_3 \text{ (dehydration)}$$

The evidence in the literature suggests that hydration and dehydration phenomena are closely involved in the anodising mechanism. Hence, the following sections consider the effect on stress of (a) hydration and (b) subsequent dehydration by the passage of an anodic current through the hydrated oxide.

b. The Effect of Hydration on Stress

The entry of water into an oxide would be expected to cause expansion and hence compressive stresses. An immediate example of compressive stresses associated with hydration was found by oxide thinning which revealed a stress gradient in an oxide grown at low current density (Figure 14). The thickness, 70-80 Å, of this region of compressive stress coincides with that of the hydrated layer which has been reported to be present after growth at low current density[69]. It is thought that the low anodic field permits protons to diffuse into the oxide and set up an electrostatic charge which attracts hydroxyl ions, producing a hydrated layer about 50Å thick. The formation of this layer occurs only in aqueous electrolytes and at low current efficiences, where the evolution of oxygen may also favour oxide hydration.

$$4OH^- = 2H_2O + O_2 + 4e^-$$

During immersion in alkaline K_2CrO_4 solutions the electrical resistance and reciprocal capacitance of alumina films decrease rapidly. Some dissolution of the oxide occurs during the period shown (Figure 16a) but this is less than 10% when measured optically[92]. A large portion of the impedance decrease is recovered on leaving the specimen in air for one or two days. This reversible process has been attributed to the uptake of physically held water. Hydration rates are known to increase with pH[91, 103], so higher alkalinity of the chromate solutions should cause greater compressive stresses in a given time. As expected, aluminium foils bearing 100 volt anodic films deflected in the direction indicating compressive stresses in the oxide, when immersed in N/10 K_2CrO_4. The deflections were greater the more alkaline the solution, and approximately obeyed a parabolic relation with time, suggesting that a diffusion mechanism was operative.

Anodic alumina can be hydrated by boiling in water; this is the basis of the technique used for sealing porous films. Water reacts with the porous oxide forming boehmite[90] which has a greater volume, blocks the ends of the pores and imparts added corrosion resistance. Since barrier anodic films can also be hydrated in this way, the boiling treatment was chosen as a standard method of hydration.

The hydration process consists of at least two parts[91],

(i) the penetration of the initial barrier layer and (ii) the formation of a corrosion product on top of it. This is also suggested by the impedance changes (Figure 19) in which conductivity and capacity increase during the first two minutes and then begin to decrease as though the corrosion product exerts a sealing effect. During the penetration of a 40 volt barrier film a considerable volume increase occurs; 1Å of barrier layer produces 2.5Å of hydrate before the corrosion product begins to form[91]. Assuming constant substrate area this implies that hydration causes 150% increase in volume.

During hydration the amorphous nature of the anodic film disappeared and the hydrated oxide, consisting of an irregular array of minute crystals, showed a pronounced α-monohydrate (boehmite) structure[91], which disappeared after prolonged hydration.

The presence of boehmite in the hydrated film has been shown also by X-ray measurements[105] but gravimetric experiments on the oxide indicated that as much as 32 w/o water was present[105] - considerably in excess of that in the monohydrate. It was concluded that the hydrate also contained loosely bound water which was not combined as boehmite.

Not surprisingly, the large volume change occurring during hydration, causes a foil of aluminium bearing a 150 volt film to

develop large compressive stresses during immersion in water at 90°C (Figure 20b).

c. The Dehydration of Hydrated Alumina by Anodic Polarisation and its Effect on Stress

Hydration causes compressive stresses by increasing the volume of the oxide. In principle, therefore, tensile stresses could arise through the shrinkage due to dehydration.

Applying a constant anodic voltage to a film hydrated by boiling in water, causes a large current surge (Figure 21), and an increase in the reciprocal capacity (Figure 20a). During the passage of this current the stress becomes tensile (Figure 20b), the deflection being about equal but opposite to that due to hydration. These observations suggest that anodic polarisation can cause tensile stress by dehydrating alumina, although the mechanism by which this is accomplished is not clear.

It was decided to examine the dehydration mechanism by measuring the rate of production of barrier oxide at constant current density. Owing to the presence of the overlying hydrated layer, it is necessary to use the indirect method of measuring the barrier thickness and to compute the oxide weight from its density. The reciprocal capacity of the oxide produced

in the hydrate's presence indicates that it is thinner than the normal barrier film. Recently it has been suggested[112] that growth of fresh oxide in the interstices of the hydrate, results in a more compact oxide containing less microfissures than the normal barrier oxide whose density (3.17 g/cm.^{3}), is considerably less than the theoretical value for alumina (3.66 g/cm.^{3})[56]. Thus three assumptions can be made to attempt to assess the quantity of barrier oxide by calculating growth rates from:

a. Voltage[104] - assuming the Å/V ratio and density of the normal barrier oxide.

b. 1/C - assuming the dielectric constant and density of the normal oxide.

c. 1/C - assuming the theoretical density 3.66 and the normal dielectric constant.

Since the apparent growth efficiencies derived from assumption (c) are similar to those obtained from assumption (a) (Table 8) it seems quite feasible that the change in 1/C results from a density increase. On the basis of this consistency it has been assumed that the dehydration growth rate is better expressed by dV/dt than by d(1/C)/dt. The true rate of formation may lie between the values obtained from (a) and (c) and from (b); this can only be resolved by detailed investigation to determine the density, dielectric constant and composition of

the new oxide.

Nevertheless, it is important to note that the efficiency in the second stage of dehydration (Table 8), even according to the conservative estimate made from assumption (c), is far greater than 100%. Reanodisation of hydrated alumina definitely produces more barrier oxide for the passage of a given ionic charge than would be expected from Faradaic principles. A theory for this anodisation process must account for three periods in which growth efficiencies are at least 96-102%:127-136%: 96-102%, but in all probability are as high as 121-128%: 160-170%: 121-128%.

Faraday's law is not violated if the anodisation involves the dehydration of oxide which is already present. The normal growth reaction occurring at 100% efficiency requires six Faradays of charge to produce 1 mole of oxide.

$$2Al + 3H_2O = Al_2O_3 + 6H^+ + 6e^- \qquad \text{(1 molecule/6 electrons)}$$

If the hydrated oxide were pure boehmite, the Al^{3+} ions moving through the barrier portion of the oxide would react with the hydrated layer producing more oxide and protons. This can be represented in various ways but for convenience is written:

$$Al + 3AlO(OH) = 2Al_2O_3 + 3H^+ + 3e^- \quad \text{(2 molecules/3 electrons)}$$

This reaction produces four times as much anhydrous oxide, for the passage of a given anodic charge, as the normal reaction of metal with water. Hence, the dehydration rate could in principle be equal to an apparent growth efficiency of 400%, without contradiction of Faraday's Law. It will be seen (Table 5) that the apparent growth rate is dependent on the state of hydration of the alumina. The dehydration rates shown (Figure 28) will be considered in detail since they appear to be limiting cases, suggesting that hydrates of constant composition are present. After about 15 minutes boiling the apparent growth (dehydration) rates attain the fixed values listed below.

	dV/dt (volt/min.)	Apparent Efficiency
Stage 1	34-36	121-128%
Stage 2	45-48	160-171%
Stage 3	34-36	121-128%
	(28 volt/min. at 1.0 mA/cm.^{2} = 100% efficiency)	

After stage 3 is completed dV/dt decreases and breakdown of the oxide occurs. The dehydration rates (above), which have anomalously high apparent growth efficiencies, can be explained by considering (a) the degree of hydration of the oxide, and

(b) the relative mobility of anions and cations during anodic polarisation.

The three stage dehydration suggests that three discrete layers of hydrates comprise the product of boiling in water. Exactly the same voltage/time behaviour is obtained when "bare" aluminium (etched 10 minutes in 10w/o KOH) is boiled in water for 30 minutes and then re-anodised (Figure 30). It is well established that the corrosion product of aluminium in water at 80°C and below consists of three layers of hydrated oxides. Hart[100] has shown by electron diffraction that initially an amorphous layer is formed and is subsequently overlaid first by boehmite, AlO(OH), and then by bayerite, $Al_2O_3.3H_2O$. After prolonged corrosion the oxide still consisted of three separate layers; the hydrates did not transform during growth. At temperatures more than 200°C the oxides of aluminium may even consist of four layers of oxides[107]. The initial amorphous layer is most probably the hydroxide $Al(OH)_3$. This means that the water content of the oxide does not increase evenly with distance away from the metal, as would normally be expected, because the hydroxide has the same molecular formula as the trihydrate, i.e. $2Al(OH)_3 \equiv Al_2O_3.3H_2O$. It is, however, possible for the monohydrate, AlO(OH), to be sandwiched between two layers of trihydrate because $Al(OH)_3$ has a less negative free energy of formation than corundum Al_2O_3 or any of the hydrates of

alumina[93].

From this evidence it is reasonable to assume that the oxide consists of three layers of different hydrates, the second layer containing some boehmite as shown from previous work on the hydration of anodic films[91, 106]. The innermost and the outer layer possibly have the same composition, although different structures, since they produce the same dehydration rates.

The degree of hydration of this complex hydrate of alumina can be calculated from density changes caused by water[91] and from thermogravimetric data[106]. By taking density values for the anodic oxide and two hydrates from the literature it is found that the density of a hydrate decreases linearly with the fraction of water (Figure 33). During the formation of the first layer of hydrate the thickness increased by 150%[91]; the appropriate density decrease implies that the anodic film is converted to $Al_2O_3.4.5H_2O$. The second hydrated layer contains boehmite and water but the proportions are not known. However, these can be deduced from gravimetric measurements made on a hydrated film produced by boiling in water for an hour[16]. The water content was 32 w/o, i.e. $\simeq Al_2O_3.3H_2O$ is the average composition of the three layer oxide. To determine the water content of the layer containing boehmite one must refer to the voltage/time graph (Figure 29). The extent of each stage of

dehydration is determined by the thickness of the hydrated layer. During stage 1 the total amount of anhydrous oxide produced is about 70 volts. This is equal to the amount of Al_2O_3 originally present in the first layer plus the Al_2O_3 that would be grown at 100% efficiency by the anodic current. Hence,

Al_2O_3 in hydrated layer = Anhydrous oxide produced by dehydration - Oxide produced by anodic current

$$= V_1 - (28 \text{ v/m} \times t_1)$$

From Figure 29 one can calculate the relative proportions of Al_2O_3 that were originally present in each layer of the hydrate. The oxide consists approximately of 10 parts $Al_2O_3.4.5H_2O$/ 49 parts $Al_2O_3.xH_2O$/ 37 parts $Al_2O_3.4.5H_2O$. x, the amount of water in the second layer, is 1.6 calculated from the average composition of the total hydrate. It is seen from Table 5 that the following dehydration reactions will produce the apparent efficiencies seen in stages 1 and 3, and stage 2. Although these reactions involve Al^{3+} ions reacting with the hydrate they are written in the equivalent form below to emphasise that electrons and therefore current are involved.

Stages 1 and 3

$$8Al + Al_2O_3 + 12H_2O = 5Al_2O_3 + 24H^+ + 24e^- \quad (125\%)$$

Stage 2

$$10Al + 3Al_2O_3 + 15H_2O = 8Al_2O_3 + 30H^+ + 30e^- \quad (160\%)$$

These equations require more water than is actually present in the oxide. The 7.5 molecules of water to balance the first expression above, are brought in from the electrolyte as hydroxyl or oxygen ions which move inwards during anodising (Figure 34). The reaction consists of two processes occurring simultaneously (a) a cationic deprotonation which can result in anomalously high rates of formation of anhydrous oxide by consuming the hydrate, and (b) anion migration which produces growth at the metal/oxide interface at 100% efficiency. It has been assumed that oxide produced by anionic transport grows at 100% efficiency because the dehydration rates are independent of the growth electrolyte. The hydrated oxide behaves as if it were the electrolyte so metal dissolution and oxygen evolution are negligible.

In stages 1 and 3 cationic dehydration is produced by Al^{3+} ions reacting with the hydrate $Al_2O_3.4.5H_2O$.

$$3Al^{3+} + Al_2O_3.4.5H_2O = 2.5Al_2O_3 + 9H^+$$

alternatively expressed as

$$3Al + Al_2O_3.4.5H_2O = 2.5Al_2O_3 + 9H^+ + 9e^-$$

The anionic growth occurs by uptake of water (as OH^- or O^{--})

$$5Al + 7.5H_2O = 2.5Al_2O_3 + 15H^+ + 15e^-$$

Similarly the relative ionic mobility influences the dehydration of the second hydrated layer which contains boehmite and has an average composition of $Al_2O_3.1.6H_2O$.

Cationic $\quad 3.2Al + 3Al_2O_3.1.6H_2O = 4.6Al_2O_3 + 9.6H^+ + 9.6e^-$

Anionic $\quad 6.8Al + 10.2H_2O = 3.4Al_2O_3 + 20.4H^+ + 20.4e^-$

Ionic transport numbers can be calculated from the amount of water taken up in the anionic process as OH^- or O^{--} ions.

$$\text{Transport number of aluminium} = \frac{\text{number of } H_2O \text{ molecules in the hydrate}}{\text{number of } H_2O \text{ molecules in the total reaction}}$$

The cation transport fraction in stages 1 and 3 is 0.35 - 0.49 and in stage 2 is 0.32 - 0.37. These figures are lower than the transport numbers measured by Davies et al. (Table 1). They represent the lowest values that the cationic transport number deduced by this method can have. Any appreciable electronic current during reanodisation will require greater metal conduction to achieve the same apparent efficiency. Also if the roughness factor, which was assumed to be unity in calculating the dV/dt

value at 100% efficiency is actually greater than one, the real current density will be reduced. It follows that the apparent efficiency and therefore the cation transport fraction will be greater. The calculated amount of metal conduction is extremely sensitive to the roughness factor. Values are given (Table 6) determined using typical roughness factors quoted in the literature. It is seen that during reanodisation aluminium's transport number is not less than 0.32 and unlikely to be greater than 0.82. Assuming a probable roughness factor such as 1.07 gives a value of 0.40-0.53 in the range of data obtained experimentally[61].

The deprotonation differs from electro-osmosis in that additional oxide is produced during the former process. This was shown by weight gain of an anodic film which formed a corrosion oxide above it during cathodic polarisation. The constant total weight of oxide measured after several days was equivalent to that of a 70 volt anodic film. When the reanodisation of this oxide was completed (Figure 27) the oxide was about 220 volts, i.e. an increase of ≈200% in thickness occurred during deprotonation.

In the dehydration by cation diffusion it is not immediately obvious that a volume reduction results from the process, since more oxide is produced in the space occupied by the hydrate. However, an overall shrinkage does occur and this increases with the water content of the hydrate. Since the density of alumina

decreases linearly with water content (Figure 33) the volume of any hydrate can be found and hence the volume reduction involved in deprotonating it. The volume strains ($\frac{\Delta V}{V}$) caused by deprotonating a range of hydrates increased with the amount of water originally present in the oxide (Figure 35). A volume reduction of 0.02 is involved in the deprotonation of the hydroxide $Al(OH)_3$ which is equivalent to the trihydrate.

$$2Al + Al_2O_3.3H_2O \quad (2Al(OH)_3) \quad = \quad 2Al_2O_3 + 6H^+ + 6e^-$$

66 volumes → 64 volumes

From the volume change it is possible to calculate the tensile stress arising from this process by Mortons[108] analysis. The tensile stress, P, arising in the oxide acting parallel to its surface is

$$P = \frac{E}{3(1 - \nu)} \left(\frac{\Delta V}{V} \right) \qquad (10)$$

where E = Young's modulus of anodic alumina = 4.2×10^5 kg/cm.^{2} [45]

ν = Poisson's ratio of the oxide assumed to be 0.2.

Assuming elastic deformation of the oxide, the stress would be of the order of 4,000 kg/cm.^{2} if the intermediate hydrate were the hydroxide. These calculations show, despite the unknown identity of the intermediate, that cation induced deprotonation

causes sufficient strain to explain the magnitude of the tensile stresses in anodic alumina.

d. A Mechanism to Explain Stresses in Anodic Alumina

The occurrence of tensile stresses in alumina can be explained on the basis of the dehydration mechanism described above. It is necessary to postulate the formation of a hydrated oxide at the oxide/electrolyte interface. Being under no constraint at an outside surface the hydrate should be stress-free. Al^{3+} ions from the metal react with the hydrate, producing anhydrous oxide and protons, e.g.

$$Al^{3+} + Al(OH)_3 = Al_2O_3 + 3H^+$$

An overall volume reduction occurs. If the oxide forms on a rigid substrate it is prevented by adhesive forces from reducing its area of contact and a biaxial tension is imposed upon it.

The formation of a hydrated intermediate phase during the anodising of aluminium is very probable. A scheme outlined by Lonergan[101] suggested that the hydroxide and boehmite were formed during growth. The cation induced deprotonation explains how anhydrous oxide can form in an aqueous environment in which, in the absence of the anodic field, the hydrated oxide is the

natural corrosion product.

Oxide thinning revealed a hydrated layer approximately 70Å thick in an oxide grown at low current density but nothing was found at higher growth rates. This implies that the intermediate hydrated layer is quite thin and probably forms as an adsorbed phase precipitated at the oxide surface. Pourbaix states[93] "the dissolution of aluminium is always accompanied by the formation of a precipitate $Al(OH)_3$". The precipitation of $Al(OH)_3$ formed by the passage of Al^{3+} ions into solution, will depend on the local pH which controls saturation. At neutral pH's the precipitate will form and be converted by further Al^{3+} ions into the anhydrous anodic film. In alkaline electrolytes (pH > 9.0) the $Al(OH)_3$ will not form as readily and a porous oxide, similar to those formed in acids, should result. The formation of a barrier or a porous film depends on the balance between precipitation and dehydration which form oxide, and degradation of the oxide by hydration and dissolution. The dominant hydrating species may cause dissolution in the following way.

$$MeO \xrightarrow{2H^+} Me^{++} + H_2O \qquad \text{acid}$$

$$MeO \xrightarrow{2OH^-} MeO_2^{--} + H_2O \qquad \text{alkaline}$$

The pH of the growth electrolyte has an important influence on the structure and the stresses of anodic alumina. In solutions

of pH > 9.0 alumina dissolves rapidly. A foil of aluminium anodised in pH = 10 electrolyte (Figure 12) deflected in a similar way to those bearing porous films formed in dilute H_2SO_4[45]. The extremely compressive stresses developed after an initial tensile layer was formed are probably caused by ingress of electrolyte into the pores and possibly also by hydroxylation of the porous oxide.

Previous workers have suggested that tensile stresses were caused by (a) deprotonation[36], (b) cation conduction[33]. The mechanism of dehydration discussed above combines both these principles; tensile stresses arise because of the volume reduction caused by deprotonation which, in turn, cannot occur without cation conduction. Overall stress in the oxide depends on (a) the relative thicknesses of the compressive/tensile layers and (b) the magnitude of the stresses. Increased overall tension would result from (a) increased metal migration or (b) increased water removal. The relative thickness of the tensile layer will depend on the cationic transport number. From calculations based on dehydration rates at different current densities (Table 7) it appears that the transport number of Al^{3+} is not a function of growth rate.

The voltage attained during the passage of a given anodic charge was lower at 0.1 mA/cm.^{2} than at 1.0 mA/cm.^{2}. However, by growing an oxide to a given voltage at 1.0 mA/cm.^{2} and switching immediately to the lower growth rate, it was noticed that the

voltage dropped, giving an estimate of the change in Å/V ratio with current density. Values of anhydrous oxide per charge passed V_1/C_1 and $(V_2-V_1)/C_2$ when corrected for the change in Å/V were the same.

Faster growth rates have been shown to increase the uptake of silicon, carbon and boron from the electrolytes during the growth of anodic zirconia[109]. Increased water trapping (and subsequent removal) will cause increased tension at high growth rates. At extremely low growth rates dehydration becomes less effective and the outer oxide layers become heavily hydrated[69]. Hence the outer oxide can be tensile at high growth rates and compressive at leakage currents (Figure 14).

The increased tension due to anodising in higher pH's (Figure 11a)is caused by increased uptake of hydroxyl ions at greater pH's. Greater tension results from the increased volume change on deprotonation.

It has been suggested from electron microscopy of separated anodic films that anion migration produces crystallites of γ-alumina at the oxide/metal interface and that metal migration gives rise to amorphous oxide[58]. This may occur because the oxygen ions have the metal lattice to form a basis for the oxide lattice, whereas the amorphous structure is produced via cation migration into an adsorbed array[110]. It is interesting to compare these findings with the observations on aluminium oxides

formed at high temperatures[111]. Again it is postulated that crystallites are formed by anion migration and penetrate into the metal a little way before growing laterally. The amorphous oxide at the outside formed by metal migration.

The average aluminium transport number according to Davies is 0.56 during anodic growth in a non-dissolving electrolyte[61]. If this figure is correct, the volume of oxide formed by anion migration should be less than that of the outgoing cations. However, chemical thinning of anodic films consistently revealed that a compressive stress remained after prolonged immersion in the solvent. It has been reported that the crystalline anodic oxide is only slowly soluble in acid solution used[113], so it is quite possible that the compressive stress was located in undissolved crystallites. If the cation vacancy excess is lost to the bulk of the metal it is possible that anion migration will produce an inner crystalline layer in compression. Cation migration will result in an outer amorphous oxide in tension, resulting from the deprotonation of a hydrate. It appears that the anodic oxide formed at high growth rates should consist of two layers, (a) an inner, crystalline layer in compression and (b) an outer, amorphous layer in tension.

At low growth rates entry of protons into the oxide after it has formed promotes hydration giving rise to compressive stresses, in the outer layers. The change from compressive

to tensile stresses with increasing growth rate may be due also to increased water trapping in the intermediate phase which will result in greater tension after the deprotonation of the higher hydrate.

Part 2. The Effect of Cathodically Polarising Anodic Oxides

Cathodic polarisation causes a decrease in the electrical resistance of anodic oxide films. This has been attributed to the presence of hydrogen, which acts as a donor impurity in the semiconducting oxide, making n-type oxides highly conducting while increasing the resistance of p-type oxides[20, 114]. Hydrogen is thought to be introduced by the entry of protons whose charge is neutralised by electrons removed from the metal substrate. High Faradaic capacities can be induced by protons entering oxides of metals with variable valancies[115] such as titania.

$$MO + H^+ + e^- \rightleftharpoons MOH$$

From this evidence and from cathodic reduction of oxides[116] it appears that cathodic polarisation of oxides causes the entry solely of protons. However, it has been suggested[106] that when aluminium (bearing barrier films) is made the cathode in aqueous electrolytes (or in fuming H_2SO_4), water (or H_2SO_4) enters the oxide by an electro-osmotic mechanism.

The present work suggests that cathodic polarisation of alumina may well involve electro-osmotic hydration phenomena, whereas anodic zirconia is simply protonated.

a. Proton Gradients in Anodic Zirconia

The hydrogen content of an oxide can be determined from the anodic charge necessary to restore the original impedance. This has been shown[117] to be:

$$Q = ixt = CV + Q_H \qquad (11)$$

CV the capacitor charge is negligible, hence the charge to expell n protons (electronic charge e) is Q_H.

$$Q_H = ixt = ne \qquad (12)$$

If i, the anodic current, is kept constant the distribution of protons in the oxide can be calculated from the rate of voltage rise dV/dt. Differentiating the above expression gives:

$$\frac{dn}{dt} = \left(\frac{i}{e}\right)$$

Now

$$\frac{dn}{dV} = \frac{dn}{dt} \Big/ \frac{dV}{dt}$$

The oxide thickness, b, is linearly related to the voltage, V, hence

$$dV = \left(\frac{1}{\rho_{A/V}}\right) db$$

Thus the number of protons in each incremental layer of oxide of unit area is

$$\frac{dn}{db} = \frac{i}{e\left(\frac{dV}{dt}\right)\left(\frac{\rho_A}{V}\right)} \qquad (13)$$

From the distribution obtained in this way it is seen (Figure 31) that the proton concentration (perhaps the saturation amount) is greatest at the oxide/electrolyte interface, decreasing towards the metal. The oxide layer adjacent to the metal is almost free of protons. The maximum proton concentration, about 4 protons/zirconia molecule, is considerably higher (by two orders of magnitude) than those measured by Isaacs and Wanklyn[117] but is of the same order as those calculated from the anodic charge from zirconia at potentials slightly greater than $E_{HA} = 0$ but below oxygen evolution potentials, approximately 1 proton/oxide molecule[118].

The curious downward inflection in the v/t curve for re-anodised zirconia immediately the original formation voltage had been reached is consistent with the deprotonation of a corrosion film which could have formed above the original anodic film. After a short voltage increase the normal growth rate during anodising resumed.

b. Anodic Alumina - Electro-osmosis or Protonation?

The following information suggests that cathodic polarisation of alumina films on aluminium may involve hydration and not simply protonation as observed with anodic films on zirconium.

Radiotracer techniques have been used by Schwabe[106] to study the movement of water and sulphuric acid in Al_2O_3 and $ZnSO_4$ barrier layers. A barrier oxide was grown in a tritiated borate solution to a low leakage current at which the radioactive species could enter. After transfer of the specimen to an inactive solution and allowing equilibrium to be reached, an applied anodic voltage produced an increase in the tritium activity of the inactive electrolyte (Figure 22). To show that not only protons were ejected, a similar experiment was performed using sulphuric acid tagged with S^{35}. Anodic polarisation again caused an increase in activity. On the basis of the ejection of both protons and anions it was concluded that anodic dehydration occurred by electro-osmosis, cathodic polarisation was alleged to return the water.

Although it is known that increasing pH and temperature[91] assist hydration, and the electrolyte anion can exert an effect[91], the mechanism by which water entry occurs is not well understood. Several theories have been put forward.

i. Advanced Proton Theory. Hoar and Wood[90] postulated that the sealing of anodic films by hydration occurs by the entry of protons

into the oxide which set up a high electrostatic charge and attract hydroxyl ions in to form a hydrate.

ii. Ion Exchange. Heine and Pryor[70] consider that hydroxyls are substituted for O^{--} ions on the oxide lattice.

iii. Electro-osmosis. This involves the movement of liquid through a capillary (or porous membrane) across the ends of which an electric field, E, is applied. In the liquid adjacent to the solid surface there is a diffuse layer, with zeta potential, ζ. The electric field acts on this layer with a force qE where q is the charge in the layer. The direction in which the liquid is drawn depends on the sign of the dominant ion and of the field.

The approximately parabolic relationship between deflection and time of immersion in K_2CrO_4 suggests that the movement of the entrant species is a diffusion process under a constant activity difference, which is controlled by the electrolyte pH. Electrokinetic measurements on corundum[119] show that OH^- and H^+ are the potential determining ions in the electrical double layer, so greater OH^- activity would be expected to increase the rate of OH^- diffusion in the oxide. It is tempting to conclude that, in the absence of applied polarisation hydration occurs, which involves hydroxylation as the slowest and therefore rate-controlling step in the process.

However, the rest potential of a "bare" aluminium electrode

which should be covered by an oxide of about 50Å thickness, was increasingly cathodic of the hydrogen evolution potential as the pH was raised (Figure 16b). Thus the changes in impedance and development of compressive stresses could conceivably be caused by the entry of protons alone, since cathodic polarisation of oxides produces similar effects. The magnitude of the anodic charges necessary to restore the original barrier voltages of oxides which have been immersed in K_2CrO_4 or cathodically polarised are large enough to remove about 1-4 protons per oxide molecule present. This concentration of protons is little different from that of hydrogen expected in a hydrate. In view of the fact that deprotonation accompanied by the growth of more oxide can even result in a volume reduction, it seems quite likely that the cathodic introduction of protons could cause the compressive stresses and impedance changes seen in the present work. This would not explain the radiotracer experiments conducted by Schwabe, however. To resolve this ambiguity between protons and water is beyond the scope of this work but the combined entry of anions and protons can be explained by the following tentative hydration mechanism.

The electro-osmotic hydration can be described by combining the model for hydrogenation[114, 117] described above with the advanced proton theory of hydration[90]. Cathodic polarisation

effects the entry of protons into the oxide.

$$H^+_{HYDRATED} \rightarrow H^+_{ADSORBED} \rightarrow H^+_{OXIDE}$$

These protons produce a space charge which can be neutralised by electrons from the metal and/or OH^- entry from the solution, depending on the relative availability of these species.

$$H^+_{OXIDE} + e^-_{METAL} \rightarrow (H^+ + e^-)_{OXIDE}$$

$$H^+_{OXIDE} + OH^-_{ADSORBED} \rightarrow (H_2O)_{OXIDE}$$

The sole function of polarisation is to introduce protons; the neutral species in the oxide are hydrogen atoms[117] and water molecules which diffuse under concentration gradients towards the metal. Anodic polarisation will reverse this process, producing no oxide growth during dehydration. Alumina and zirconia show different extremes of this behaviour, the former oxide appears to hydrate, the latter can obtain electrons from the metal to neutralise the protons introduced and does not hydrate.

Whatever the exact species involved, whether water or protons, it is clear that the hydrated/protonated oxide differs from the hydrates formed by boiling anodic alumina in

water. During exposure to the atmosphere the original barrier voltage and impedance of a composite oxide formed by cathodic polarisation which consisted of a corrosion product above the anodic film, completely recovered whereas the outer portion, the layer containing boehmite, was apparently unchanged. If water is introduced into the anodic oxide, it is only loosely held, and its removal can be accomplished by anodisation which does not involve the formation of more oxide. Thus protons or physically held water can be removed by an anodic current which is substantially electronic. Water which is chemically held, e.g. in the hydrates formed by boiling, can only be eliminated by an ionic current since more oxide is produced during its deprotonation.

Part 3. Growth Stresses in Anodic Zirconia

a. Tensile Stresses in Anodic Zirconia

Anodic zirconia grows almost completely by anion migration[61]. Zirconium is, therefore, an ideal metal for investigation in order to verify the volume ratio principle as a cause of growth stresses in oxides. Extremely compressive stresses would be expected from this oxide which has a volume ratio = 1.56. However, during the initial stages of anodising tensile stresses are generated; only when the oxide is thicker than 400-500Å is the overall stress compressive.

Tension in thin zirconia films has been reported elsewhere[36]. Vermilyea[36] suggested that the oxide forms first as a hydrate and is subsequently deprotonated by the anodic field. This does not appear likely since anodic zirconia is not known to hydrate readily, if at all at room temperature, and protons which enter the oxide at low leakage currents (Figure 41) or during cathodic polarisation do not have a noticeable effect on stress.

The tensile stresses are most likely to be caused by the removal of atoms (e.g. metal atoms from the substrate) or by the replacement of large atoms in the oxide by smaller ones. The principle of replacement has been demonstrated experimentally by the diffusion of various alkali ions into soda-lime glass from nitrate melts[120]. K^+ has a very much larger volume than Na^+ and causes expansion of the surface layers of a glass disc when

allowed to diffuse in and replace Na^+. Li^+ which has a smaller volume than Na^+ causes contraction. The stress arising from such volume changes can be as high as 124,000 psi (8820 kg/cm.^{2}) compressive. Cracking of the surface of the glass was caused especially by the tensile stresses.

Two suggestions as to the possible cause of tension can be made.

a. When the oxide is thin the combined effect of the chemical potential and anodic field may be sufficient to cause metal ion migration. Initially this would lead to cation vacancies in the substrate which would collapse and form a tensile layer in the substrate.

b. The electrolyte anion may play a more important role in anodising than has hitherto been realised, by first forming a compound of larger volume than the oxide. Hydrolysis of the intermediate producing the oxide would result in a volume reduction and tension.

The structure of the oxide layer in contact with the growth electrolyte is not known exactly nor is the complex mechanism of anodic oxidation fully understood. At present, therefore, one can only speculate as to the cause of tension in zirconia.

b. Compressive Stresses in Anodic Zirconia

Compressive stresses in zirconia can be explained in terms of the volume increase which accompanies oxidation. Oxygen ions formed at the oxide/solution interface by the dissociation of hydroxyls into protons and oxygen ions, diffuse into the oxide by anion vacancy migration. New oxide produced at the metal/oxide interface is constrained to fit the area of the metal. Since the oxide has a greater volume than the metal it replaces, each layer forms under a biaxial constraint, which causes internal compressive stresses. To maintain constant volume the oxide expands perpendicular to the metal surface and relieves the stress in this direction. The linear compressive strain imposed upon the oxide is approximately 19%, which according to elastic theory would produce a stress greater than 10^6 kg/cm.^{2}. Since the elastic limit in tension of anodic zirconia is 1-3%[45, 48], it seems likely that the oxide is plastically deformed and that the growth stress should be equal to the ultimate compressive strength or the flow stress at 19% strain.

The ultimate compressive strength of bulk zirconia (containing 1.6 at.% Ti) is 9900 kg/cm.^{2} at room temperature[121]. This is very close to the stresses in anodic zirconia (Figure 38 of 7000-1050 kg/cm.^{2}), calculated by the biaxial bending analysis. In previous work[77] the stresses arising during anodising of zirconium have been interpreted as attaining a constant value of

5000 kg/cm.^{2} at oxide thicknesses greater than 2000-3000Å. This value was calculated from deflections of the same magnitude as those observed in the present work; the lower value results from employing Stoney's equation for uniaxial bending of the metal foil. Examination by electron microscopy revealed that the oxide surface was ruptured[77]. The reasonable agreement between the growth stress and the compressive strength of bulk oxide, combined with the presence of cracks in the oxide suggests that anodic zirconia grows at the ultimate compressive stress by a cracking and healing mechanism. This occurs in oxides thicker than ≈500Å which are stoichiometric and less plastic[15] than the oxygen deficient inner layer.

c. The Effect of Alloying Zirconium

Stresses arising during the anodising of Zircaloy 2 were measured to establish whether the increased corrosion resistance obtained by alloying zirconium was due to a decrease in growth stresses. The present work suggests that no significant change in stress is brought about by alloying the metal. Elsewhere, it is reported that Zircaloy 2 develops higher growth stresses than pure zirconium during anodising[77].

Transition and "breakaway" during high temperature oxidation are thought to be caused by local stresses arising from preferred growth of oxide due to enhanced vacancy diffusion down grain boundaries[11]. The anodic oxide of Zircaloy 2 has a

lower a.c. resistivity than pure zirconia. An increase in the electrical and/or ionic conductivity of the whole of the oxide will lessen the difference between the diffusion rate in the grain boundary and that through the body of the oxide, resulting in more uniform oxidation. Consequently the build up of stress to a critical value where cracks develop, will be delayed and a greater protective thickness may result.

Part 4. Field Induced Stresses During Anodising

The present work shows that the compressive stresses caused by the applied field can be interpreted in terms of electrostatic pressure. Field induced stresses, measured at current densities where the temperature rise is negligible, are proportional to the square of the electric field and are of the same magnitude as the lateral component of the theoretical electrostatic stress.

The proportionality of this extra compressive stress to the square of the field can be verified in the following way. Stress σ, is related to the foil deflection Z by Stoney's equation[81] (see Section III, Part 3c.).

$$\sigma = C' \left(\frac{Z}{V_f} \right)$$

where C' = a constant

V_f = formation voltage which is proportional to oxide thickness.

If the stress is proportional to the square of the applied field, (V/V_f), then

$$\sigma = C'' \left(\frac{V}{V_f} \right)^2$$

where C'' = a constant.

By eliminating σ, it is found that

$$\left(\frac{Z}{V^2} \right) = \text{constant} \left(\frac{1}{V_f} \right)$$

(Z/V^2) versus $(1/V_f)$ obtained experimentally for anodic zirconia (Figure 53) follows the relationship above proving that the compressive stress caused by the anodic field is proportional to the square of the field.

With this relationship established, the hysteresis behaviour in Figure 51 can be understood. During growth at constant current density, the field, and hence the electrostatic stress, are constant. Therefore, the deflection increases linearly with voltage as the oxide thickens. During growth at constant voltage the oxide thickens 10-20% and the field and deflection decrease. As the applied voltage is lowered from the formation voltage the deflection decreases as the square of the field. Once the oxide has been formed, increasing or decreasing the voltage causes deflections to behave as in stage C; the hysteresis

behaviour no longer occurs.

The passage of an anodic current through an oxide involves considerable power dissipation[53]. Unless the heat produced is rapidly removed to the electrolyte and substrate the temperature will rise, causing expansion of the oxide and compressive stresses. This possibility becomes more likely at high current densities (greater than about 10 mA/cm.^{2}) where instantaneous compressive stresses have been measured[55], and were attributed to the combined effects of temperature and electrostatic pressure. At low current densities such as employed in this work (1.0 mA/cm.^{2} and less) the temperature rise is small[55] and will cause negligible stresses.

In the absence of heating effects, the field induced stresses are almost certainly caused by electrostatic pressure. Previous calculations of the total electrostatic stress suggest this is 200-500 kg/cm.^{2}[36]. This value is too low to explain the measured stresses. These calculated values are too low, however, because the effect of the barrier space charge layers on stress has been ignored. The stresses calculated from equation 9 in Section III and multiplied by the Poisson ratio of the oxide (assumed to be 0.2-0.3) are in fair quantitative agreement with the measured stress (Table 4).

The theoretical value of the lateral component of the electrostatic stress depends on the static dielectric constant and the

Poisson's ratio of the oxide. Some uncertainty arises in the calculation because values for these two quantities were not obtainable. The dielectric constant of the anodic film measured at ≈1000 c/s was assumed for the first quantity. The Poisson's ratios of the oxides were assumed to lie between 0.2, the value of a typical soft glass, and 0.3 , the value for an ideal incompressible solid. Nevertheless, when the force due to the polarisation charges is taken into account, the calculated and measured electrostatic stresses are of the same order of magnitude.

The rapid increase in deflection that occurs around V_f (Figure 52) does not present an anomaly to the relationship expected from electrostatic effects. The deflection always varies with log(current) ∴ which is a measure of the electric field. It is possible that this increase in field to the growth value is associated with the removal of water from the hydrated layer of alumina formed at low leakage currents[69]. In the case of zirconia, which does not hydrate, protons appear to be the species which enter during growth at low current densities and would be removed before further growth past the original formation voltage could occur.

SECTION VI

CONCLUSIONS

The following conclusions have been drawn from the results of the present research.

1. Compressive stresses arise in alumina when water, which causes an expansion of the oxide, is introduced by various methods. Aluminium oxides or the "bare" metal when boiled in water, form a hydrated product which consists of three discrete layers and has the estimated composition of $Al_2O_3.4.5H_2O/Al_2O_3.1.6H_2O/Al_2O_3.4.5H_2O$. These hydrates contain some water which is chemically bound, whereas almost all of the water which enters alumina from alkaline K_2CrO_4 solutions at room temperature is only physically held, being lost after one or two days exposure to the atmosphere.

2. Water can be removed from hydrated alumina by anodisation. The mechanism apparently depends on the state of hydration.

Hydrates formed in boiling water are transformed into barrier oxides by a deprotonation in which mobile cations react with the corrosion product, displacing protons and forming additional oxide. Normal anodic growth occurs simultaneously at the metal/oxide interface by anion migration. As a result of anodisation involving dehydration of oxide already present, the total amount of anhydrous oxide after the passage of a given anodic charge is greater than would be expected assuming 100% current efficiency.

From estimated water contents of hydrated oxides and the apparent growth rates during dehydration, it has been deduced

that the aluminium transport number has a value between 0.32 and 0.82, in reasonable agreement with published data, and does not vary with the current density.

The effects of hydration by immersion in K_2CrO_4 solutions can be removed without the noticeable formation of more oxide. It is possible that a mechanism similar to electro-osmosis may be responsible for the movement of physically held water.

3. The development of stresses in anodic alumina depends on hydration/dehydration phenomena associated with the oxidation mechanism and upon relative ionic migration. Tensile stresses arise from the volume reduction involved when cations react with a hydrated intermediate, possibly an adsorbed layer, and produce an amorphous barrier oxide by substitution for protons. Compressive stresses are caused by hydration of the outer layers of oxide during growth at low current densities where the flux of metal ions is too small to remove water which diffuses in. Also it is possible that compressive stresses may exist in a crystalline layer of oxide formed at the metal/oxide interface by anion diffusion. The cationic transport fraction deduced from dehydration behaviour is not a function of the current density. Therefore it is concluded that increased water trapping in the intermediate oxide at higher growth rates is partly responsible for the change from overall compression to tension since the volume reduction resulting from the complete dehydration of oxides

increases with their original water content.

4. Proton gradients existing in anodic zirconia films after cathodic polarisation can be determined from the rate of voltage rise during reanodisation at constant current. The highest concentration, approximately 4 protons/molecule of zirconia, was found at the oxide/electrolyte interface.

Cathodic polarisation of anodised aluminium electrodes results in a permanent weight gain due to the growth above the anodic film of a corrosion product which probably contains boehmite.

5. Zirconia which has a volume ratio greater than unity and grows by anion migration develops extremely compressive stresses in accordance with the concept of Pilling and Bedworth. The compressive stress is of the same order as the ultimate compressive strength of the bulk oxide thus, zirconia appears to grow at the compressive fracture stress by a crack-heal mechanism.

The improved corrosion resistance of Zircaloy 2 obtained by alloying zirconium is not associated with a uniform reduction in growth stresses.

6. The compressive stress which is caused by applying a voltage across an oxide is proportional to the square of the electric field and, at current densities where the temperature rise due to the passage of current is negligible, it is of the same order of magnitude as the lateral component of the calculated electrostatic pressure.

PROPOSALS FOR FUTURE WORK

The results of this investigation emphasise that stresses in anodic alumina are dependent on the role played by water in the mechanism of growth. It is considered that the effects of anodising conditions such as the nature of the electrolyte, pH, temperature and growth rate on stress development in alumina should be thoroughly investigated in terms of relative ionic mobility and the volume changes resulting from hydration phenomena.

Fundamental research to decide on the individual influence of the dominant ionic species and volume ratio on stresses should be directed to studying oxidation under conditions which do not involve dehydration or similar desolvation processes.

Dehydration by anodisation may be applicable to the hydrated oxides of other metals besides aluminium, and may be the cause of tensile stresses in their anodic films. The rates of production of barrier oxide (in the presence of hydrated oxide) must be more accurately measured by determination of its dielectric constant, density and composition. Together with measurements of initial surface roughness this data should permit better confirmation of the cation induced deprotonation mechanism and more accurate calculation of the ionic transport numbers.

ACKNOWLEDGEMENTS

The author is deeply indebted to his supervisor Professor J. S. Llewelyn Leach for his understanding and guidance at all times. Thanks are due to Professor J. G. Ball for his permission to use the facilities and laboratory space in the Metallurgy Department, Royal School of Mines. Acknowledgements are made for the financial assistance provided for this work by the Central Electricity Generating Board and also for the materials kindly supplied by Imperial Metal Industries and Arthur Wollacott Ltd. Finally the colleagues in the corrosion group are thanked for their helpful discussions and the sincerest gratitude is expressed to those who ensured the production of this thesis, particularly the author's fiancée, Shirley, who did the typing.

REFERENCES

1. J. S. Ll. Leach; International Conference on Properties of Reactor Materials and Effects of Radiation Damage. Berkeley Castle England (Butterworths) 1961.
2. J. Stringer; J. Inst. Metals Met. Rev. 107 113 Sept. 1966.
3. A. Y. Nehru; Ph.D. Thesis (London) 1963.
4. J. V. Cathcart, R. Bakish and D. R. Norton; J. Electrochem. Soc. 107 669 (1960).
5. J. V. Cathcart, J. J. Cambell and G. P. Smith; J. Electrochem. Soc. 105 442 (1958).
6. J. V. Cathcart; J. Electrochem. Soc. 106 442 (1959).
7. R. E. Pawel, J. V. Cathcart and J. J. Cambell; J. Electrochem. Soc. 110 551 (1963).
8. J. J. Stobbs; J. Electrochem. Soc. 112 916 (1965).
9. J. J. Stobbs and A. J. Woodward; The Oxidation of Unalloyed Uranium in CO_2 and CO C.E.G.B. Report RD/B/N594.
10. J. S. Ll. Leach and A. Y. Nehru; Part 1 Proceedings of Conference on Corrosion of Reactor Materials (I.A.E.A.) Saltzburg Austria, June 1962.
11. B. Cox; Corrosion 16 380t Aug. (1960).
12. D. L. Douglass and J. Van Landuyt; Acta Met. 13 1069 (1965).
13. J. N. Wanklyn, C. F. Britton, D. R. Silvester and N. J. M. Wilkins; J. Electrochem. Soc. 110 856 (1963).

14. A. E. Bibb and J. R. Fascia; Trans. Met. Soc. A.I.M.E. 230 415 (1964).

15. D. L. Douglass; Corrosion Science 5 pp. 255-268 (1965).

16. W. J. Bernard and J. J. Randall Jnr.; J. Electrochem. Soc. 108 822 (1961).

17. J. E. Draley, Shiro Mori and R. E. Loess; J. Electrochem. Soc. 110 222 (1963).

18. V. H. Troutner; A.E.C. Research and Development Report HW-53389 Nov. (1957).

19. J. E. Draley and W. E. Ruther; J. Electrochem. Soc. 104 329 (1957).

20. A. J. Breen, G. D. Fawkes, H. S. Isaacs, J. S. Ll. Leach and A. Y. Nehru; 3rd International Congress on Metallic Corrosion (Moscow) May 1966.

21. M. W. Burkart; Bettis Plant Report WAPD-127 Part III (1956).

22. N. B. Pilling and R. E. Bedworth; J. Inst. Metals 29 529 (1923).

23. U. R. Evans; Inst. Metals Symposium on Internal Stresses in Metals and Alloys London (1947) p. 291.

24. P. D. Dankov and P. V. Churaev; C. R. Acad. Sci. U.R.S.S. 73 1221 (1950).

25. D. J. Garibotti, H. M. Green and W. M. Baldwin Jnr.; A.E.C. Document AECU-3013 March 1955.

26. J. T. Waber; A. Review of the Corrosion of Uranium and its Alloys. Los Alamos Scientific Laboratory Report LA-1524 Nov. 1952 .

27. J. N. Chirigos; Bettis Plant Report WAPD-T-985 May 1959.

28. F. C. Frank and J. H. Van der Merwe; Proc. Roy. Soc. (London A198 216-225 (1949).

F. C. Frank; Proc. Phys. Soc. (London) 64A 941-942 (1951).

29. W. Jaenicke, S. Leistikow and A. Stadler; J. Electrochem. Soc. 111 1031 (1964).

30. B. Borie, C. J. Sparks and J. V. Cathcart; Acta Met. 10 691 (1962).

31. U. R. Evans; Nature 126 130 (1936).

32. W. N. Bradshaw and S. Clarke; J. Electrodep. Tech. Soc. 24 147 (1949).

33. D. H. Bradhurst and J. S. Llewelyn Leach; J. Electrochem. Soc. 113 1245 (1966).

34. J. A. Davies, J. P. S. Pringle, R. L. Graham and F. Brown; J. Electrochem. Soc. 109 999 (1962).

35. E. C. Potter and G. M. W. Mann; First International Congress on Metallic Corrosion p. 417 (Butterworths, London) (1961).

36. D. A. Vermilyea; J. Electrochem. Soc. 110 345 (1963).

37. R. Scott, A. R. Hall and J. Williams; J. Nucl. Mat. 1 39 (1959).

38. J. A. Sartell, R. J. Stokes, S. H. Bendell, T. L. Johnston and C. H. Li; Trans. A.I.M.E. 215 420 (1959).

39. D. Caplan and M. Cohen; Corrosion Science 3 139 (1963).

40. J. D. Mackenzie and C. E. Birchenall; Corrosion 13 12 pp. 783t-786t (1957).

41. R. F. Tylecote; J. Iron Steel Inst. 195 380 (1960).

42. R. F. Tylecote; J. Iron Steel Inst. 196 135 (1960).

43. D. A. Vermilyea; Acta Met. 5 492 (1957).

44. C. Edeleanu and T. J. Law; Phil. Mag. 7 573 (1962).

45. D. H. Bradhurst and J. S. Ll. Leach; Trans. Brit. Ceram. Soc. 62 693 (1963).

46. J. W. Beams, J. Brezeale, W. L. Bart; Phys. Rev. 100 1657 (1955).

47. A. A. Griffith; Phil. Trans. Roy. Soc. London 221A pp. 163-198 (1920).
International Congress Appl. Mech. Delft p. 55 (1924).

48. S. F. Bubar and D. A. Vermilyea; J. Electrochem. Soc. 113 892 (1966).

49. J. S. Ll. Leach and P. Neufeld; Proc. Brit. Ceram. Soc. 6 49 (1966).

50. L. Young; "Anodic Oxide Films" Academic Press London and New York (1961).

51. H. F. Church; Inst. Electr. Engineers paper 3601 p. 399 (1961).

52. T. P. Hoar and J. Yahalom; J. Electrochem. Soc. 110 614 (1963).

53. D. A. Vermilyea; Acta Met. 1 282 (1953).

54. L. Young; Trans. Faraday Soc. 53 229 (1957).

55. P. Neufeld; Ph.D. Thesis (London) 1967.

56. E. M. Field and D. R. Holmes; J. Electrochem. Soc. 111 755 (1964).

57. P. E. Doherty and R. S. Davis; J. Appl. Phys. 34 619 (1963).

58. J. E. Lewis and R. C. Plumb; J. Electrochem. Soc. 105 496 (1958).

59. J. P. S. Pringle and J. A. Davies; Abstract for Meeting of Electrochem. Soc. Pittsburgh (1963).

60. J. A. Davies, B. Domeij; J. Electrochem. Soc. 109 999 (1962).

61. J. A. Davies, B. Domeij, J. P. S. Pringle and F. Brown; J. Electrochem. Soc. 112 675 (1965).

62. F. Keller and A. H. Geisler; Trans. A.I.M.E. 156 82 (1944).

63. C. J. L. Booker and J. L. Wood; Proc. Phys. Soc. (London) 721 (1960).

64. D. J. Stirland and R. W. Bicknell; J. Electrochem. Soc. 106 481 (1959).

65. H. G. Wilsdorf; Nature 168 600 (1951).

66. D. A. Vermilyea; J. Electrochem. Soc. 104 542 (1957).

67. E. J. W. Verwey; Z. Krist. 91 317 (1935).

68. W. J. Bernard and J. W. Cook; J. Electrochem. Soc. 106 643 (1959).

69. A. J. Brock and G. C. Wood; Electrochim. Acta 12 395 (1967).

70. M. A. Heine and M. J. Pryor; J. Electrochem. Soc. 110 1205 (1963).

71. M. A. Heine and P. R. Sperry; J. Electrochem. Soc. 112 361 (1965).

72. G. C. Wood and C. Pearson; Nature 208 547 (1965).

73. G. A. Dorsey; J. Electrochem. Soc. 113 169 (1966).

74. G. A. Dorsey; J. Electrochem. Soc. 113 172 (1966).

75. G. A. Dorsey; J. Electrochem. Soc. 113 204 (1966).

76. J. F. Murphy; Paper in Anodising Symposium at Birmingham April 1967.

77. S. Nomura, C. Akutsu and I Saruyama; Denki Kagaku 33 723-729 (1965).

78. A. Charlesby; A.E.R.E. Report M/R-1014 282 (1952).

79. N. J. M. Wilkins; private communication (1967).

80. D. Michell and G. J. Ogilvie; Phys. Stat. Sol. 15 83 (1966).

81. G. G. Stoney; Proc. Roy. Soc. London (A) 82 172 (1909).

82. D. Wilcock; private communication.

83. A. Brenner and S. Senderoff; J. Research Nat. Bureau of Standards 42 105 (1949).

84. W. Beck, J. Danovich and S. J. Ketcham; J. Electrochem. Soc. 106 1063 (1959).

85. N. J. M. Wilkins; J. Electrochem. Soc. 109 998 (1962).

86. I. H. Khan, J. S. Ll. Leach and N. J. M. Wilkins; Corr. Sci. 6 483 (1966).

87. N. J. M. Wilkins; Corr. Sci. 4 17 (1964).

88. Smithells - Metals Reference Book (Butterworths) 1965.

89. G. L. Miller; "Zirconium" (Butterworths) 1957.

90. T. P. Hoar and G. C. Wood; Electrochim. Acta 7 333 (1962).

91. M. S. Hunter, P. F. Towner and D. L. Robinson; Tech. Proc. Amer. Electroplaters Soc. 46th Ann. Conf. 3 220 (1959).

92. I. H. Khan; Ph.D. Thesis (London) 1966.

93. E. Deltombe and M. Pourbaix; Corrosion 14 16 (1958).

94. L. Page and N. I. Adams; "Principles of Electricity" Van Nostrand 3rd edition pp. 42-45 (1958).

95. D. R. Kennedy; ERA Report ref. L/T374/1958.

96. R. W. Franklin; Inst. Elec. Engrs. Paper No. 3655 412 (1962).

97. J. Patrie; Contribution à l'Etude des Phenomenes de Passivation de l'aluminium Immergé en Milieu Nitrique, Thèse, Grenoble (1952).

98. R. W. Franklin; p. 214 "Anodic Oxide Films" L. Young Academic Press London and New York (1961).

99. G. M. Krembs; J. Electrochem. Soc. 110 938 (1963).

100. R. K. Hart; Trans. Faraday Soc. 53 1020 (1957).

101. G. A. Lonergan and W. B. Simpson; Electrochim. Acta 11 1495 (1966).

102. S. TAjima, N. Baba and T. Mori; Electrochim. Acta 9 1509 (1964).

103. J. C. Bailar; "The Chemistry of the Co-ordination Compounds" New York Rheinhold (1956).

104. M. S. Hunter and P. Fowle; J. Electrochem. Soc. 101 481 (1954).

105. W. J. Bernard and J. J. Randall Jnr.; J. Electrochem. Soc. 107 483 (1960).

106. K. Schwabe; J. Electrochem. Soc. 110 663 (1963).

107. J. H. Greenblatt; J. Electrochem. Soc. 109 1139 (1962).

108. V. M. Morton; A Note on the Calculation of Stress Developed During Oxidation, C.E.R.L. (1967).

109. G. T. Rodgers; A paper on "Anion Impurities in Anodic Films on Zirconium, 8th Corr. Sci. Symp., Leeds (1967).

110. G. Aronowitz and N. Hackermann; J. Electrochem. Soc. 110 633 (1963).

111. A. F. Beck, M. A. Heine, E. J. Caule and M. J. Pryor; Corr. Sci. 7 1 (1967).

112. R. S. Alwitt; J. Electrochem. Soc. 114 843 (1967).

113. D. Altenpohl; Inst. Radio Engrs. Com. Rec. 111 35 (1954).

114. J. S. Ll. Leach; J.I.M. 88 24 (1959-60).

115. H. S. Isaacs and J. S. Ll. Leach; J. Electrochem. Soc. 110 680 (1963).

116. D. Boden, C. J. Venuto, D. Wisler and R. B. Wylie; J. Electrochem. Soc. 114 415 (1967).

117. H. S. Isaacs and J. N. Wanklyn; U.K.A.E.A. Research Report A.E.R.E. R4604 (1964).

118. G. D. Fawkes; M.Sc. Thesis (London) 1962.

119. D. J. O'Connor, P. G. Johansen and A. S. Buchanan; Trans. Faraday Soc. 52 229 (1956).

120. S. S. Kistler; J. Amer. Ceram. Soc. 45 59 (1962).

121. H. A. Lipsitt and R. Ruh; J. Amer. Ceram. Soc. 47 645 (1964).

TABLE 1.

Growth Current Density $mA/cm.^2$	t_m in Ammonium Citrate	t_m in Sodium Tetraborate
0.1	0.33 - 0.41	0.54
0.2	0.39	-
0.3	0.44	0.56
0.5	0.59	0.63
1.0	0.56	0.60
10	0.72	0.57

Cation Transport Number, t_m, During Anodising of Aluminium[61]

TABLE 2.

Elastic Constants of Metals Used in Stress Measurements

Metal	Young's Modulus (E)	Poisson's Ratio (ν)
Aluminium[88]	9.9×10^6 p.s.i.	0.34
Zirconium[88]	13.5×10^6 p.s.i.	0.34
Zircaloy 2[89]	14.0×10^6 p.s.i.	0.31

TABLE 3.

Thickness/Voltage Ratios and Current Efficiencies During Anodising

a. Aluminium

Electrolyte	Total mA/cm^2	Growth Å/V	dV/dt (volt/min)	Ionic Current	Current Efficiency %
pH = 9	1.0	12.85	21.6	0.80	80
ammonium	0.5	13.2	10.4	0.39	78
borate	0.2	13.6	3.4	0.14	70
	0.1	13.9	0.42	0.02	20
pH = 6	3.0	12.2	53	1.91	64
ammonium	2.0	12.5	24	0.89	45
citrate	1.0	12.7	10	0.38	38
	0.5	13.0	6.4	0.25	49
	0.1	13.7	0.95	0.039	39

b. Zirconium

pH = 9	0.1	25.70	0.54	0.04	42
ammonium	1.0	24.30	10.7	0.705	70
borate	6.0	23.05	60	4.05	68
0.2N H_2SO_4	1.0	17.8	11.5	0.60	60
	10.0	11.2	132	4.30	43
1% KOH	1.0	25.3	6.5	0.48	48
	10.0	24.3	95	6.70	67

c. Zircaloy 2

pH = 9 ammonium borate	1.0	24.3	-	-	-

TABLE 4.

Electrostatic Stresses During Anodising at 1.0 mA/cm.^{2}

Metal	Specimen	Deflection per volt (cm./volt)	Growth Å/V	Dielectric Constant	Electrostatic Stresses (kg./cm.^{2})		
					Theoretical Total Stress P	Lateral Component	
						Theoretical	Measured
Al	1	1.85×10^{-4}	12.9	10	3000	600-900	1050
Al	2	1.62×10^{-4}	12.9	10	3000	600-900	950
Zr	3	3.60×10^{-4}	24.3	22	3560	712-1068	1290
Zr	4	2.8×10^{-4}	24.3	22	3560	712-1068	870
Zr	5	3.4×10^{-4}	24.3	22	3560	712-1068	1215

TABLE 5.

Apparent Growth Efficiencies of Alumina During Dehydration by Anodic Polarisation

Reaction	Degree of hydration H_2O/Al_2O_3	Al_2O_3 molecules per electron charge	Efficiency %
$2Al + 3H_2O = Al_2O_3 + 6H^+ + 6e^-$	∞	1/6	100
$12Al + Al_2O_3 + 18H_2O = 7Al_2O_3 + 36H^+ + 36e^-$	18	7/36	117
$10Al + Al_2O_3 + 15H_2O = 6Al_2O_3 + 30H^+ + 30e^-$	15	6/30	120
$8Al + Al_2O_3 + 12H_2O = 5Al_2O_3 + 24H^+ + 24e^-$	12	5/24	125
$6Al + Al_2O_3 + 9H_2O = 4Al_2O_3 + 18H^+ + 18e^-$	9	2/9	133
$4Al + Al_2O_3 + 6H_2O = 3Al_2O_3 + 12H^+ + 12e^-$	6	1/4	150
$2Al + Al_2O_3 + 3H_2O = 2Al_2O_3 + 6H^+ + 6e^-$	3	1/3	200
$Al + 3AlO(OH) = 2Al_2O_3 + 3H^+ + 3e^-$ $\{2AlO(OH) \equiv Al_2O_3.H_2O\}$	½	2/3	400

TABLE 6.

Aluminium Ion Transport Numbers Determined from Dehydration Rates

Roughness Factor	Apparent Growth Efficiency %				Calculated Metal Transport Number	
	Measured		Corrected for Roughness			
	Stage 1 & 3	Stage 2	Stage 1 & 3	Stage 2	Stage 1 & 3	Stage 2
1.00	120-130	160-170	120-130	160-170	0.35-0.49	0.32-0.37
1.03	"	"	129*	170*	0.46	0.37
1.07	"	"	134*	177*	0.53	0.40
1.20	"	"	150*	199*	0.66	0.82

* Average efficiencies

TABLE 7.

Anodisation of Hydrated Alumina at Different Current Densities

$mA/cm.^2$	1.0	0.1
V_1 (volts)	74	39
V_2 (volts)	174	106
Charge C_1 (mA.min.)	2.17	1.3
Charge C_2 (mA.min.)	2.0	1.6
V_1/C_1	34	30
$(V_2 - V_1)/C_2$	50	42
Increase Å/V from 1.0 $mA/cm.^2$ to 0.1 $mA/cm.^2$	-	18%
Barrier oxide (voltage corrected for Å/V increase) per unit charge.		
Stage 1 (v/mA.min.)	34	35.2
Stage 2 (")	50	49.5

V_1, C_1, etc. refer to Figure 29.

TABLE 8.

Growth Efficiencies during Anodisation in the Presence of Hydrated Oxide

Stage of Dehydration	Growth Rate (v/m)	Apparent Growth Efficiency (%) indicated by		
		(a) Voltage	(b) 1/C	(c) 1/C, and ρ_{THEO}
Stage 1	34-36	121-128	96-102	111-118
Stage 2	45-48	160-170	127-136	147-158
Stage 3	35-36	121-128	96-102	111-118

ρ_{THEO} = Theoretical density of alumina.

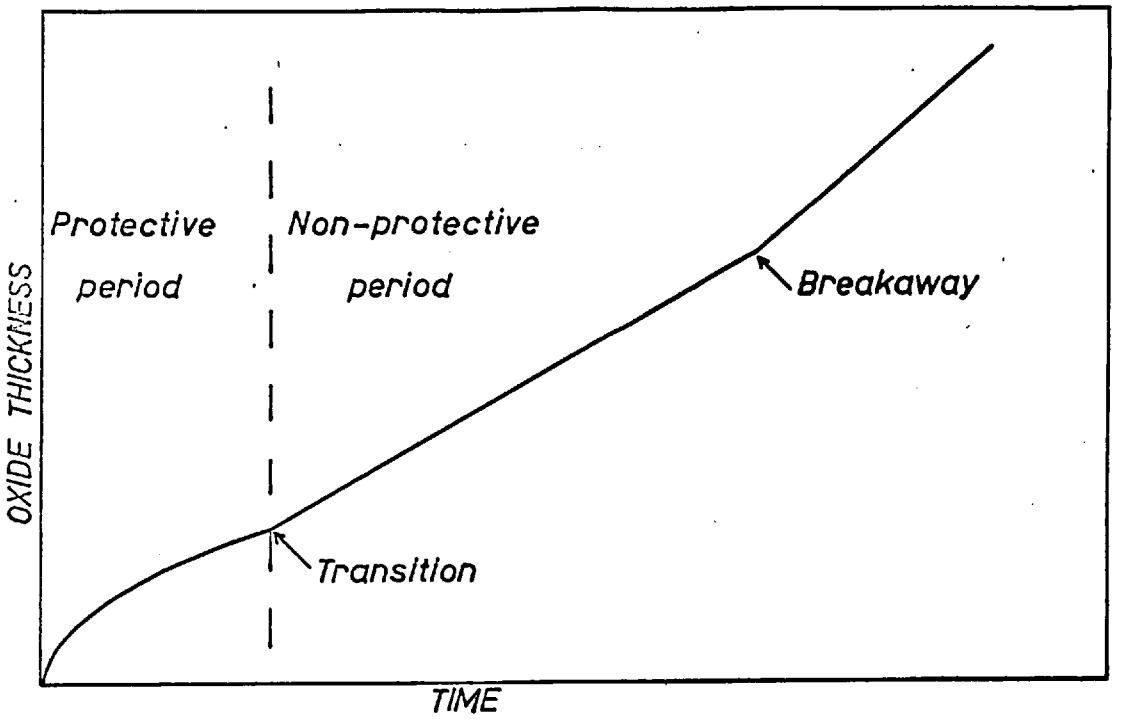

Figure 1. Typical oxidation kinetics of metals.

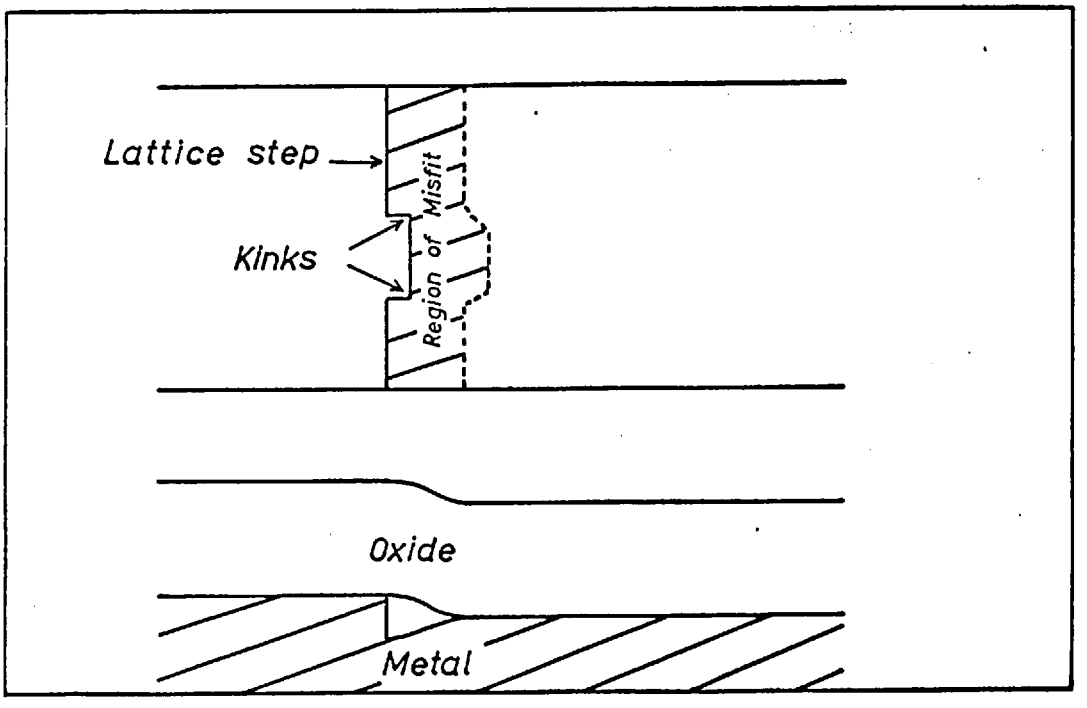

Figure 2. Growth of oxide by cation migration (after Vermilyea).

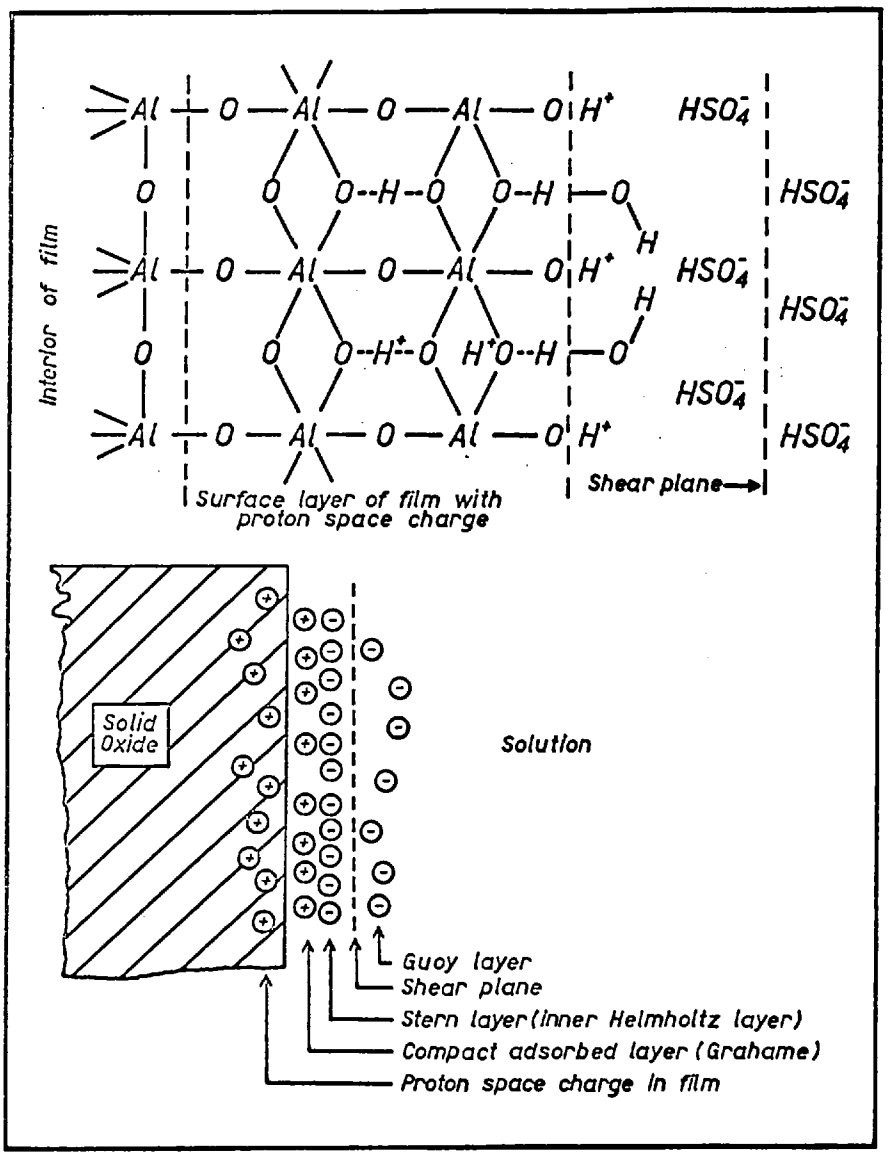

Figure 3. A possible ionic arrangement in the anodic film-electrolyte interphase showing protons in film as well as in compact adsorbed layer (after Murphy).

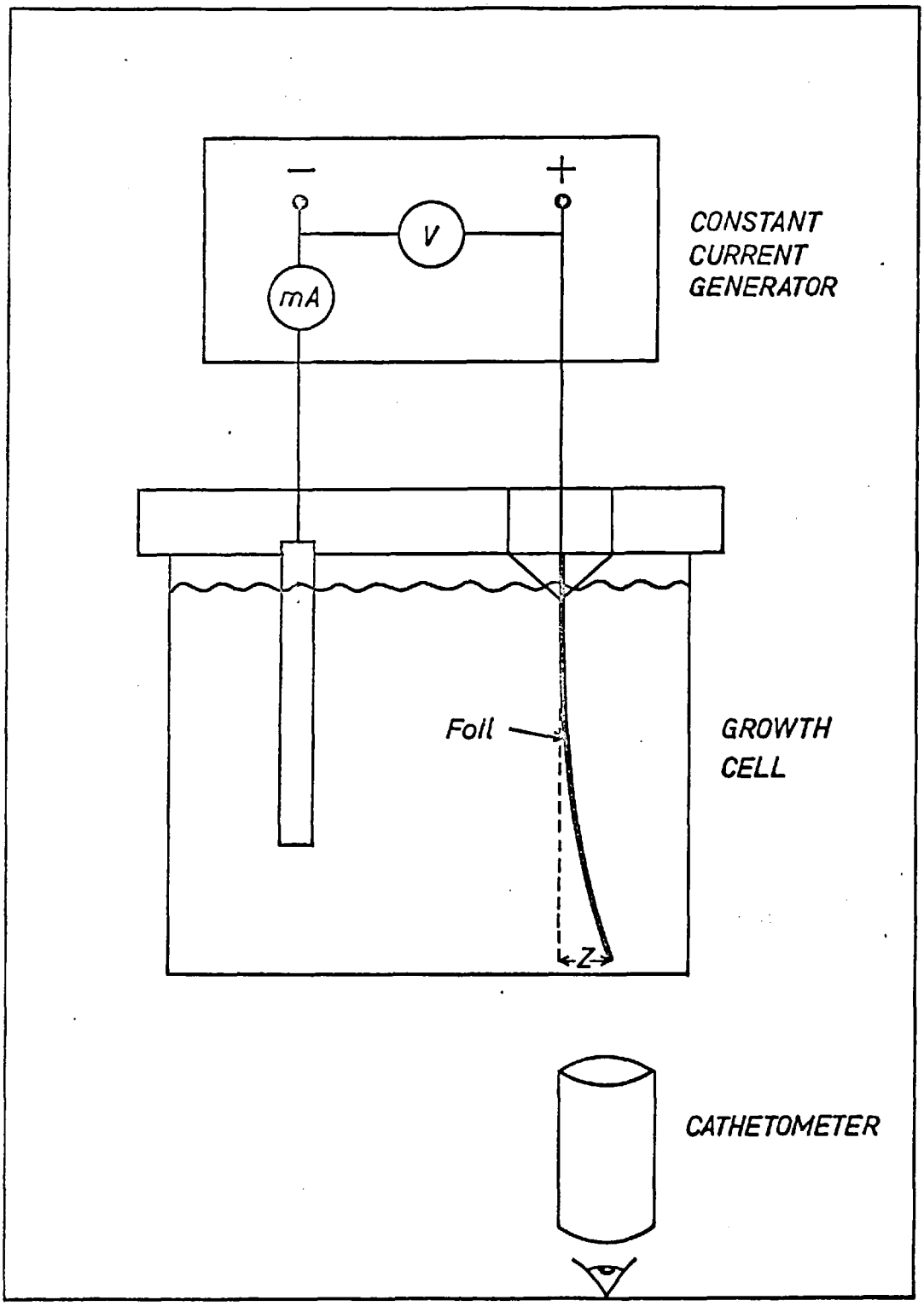

Figure 4. Apparatus for measurement of stresses in oxide films by the bending foil method.

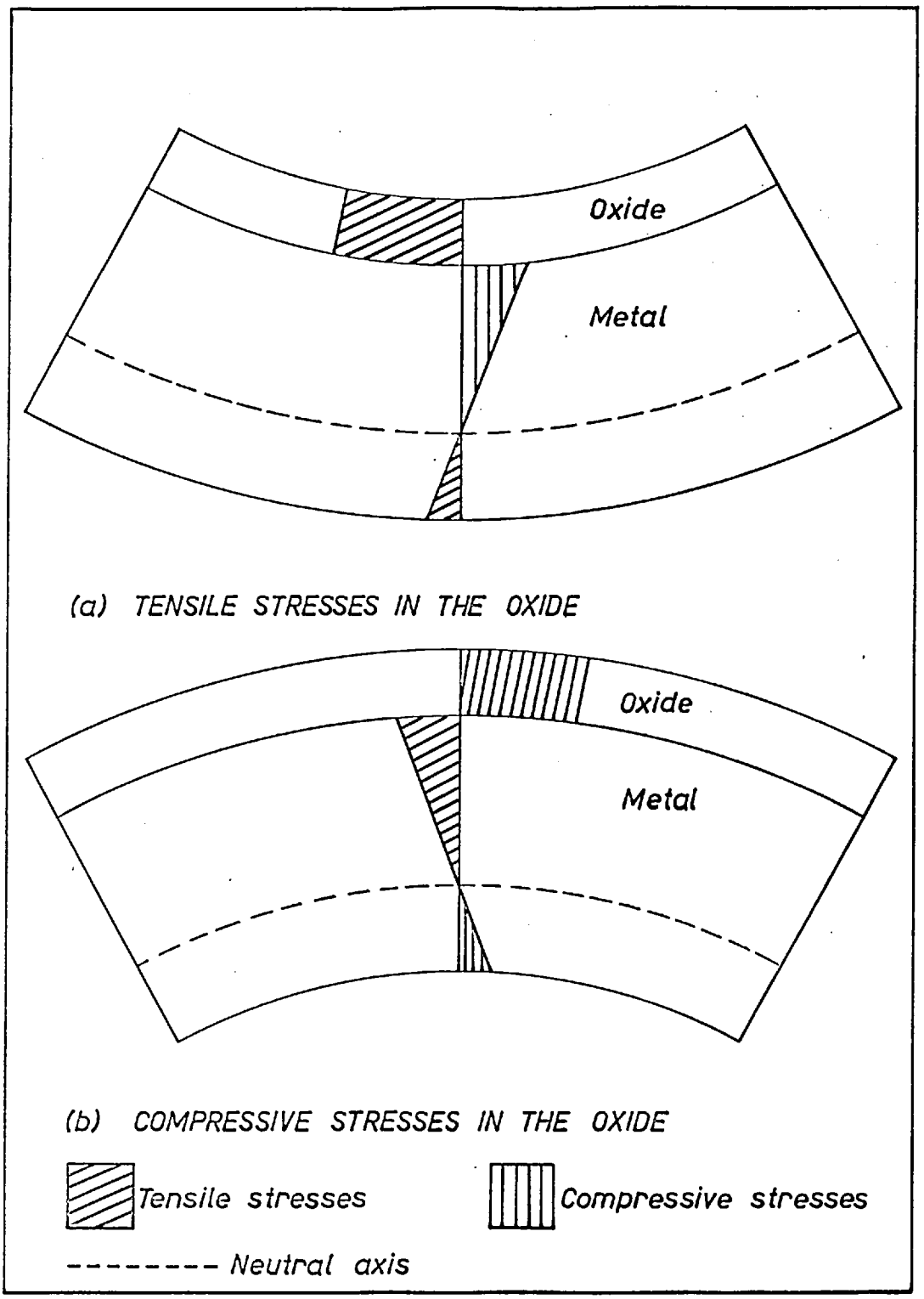

Figure 5. Bending of the substrate caused by stresses in the oxide.

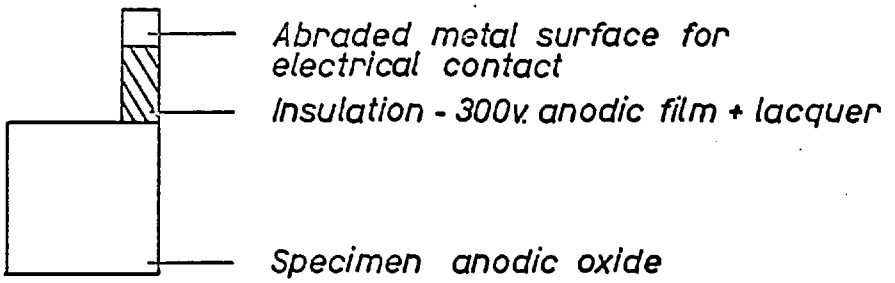

Anodised metal flag used for Impedance and Spectrophotometric Measurements

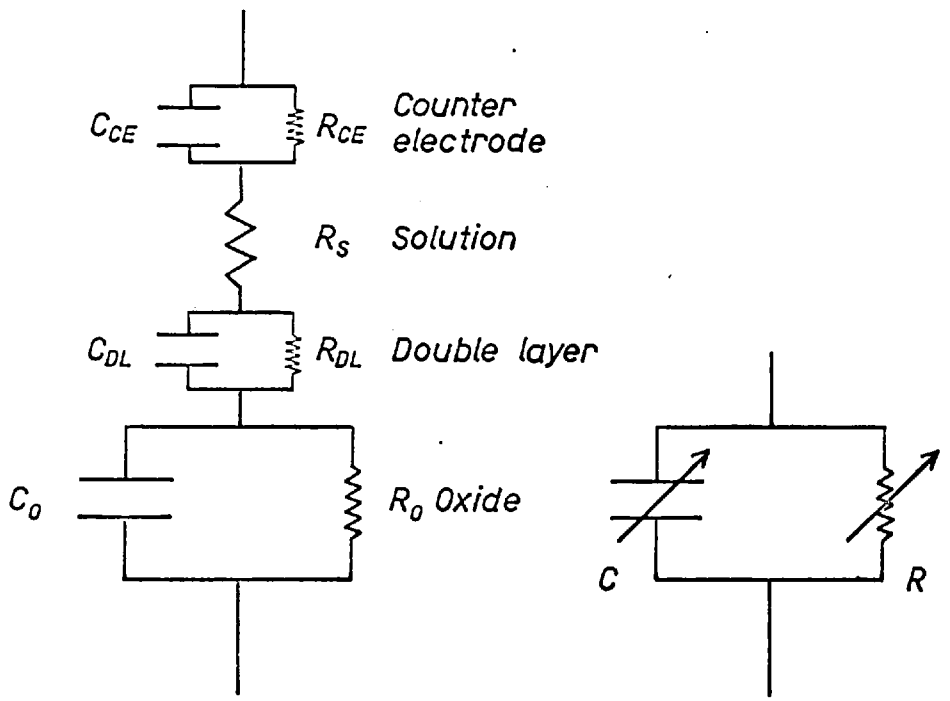

Anodic growth cell

— Analogue circuit

Bridge

— Standard impedance

C and R in parellel

Figure 6.

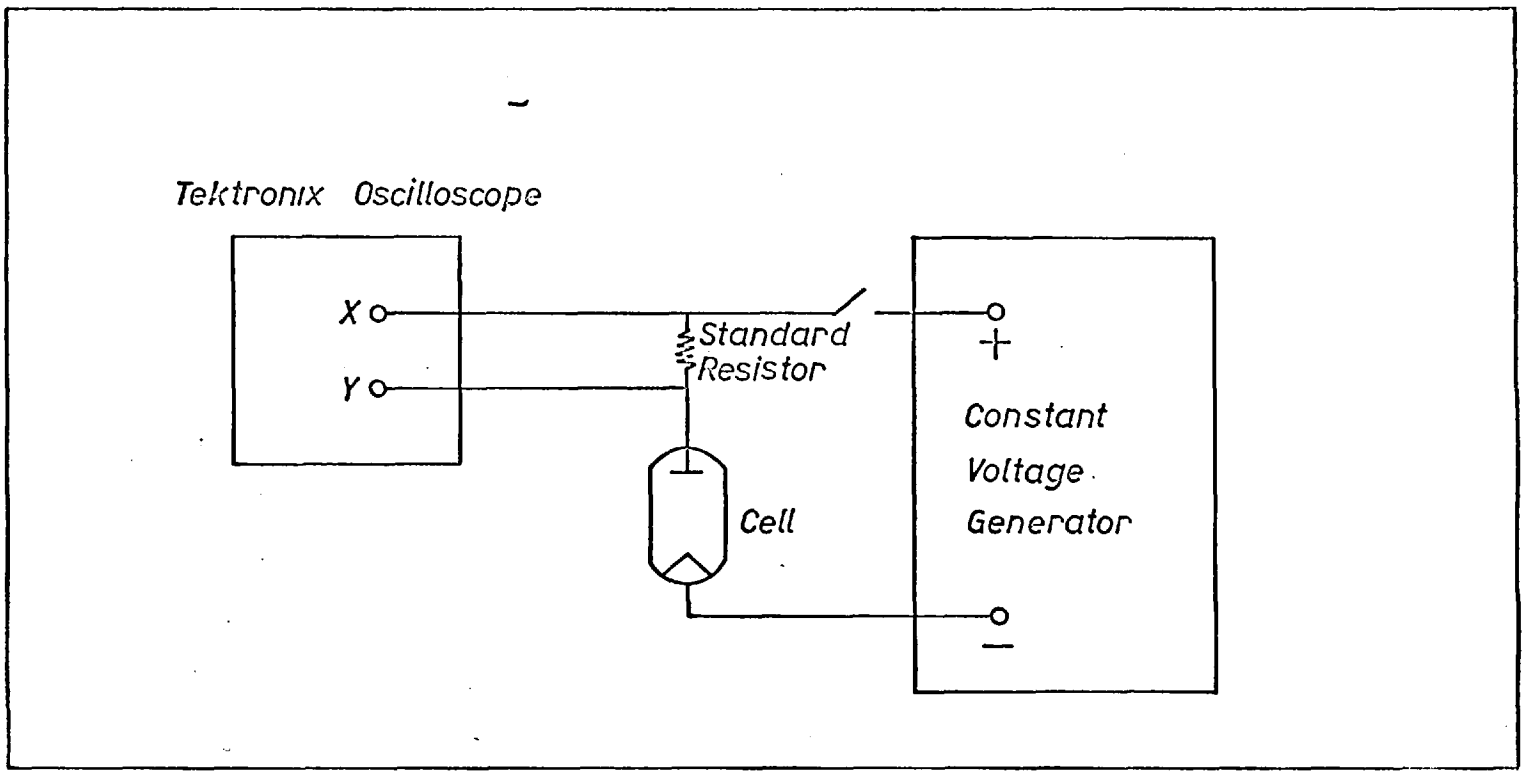

Figure 6a. Circuit for Measuring Current Transients.

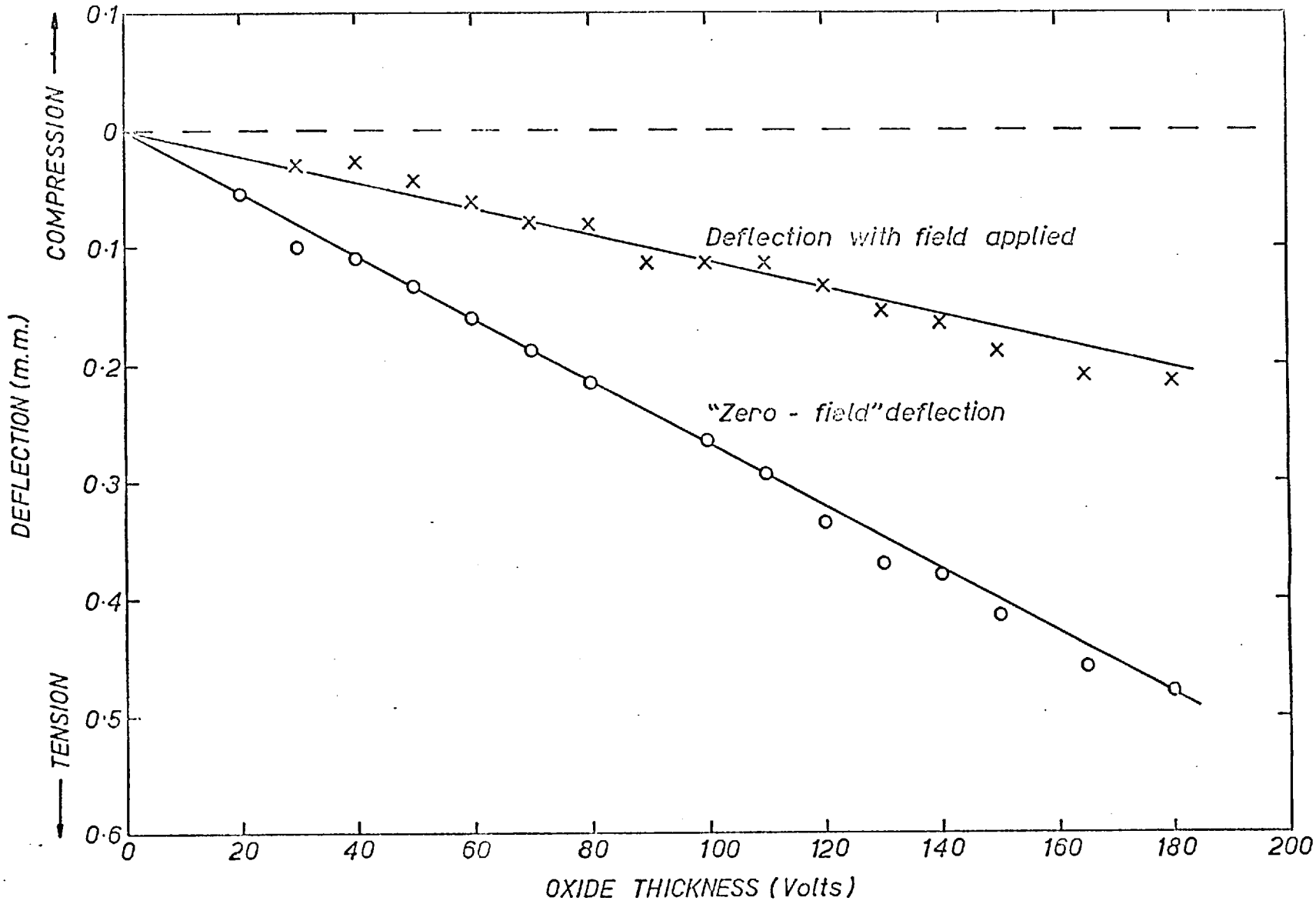

Figure 7. The effect of voltage on the deflection of an aluminium foil anodised at constant current density (1.0 mA/cm.^{2}).

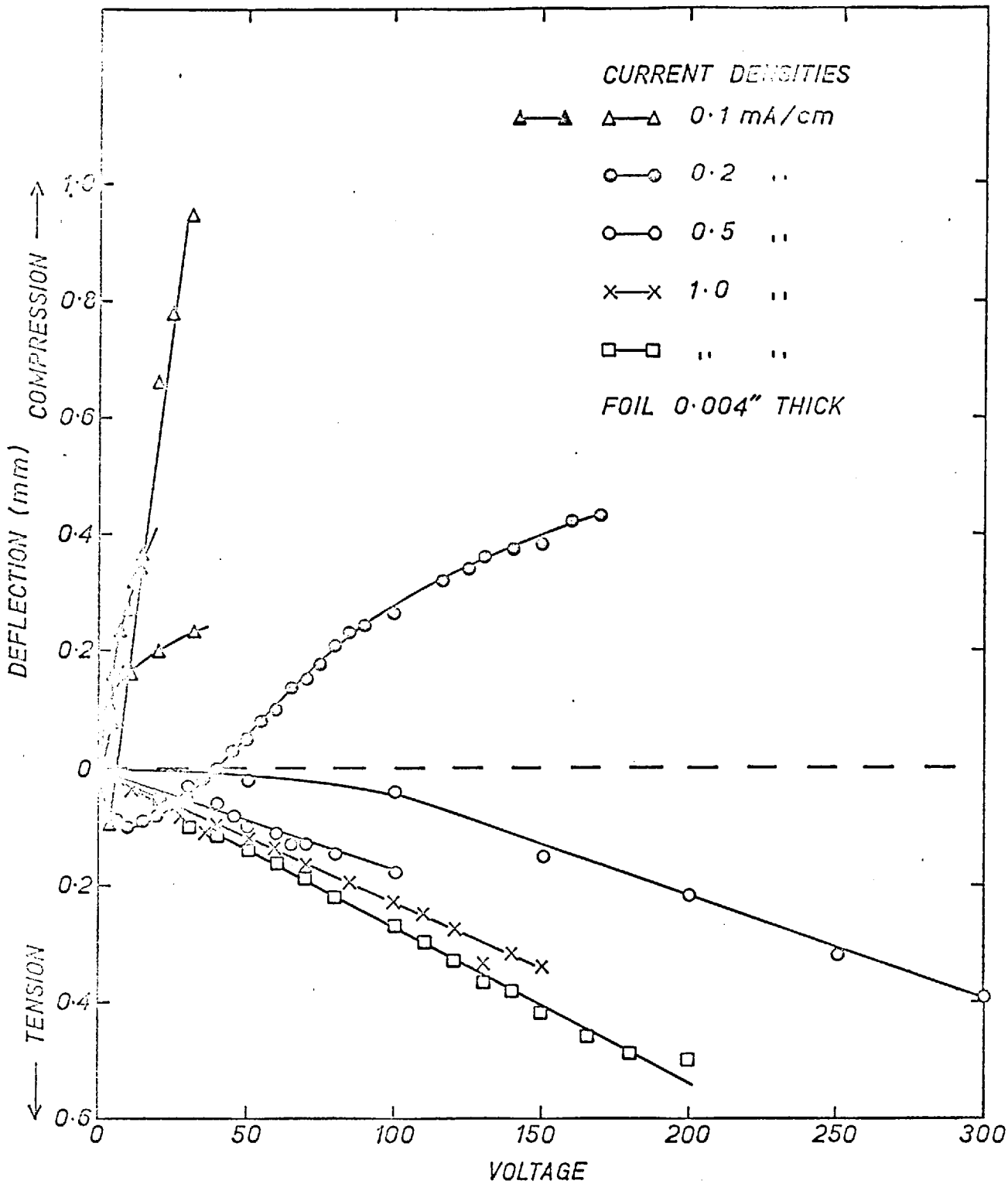

Figure 8. Deflection of aluminium foils anodised in pH = 9 ammonium borate at various current densities.

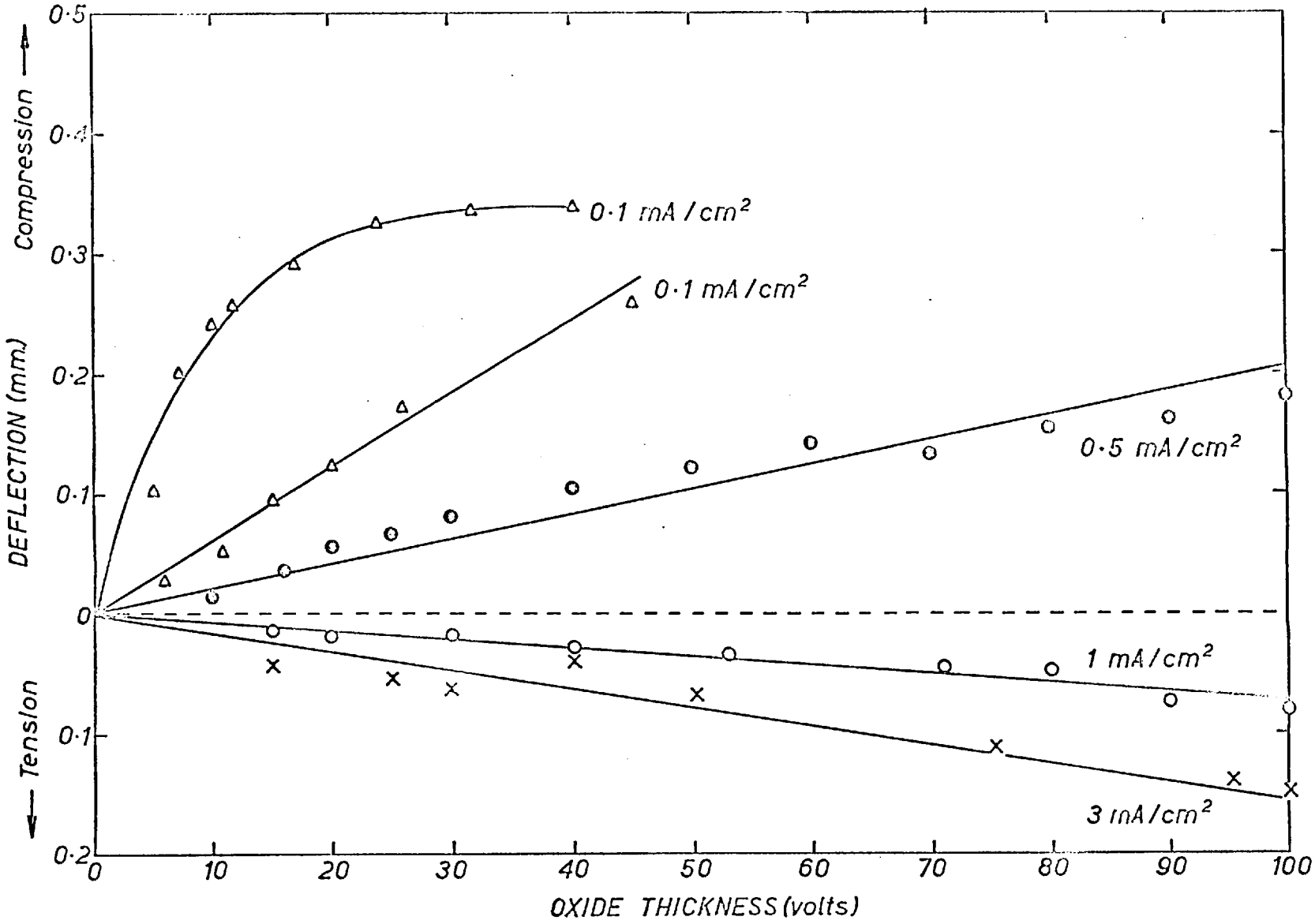

Figure 9. *Deflection of Al foil anodised in pH = 6 ammonium citrate at various current densities*

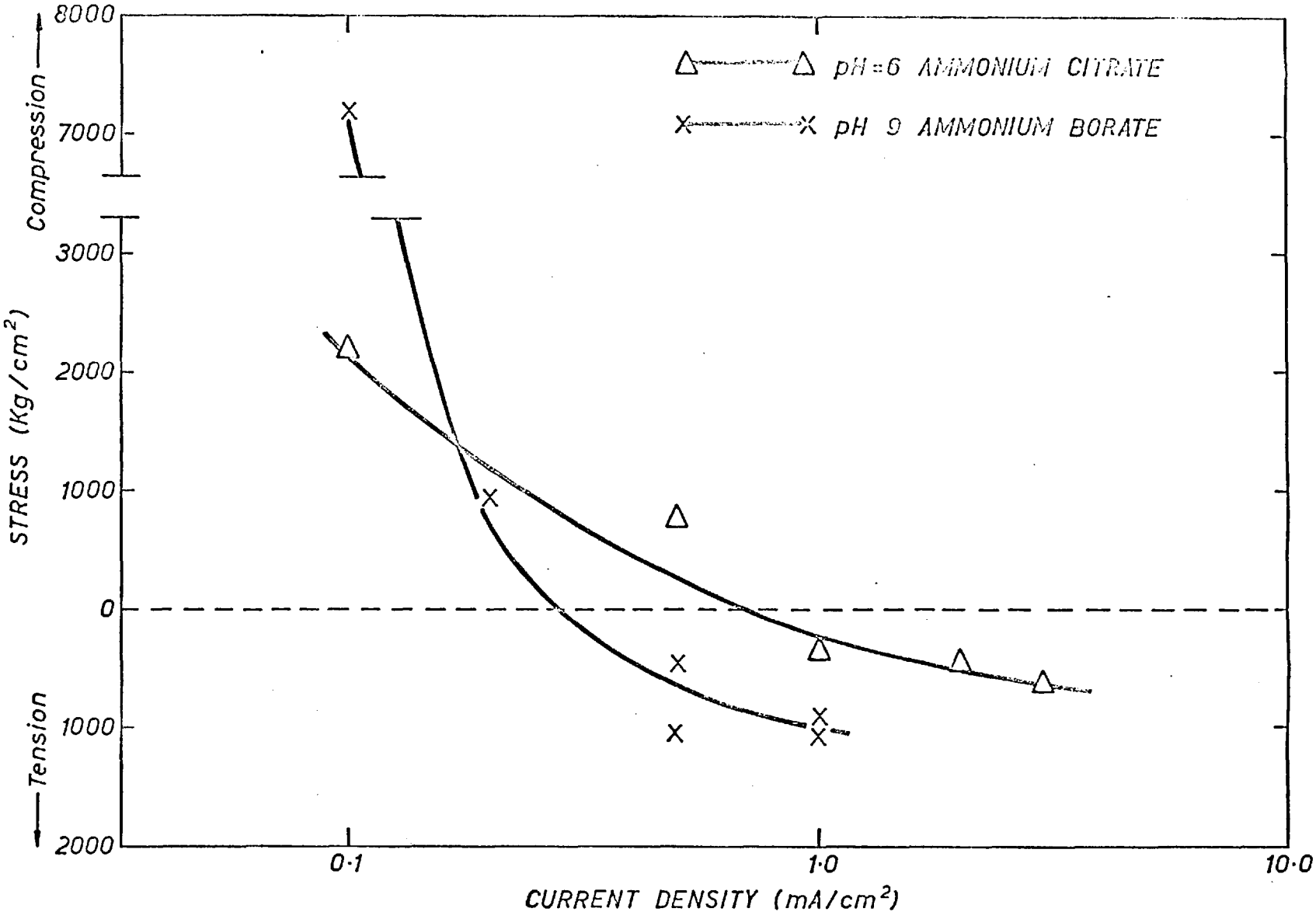

Figure 10. *The growth rate dependence of stresses developed in anodic alumina barrier films*

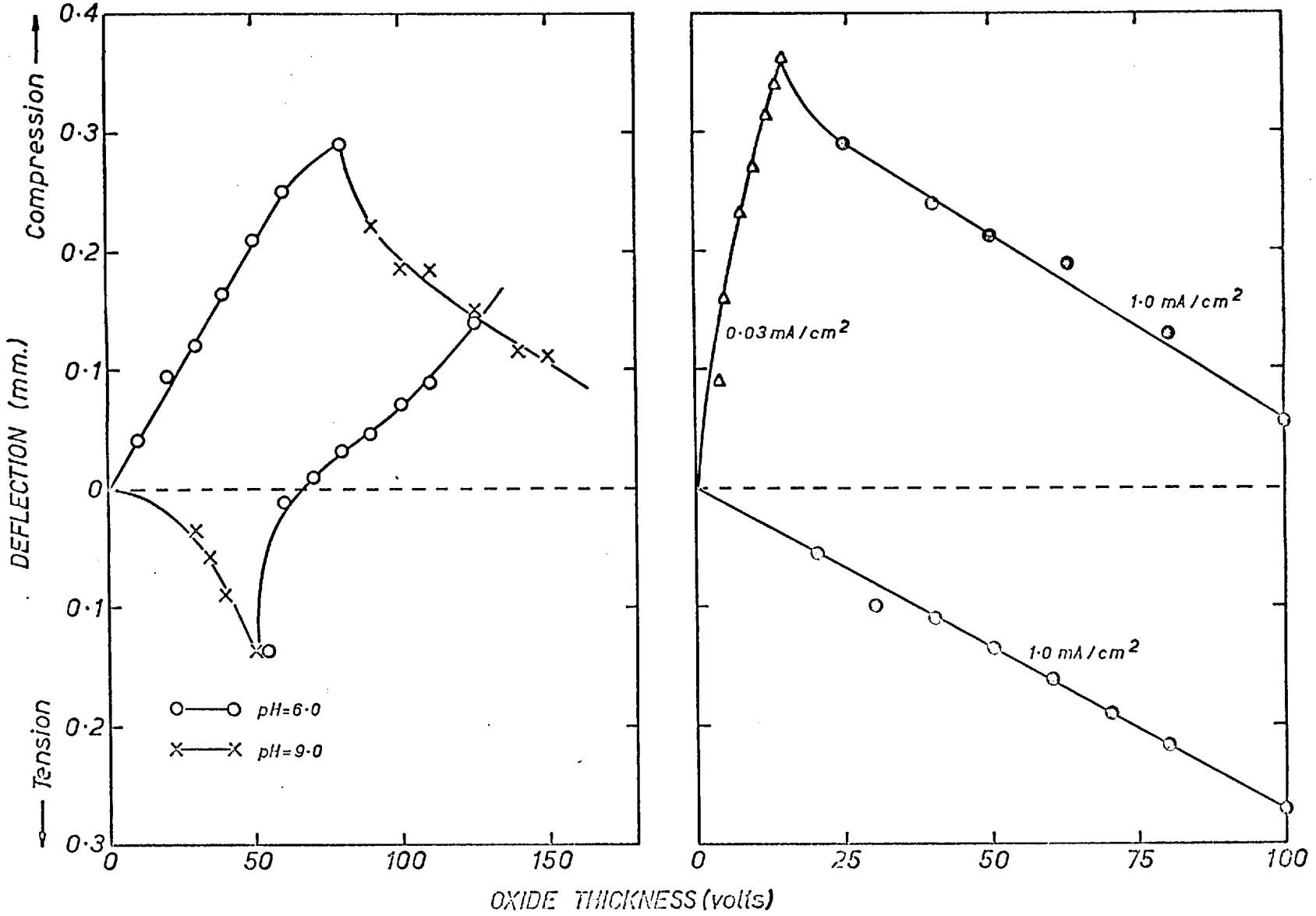

Figure 11. *(a) The effect of pH on stress. Duplex oxides grown at 1·0 mA/cm² in ammonium citrate*

(b) The effect of growth rate on stress. Duplex film formed in pH=9·0 ammonium borate.

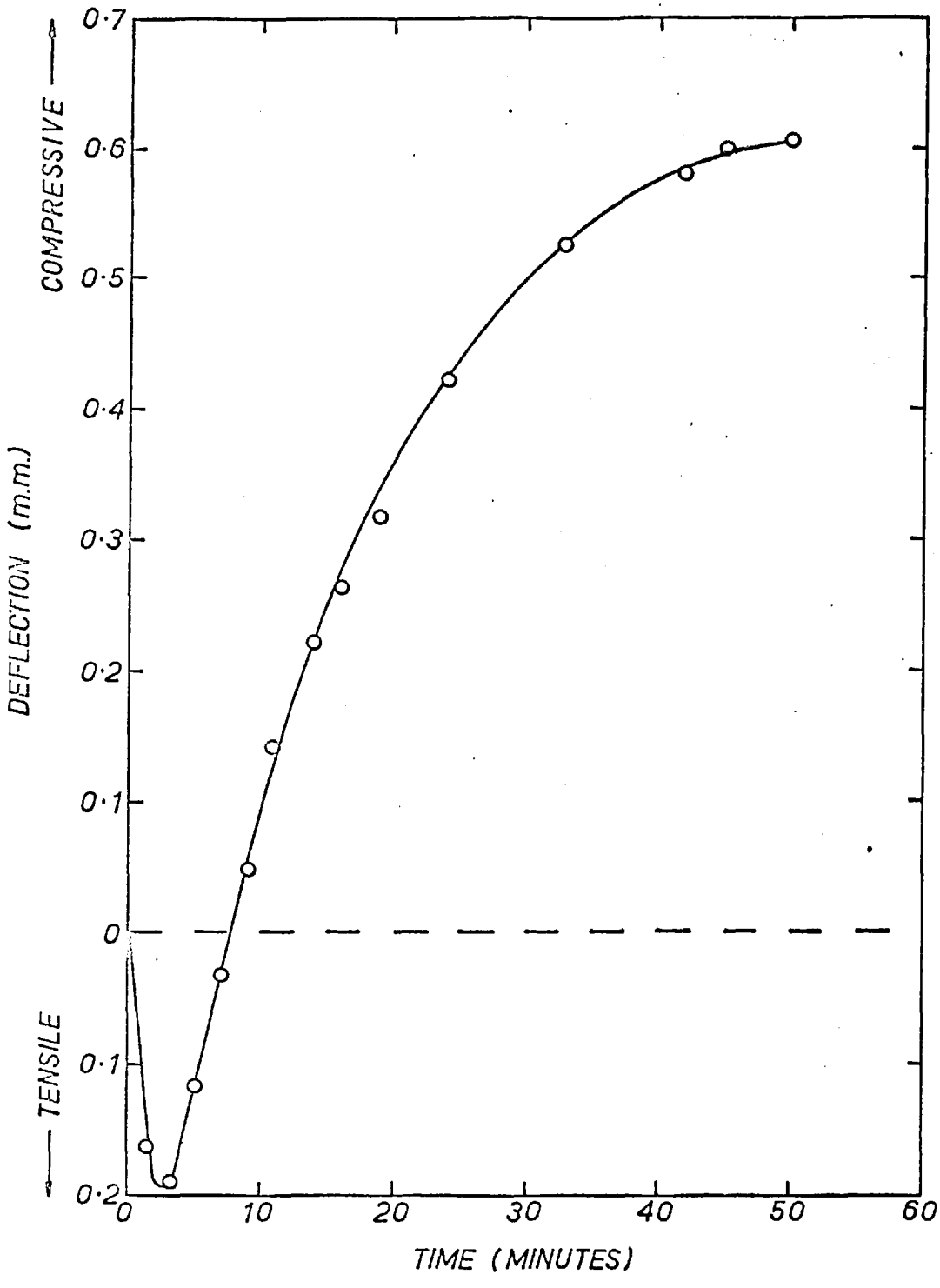

Figure 12. Deflection of an aluminium foil anodised at 1.0 mA/cm.^{2} in pH = 10.0 ammonium citrate.

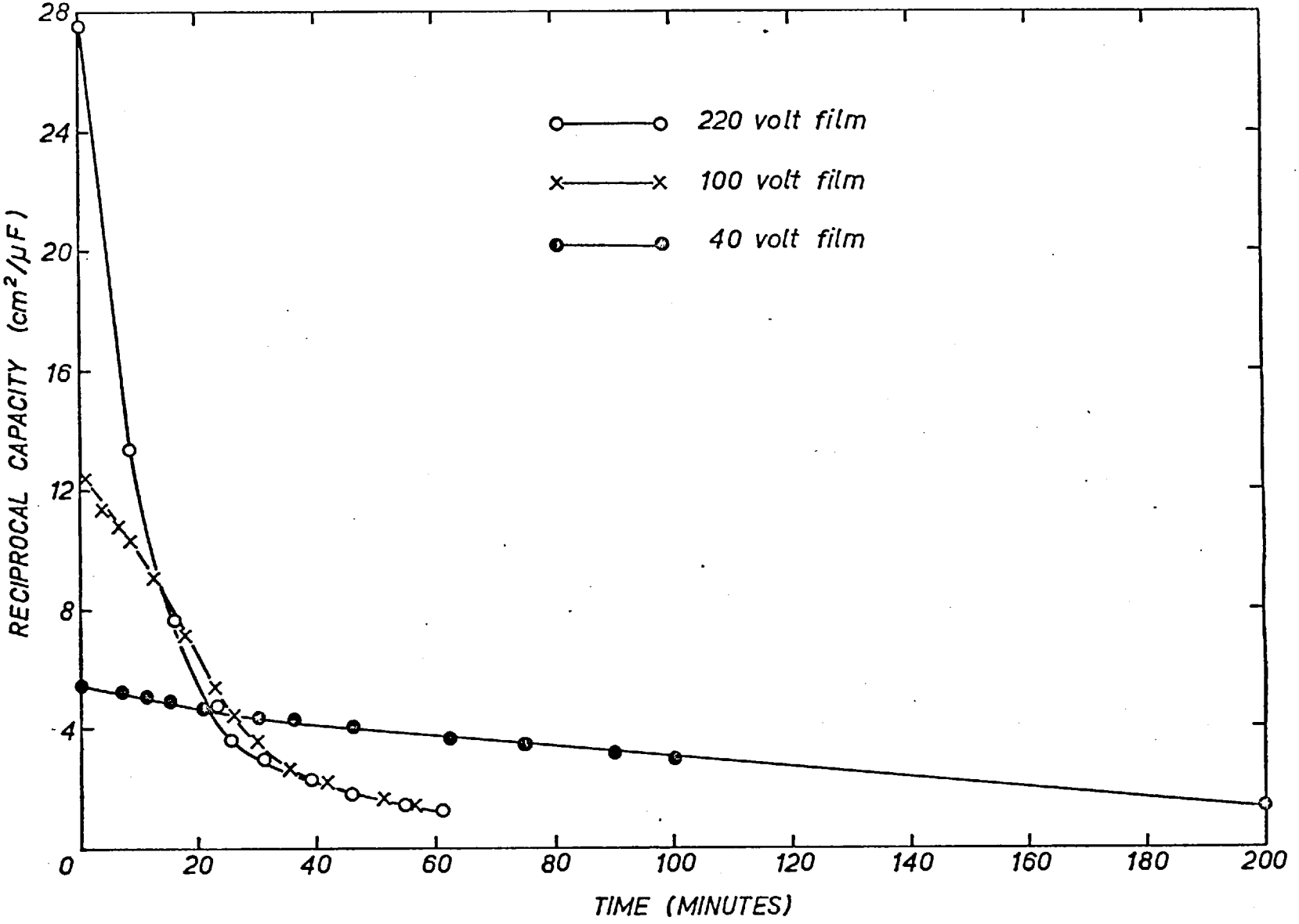

Figure 13. Variation in reciprocal capacity during oxide dissolution in 5% H_3PO_4 / 2% CrO_3

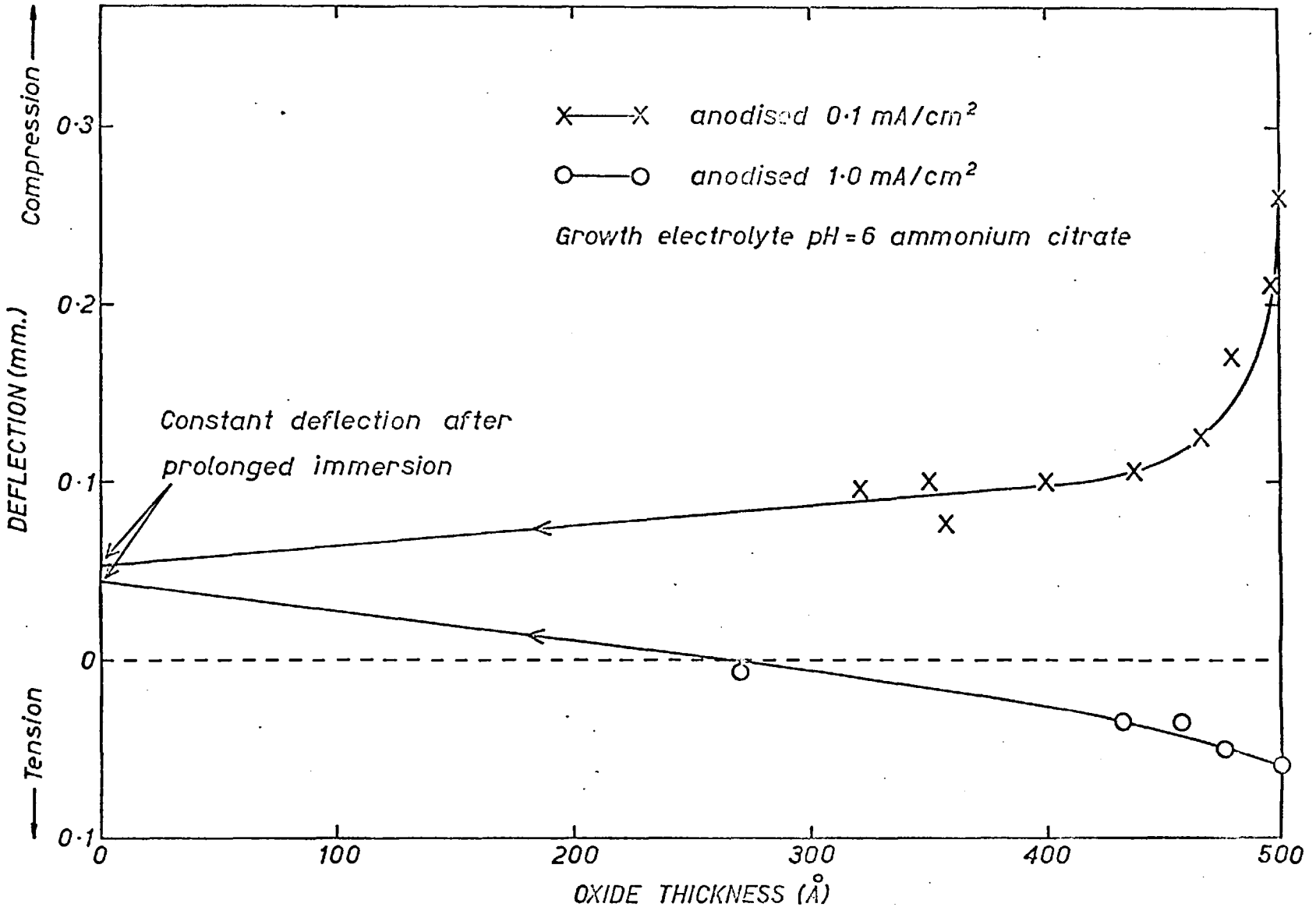

Figure 14. *Stress location - deflection of anodised Al foils during removal of oxide in 5% H_3PO_4/2% CrO_3 solution.*

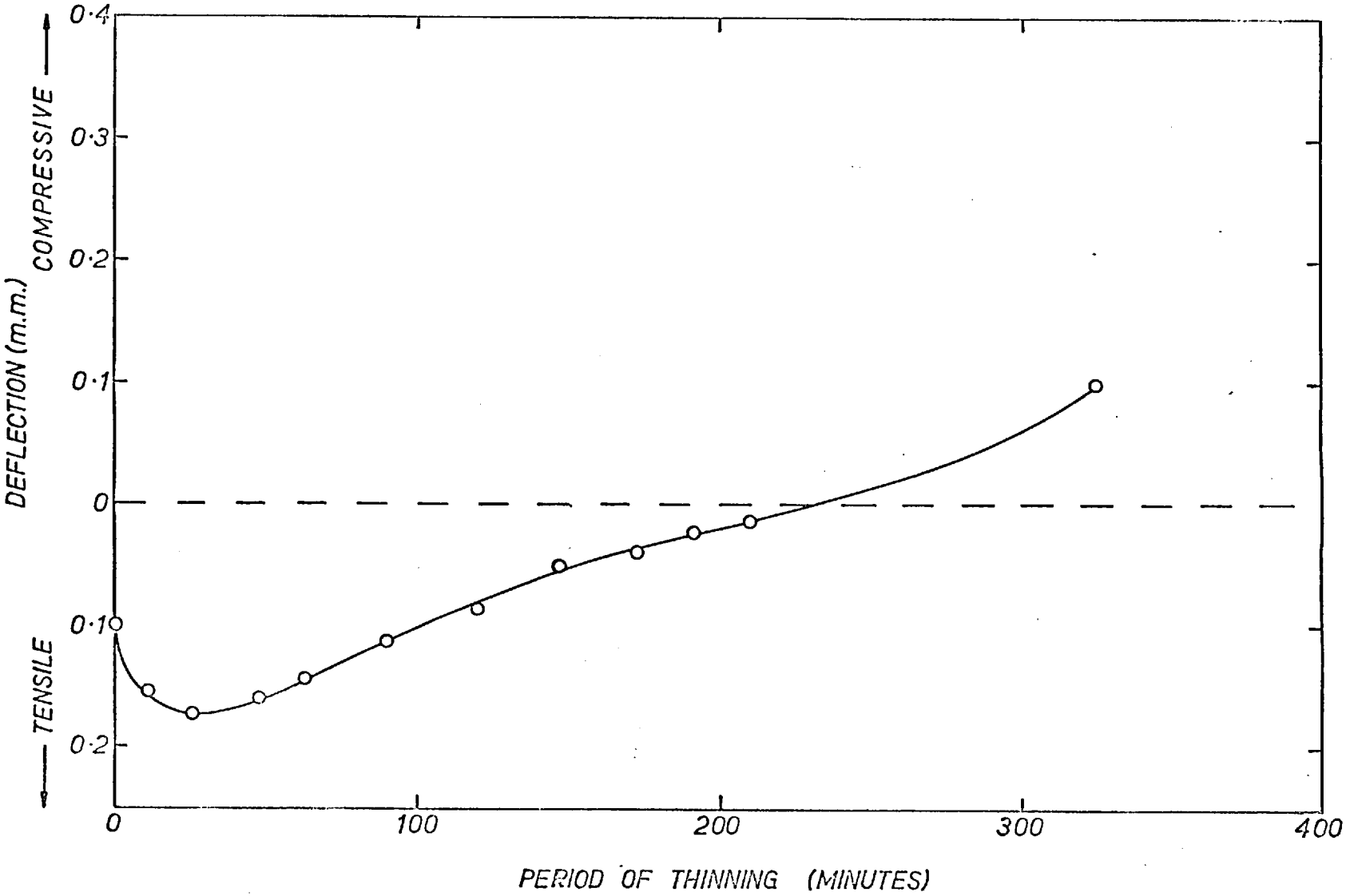

Figure 15. Deflection during thinning in H_3PO_4/CrO_3 solution. Duplex alumina oxide grown at 1.0 mA/cm.^{2} and then at 0.1 mA/cm.^{2}, in pH = 6 citrate.

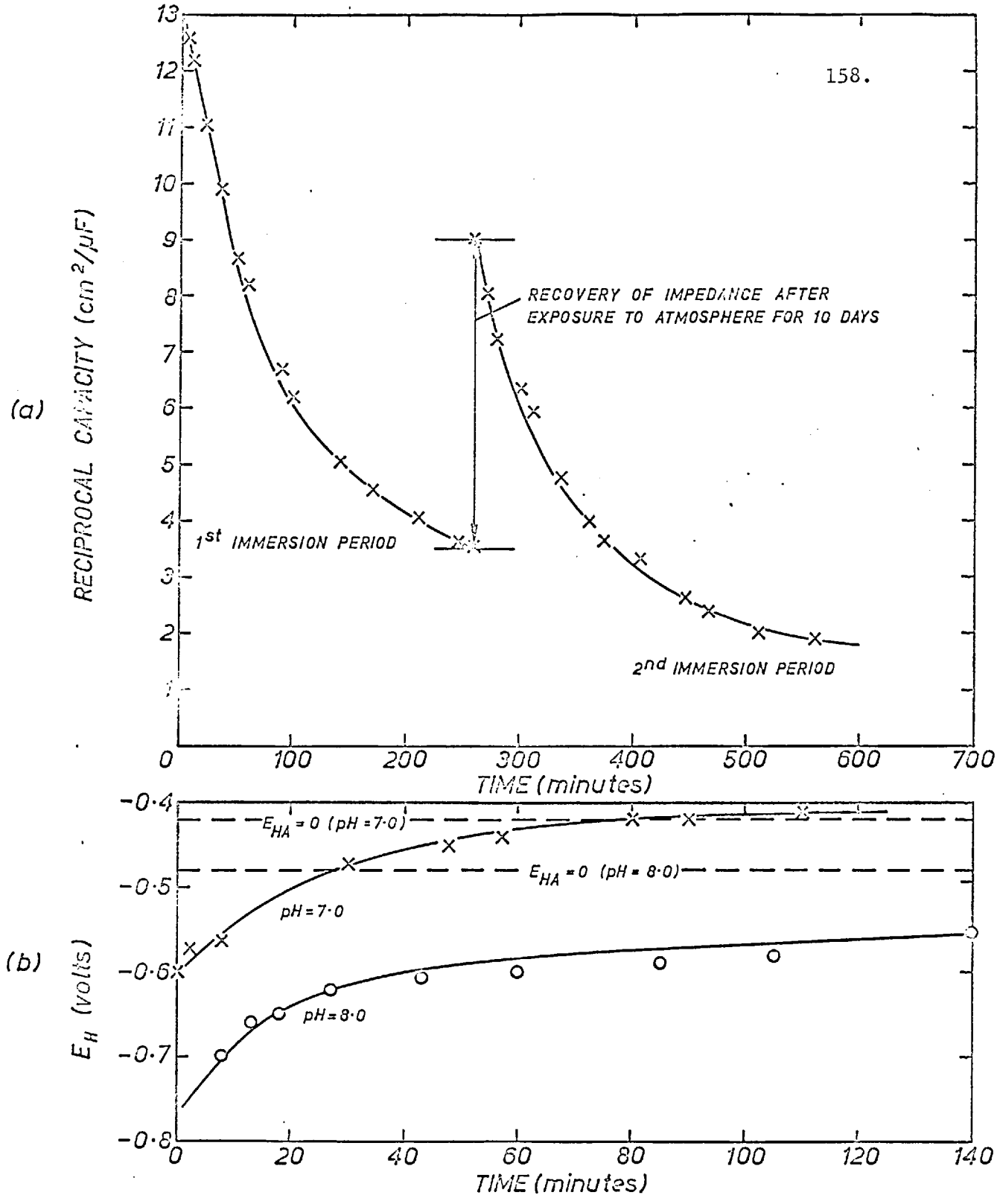

Figure 16. (a) Decrease in capacitive thickness during immersion of a 100v. anodic film in pH=9 N/10 K_2CrO_4

(b) Rest potential of a "bare" Al electrode during immersion in N/10 K_2CrO_4

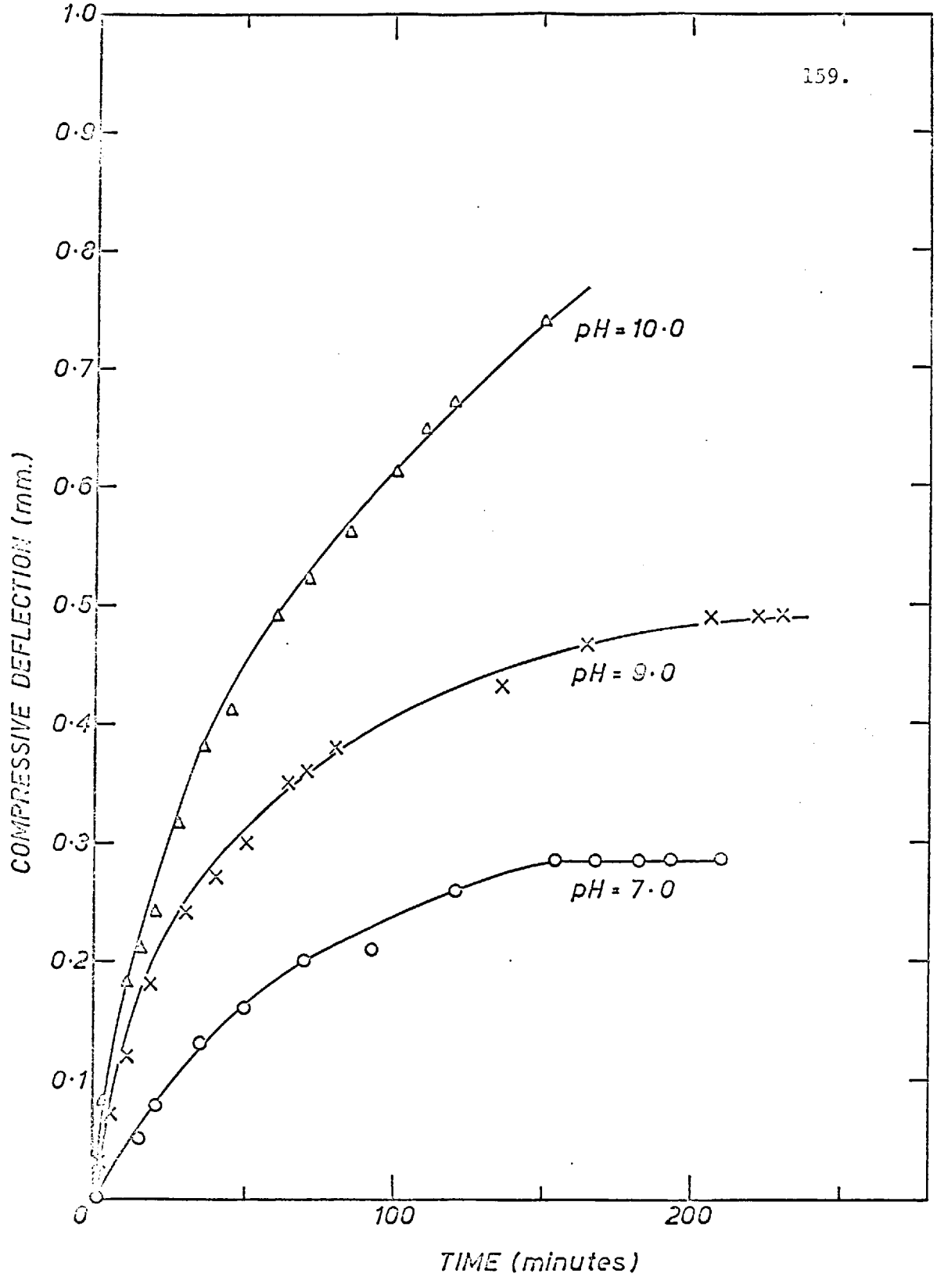

Fig. 17. *Compressive deflection of Al foils (bearing 100v. anodic films) during immersion in N/10 K_2CrO_4.*

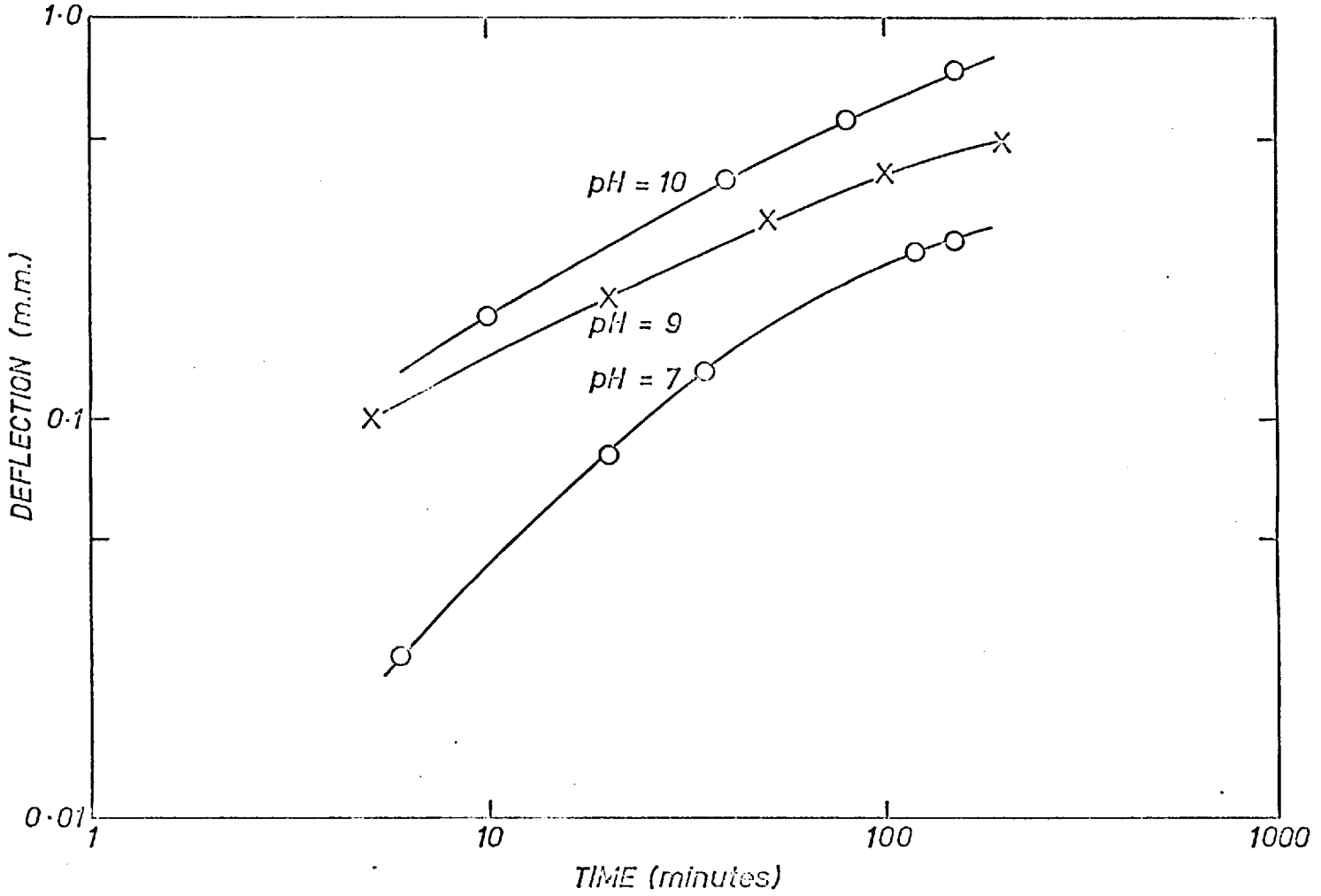

Figure 18. Deflection of anodised aluminium foils in alkaline chromate solutions.

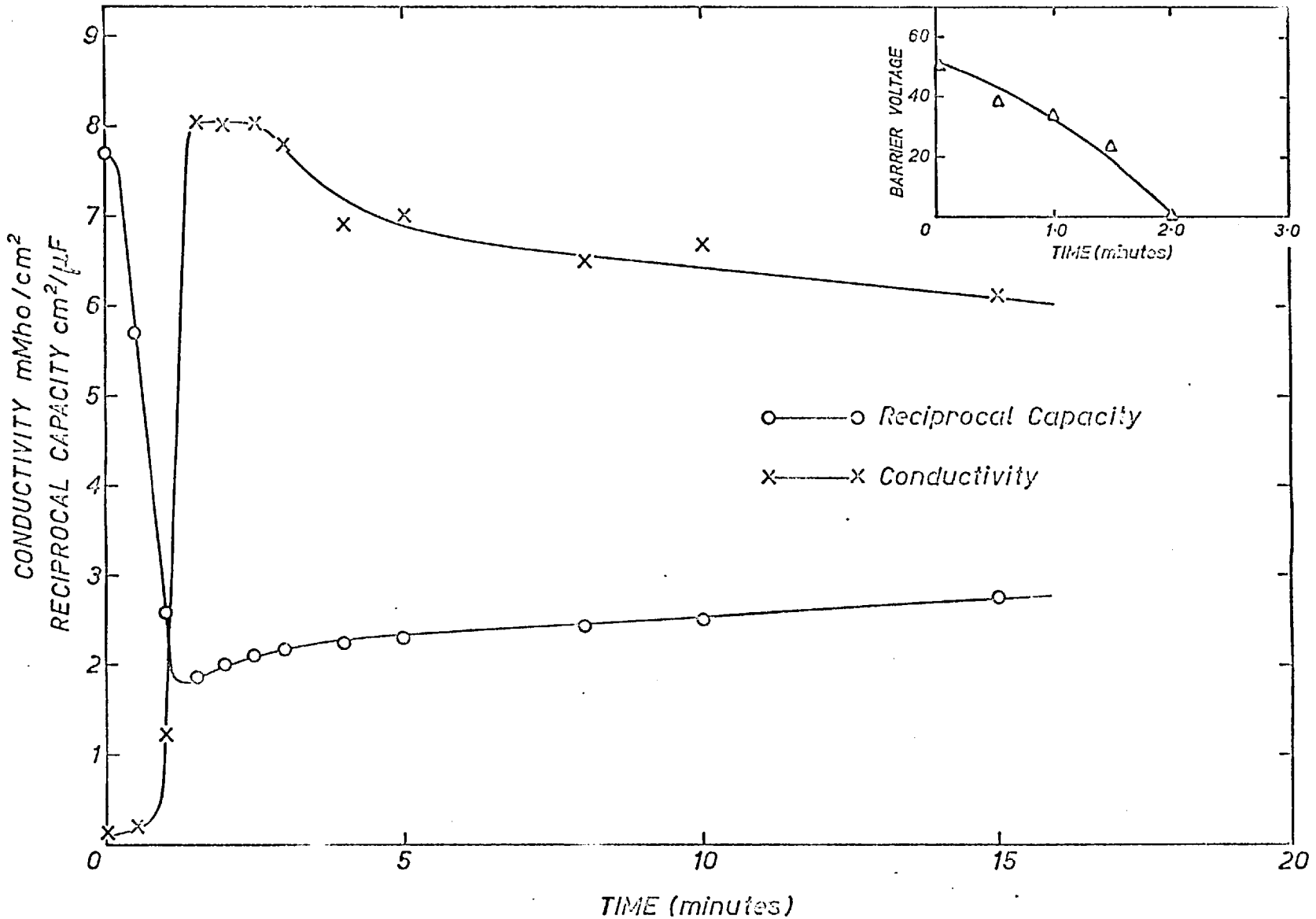

Figure 19. *Impedance of 50v. anodic film during boiling in pH = 8·0 distilled H_2O*

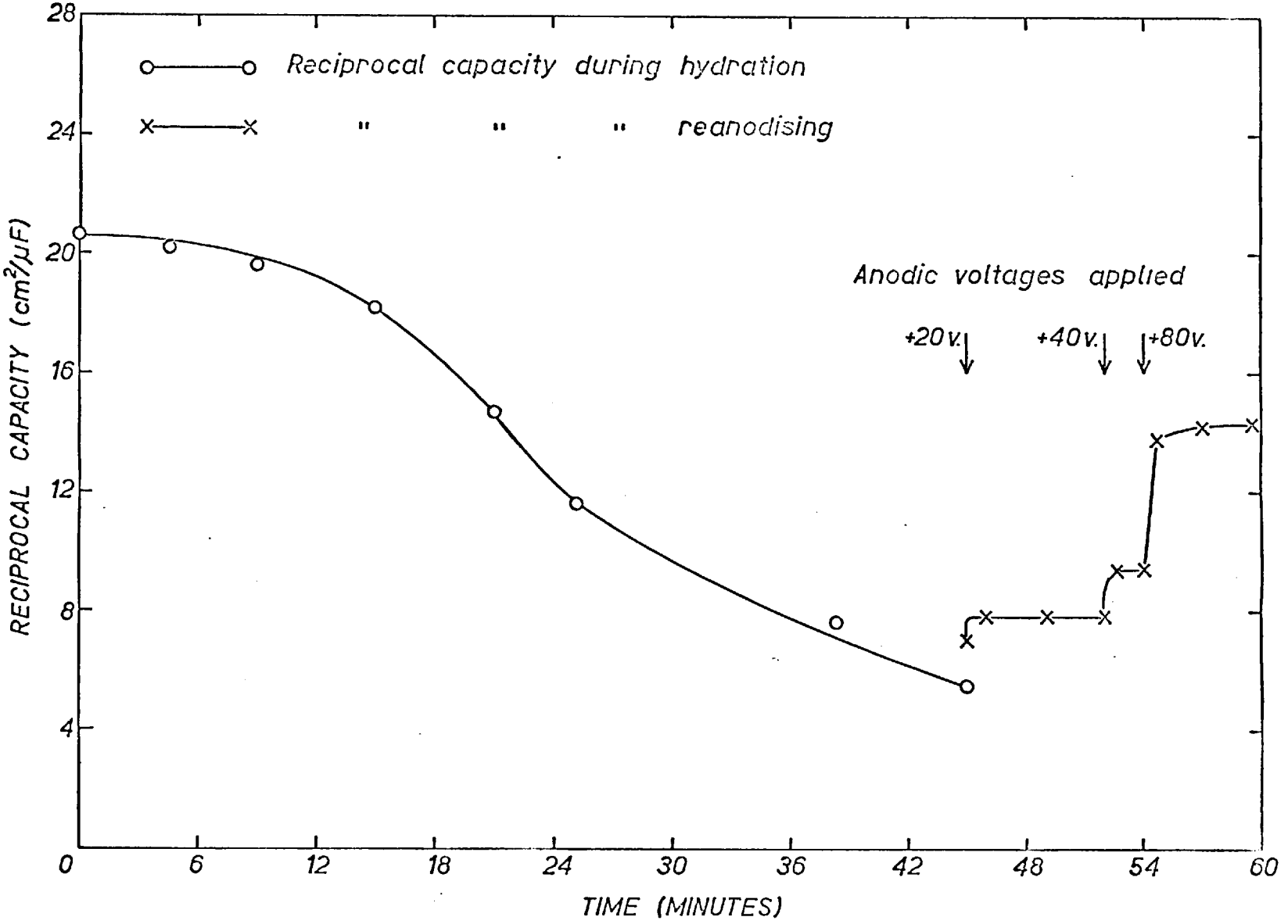

Figure 20a. Changes in reciprocal capacitance of a 150 volt anodic film during hydration in H_2O at 80°C and reanodising at room temperature.

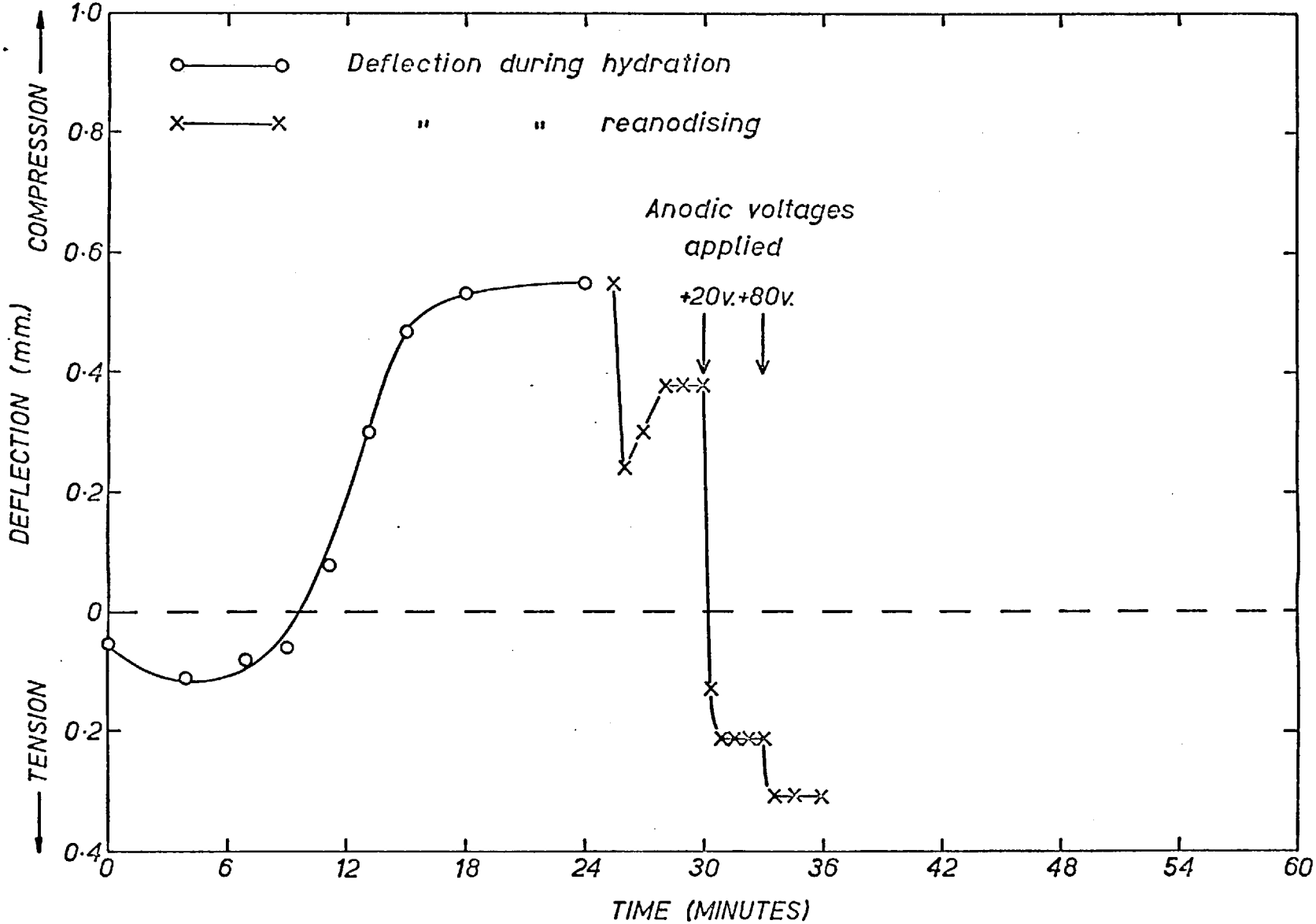

Figure 20b. Deflection of aluminium foil (bearing 150 volt film) during hydration at 90°C and reanodising at room temperature.

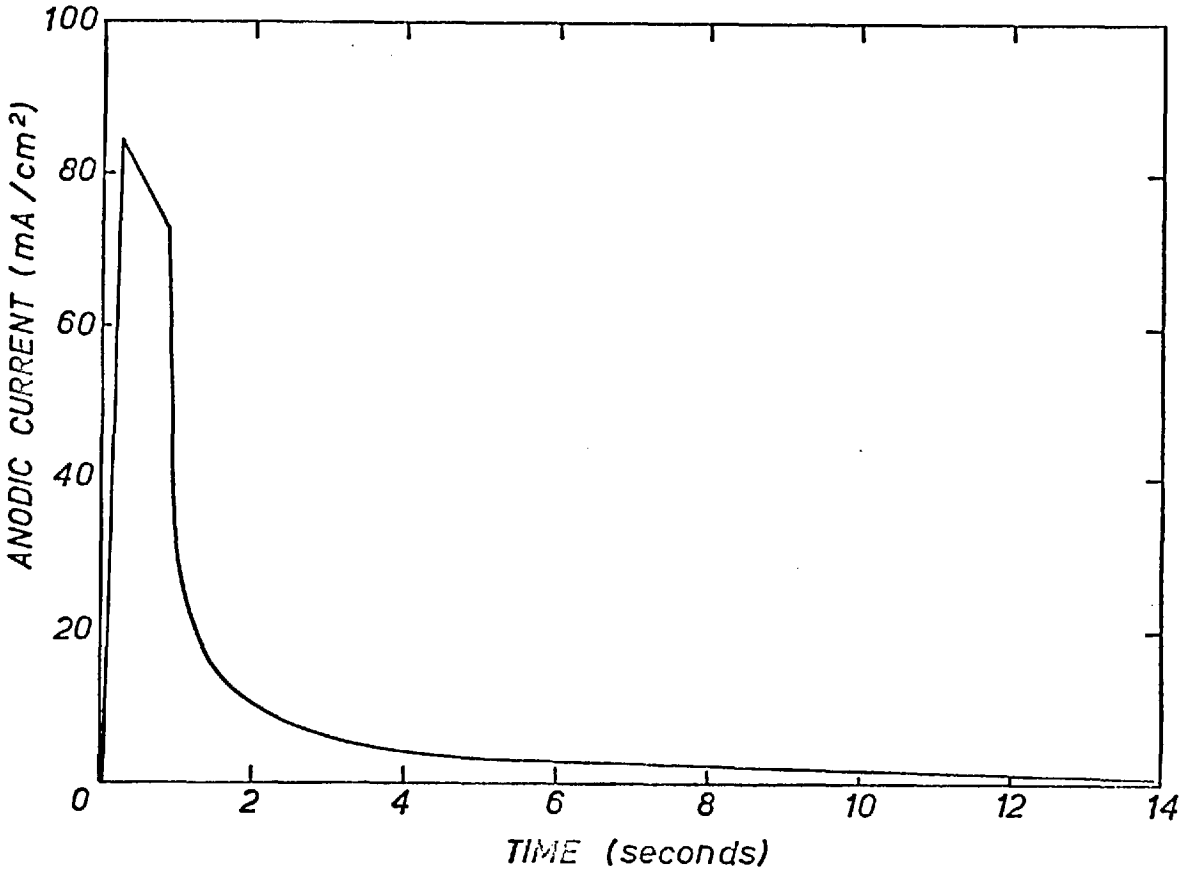

Figure 21. Current Response of a hydrated anodic alumina film (grown to 100 volts) under 40 volts constant anodic polarisation.

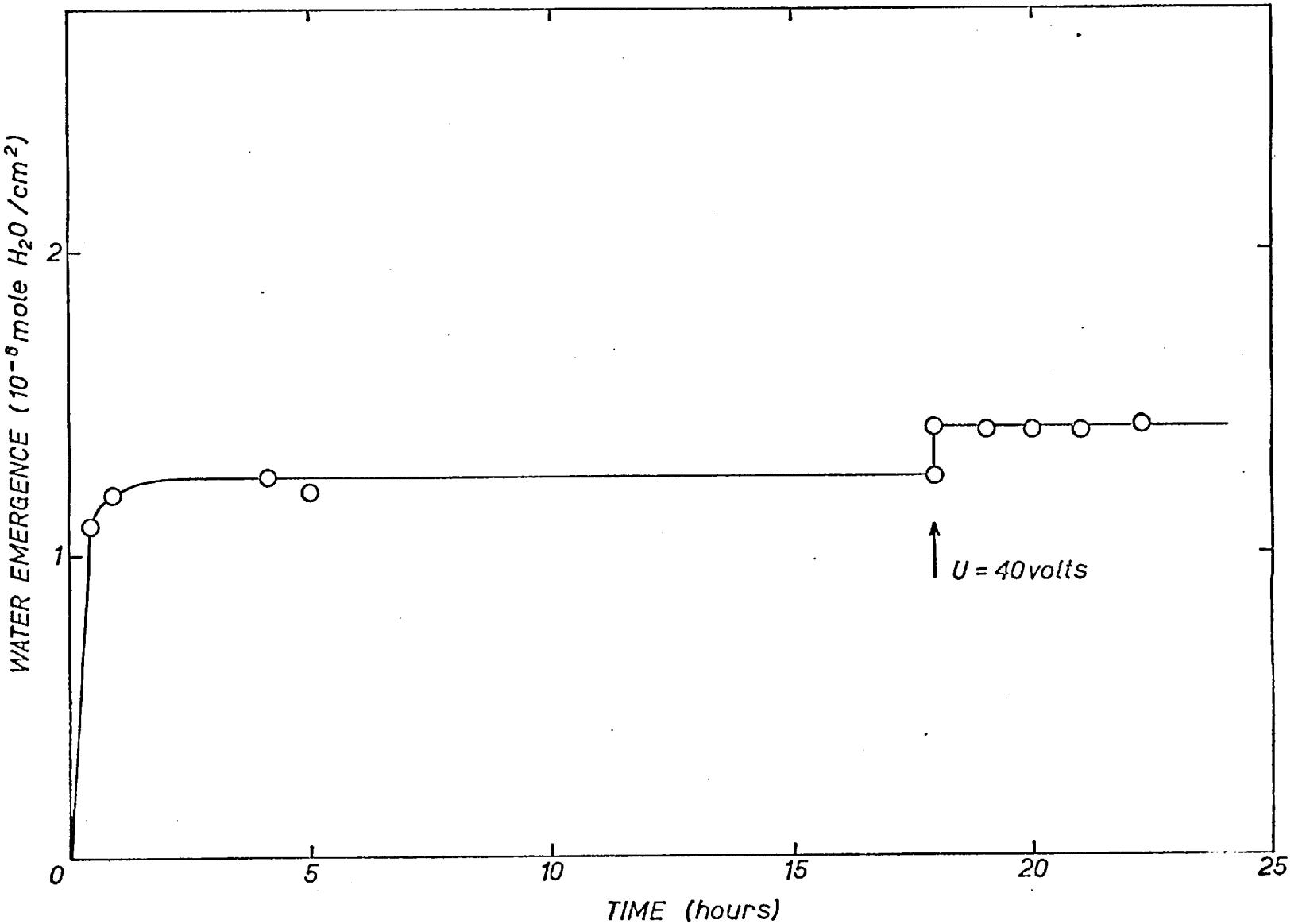

Figure 22. Dehydration of aluminium anode in ammonium borate solution (after Schwabe).

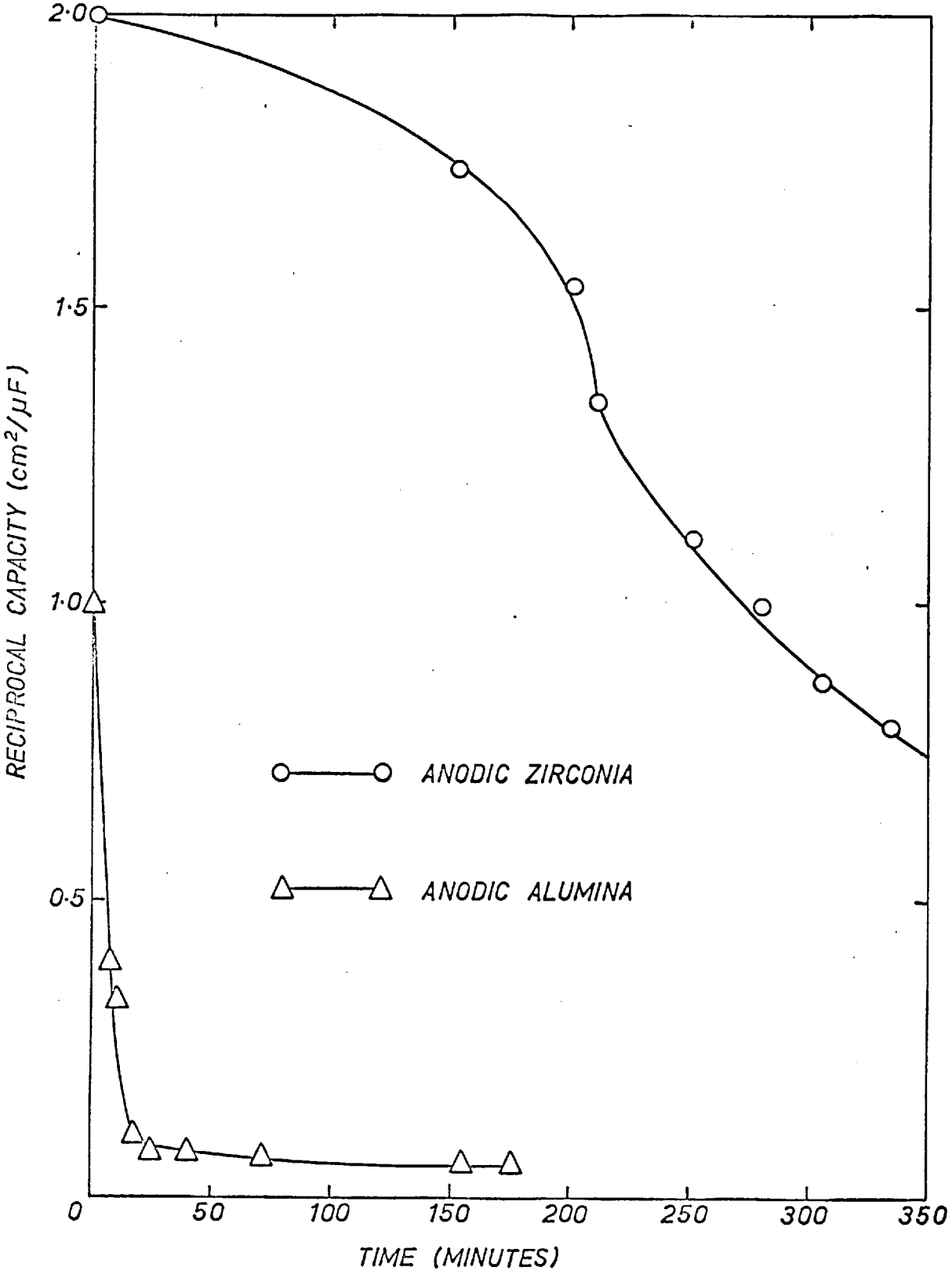

Figure 23. Change in reciprocal capacity of anodic films during cathodic polarisation.

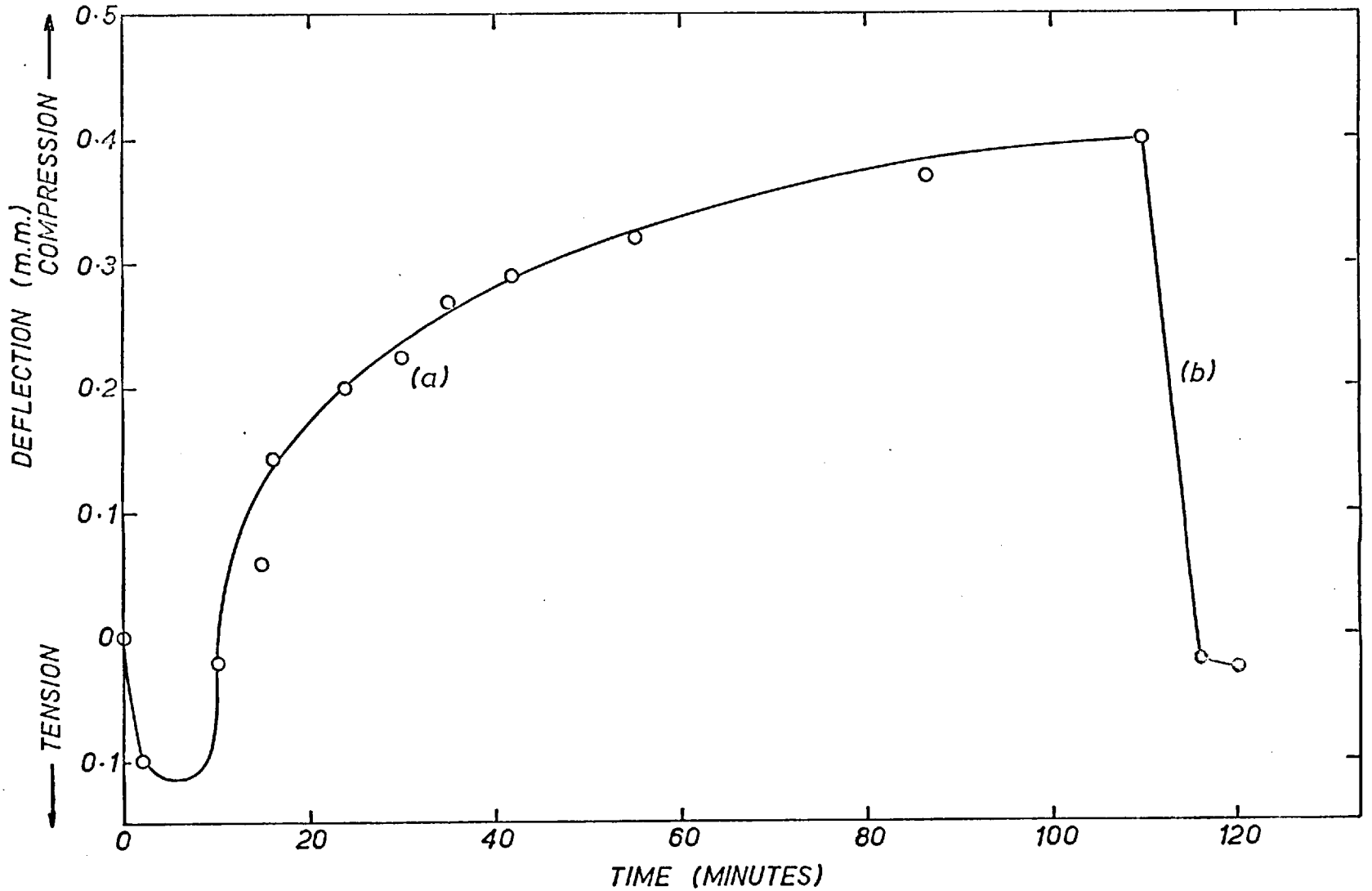

Figure 24. Deflection of aluminium foil (bearing a 150 volt film) during (a) cathodic polarisation at -7.0 mA/cm.^{2}, and (b) the application of 1.0 mA/cm.^{2} anodic current.

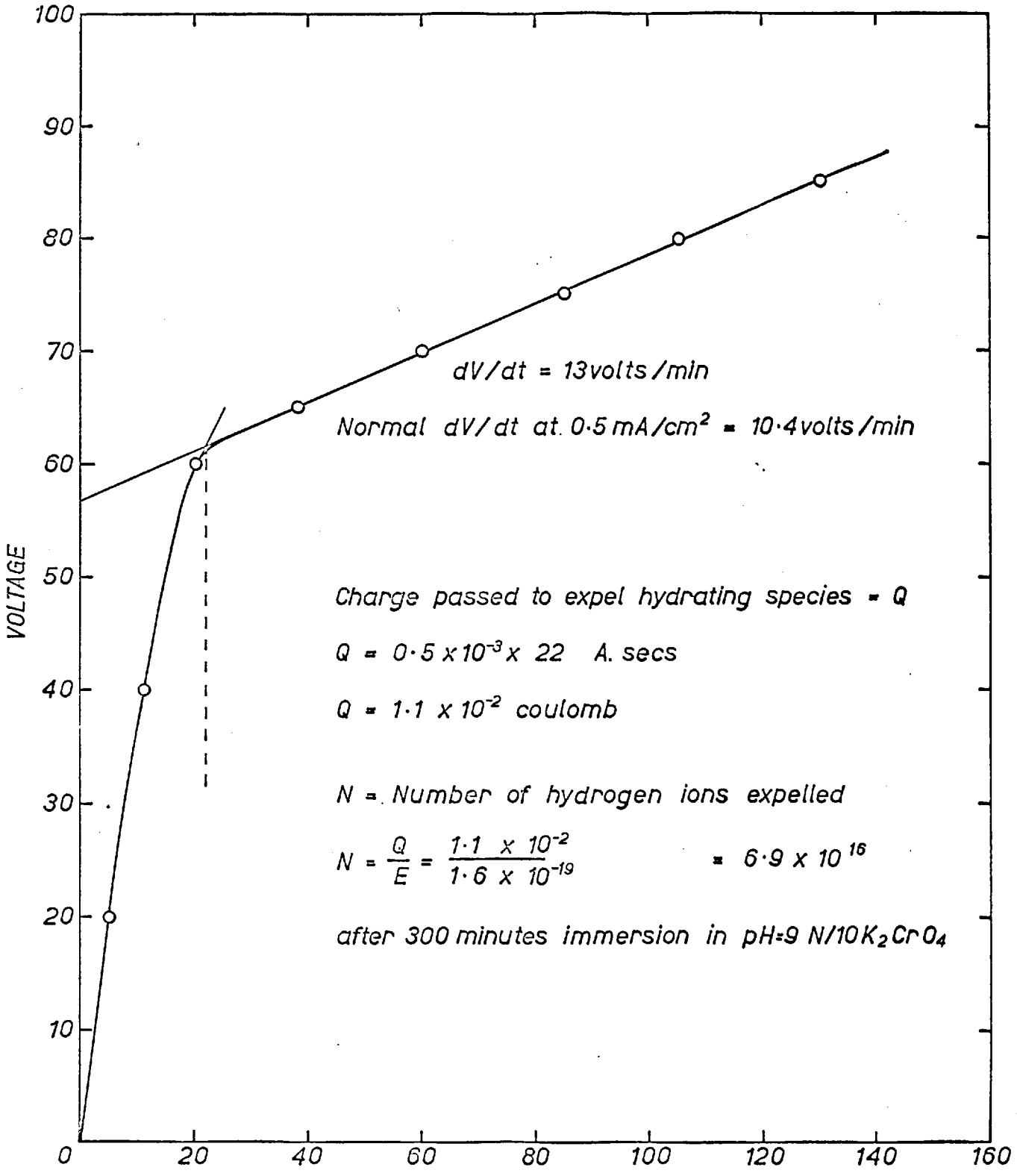

Figure 25. Anodisation of 100 volt anodic alumina film after immersion in pH = 10K_2CrO_4.

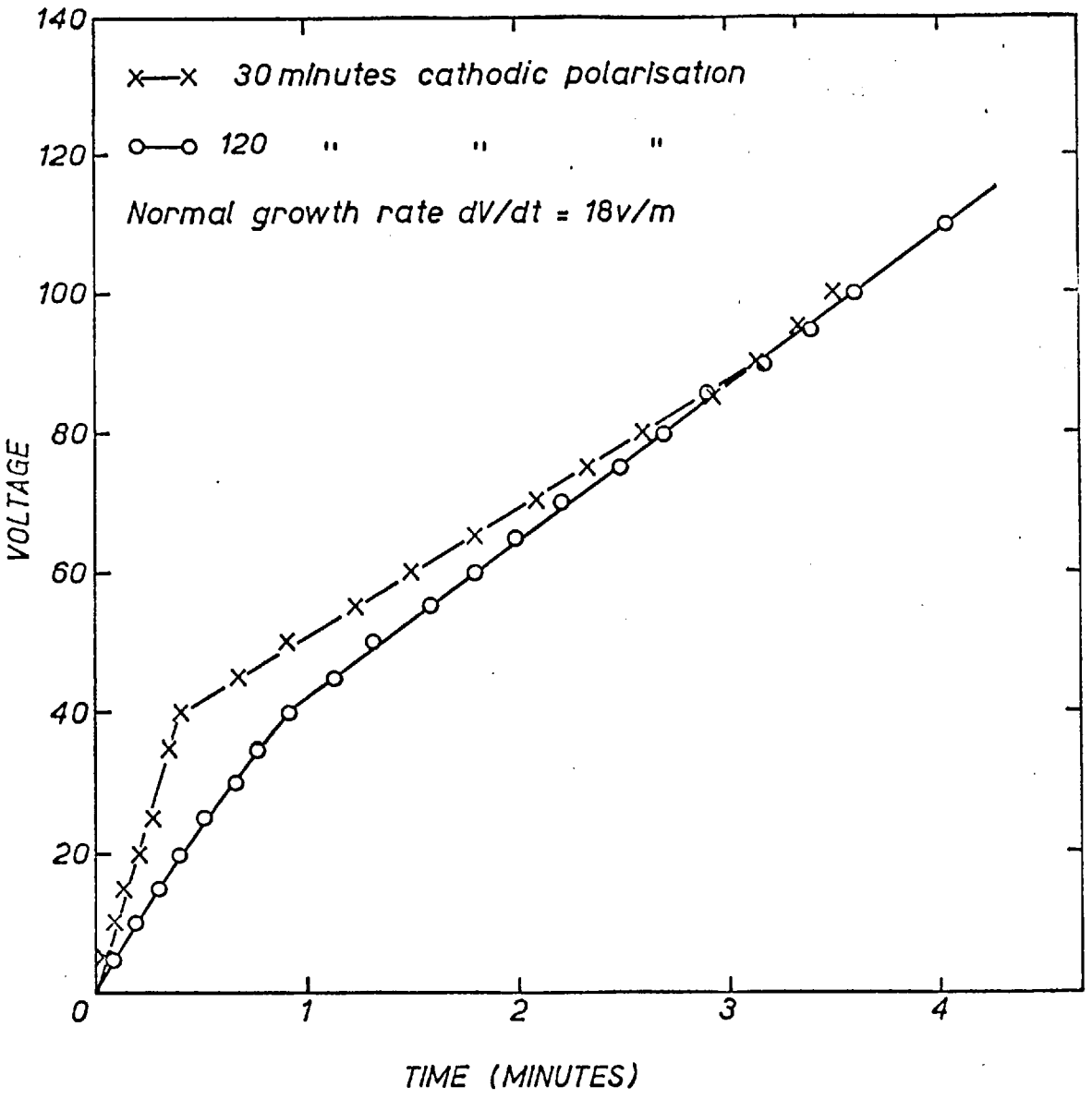

Figure 26. The voltage response during reanodising at 1.0 mA/cm.^{2} of a 40 volt anodic film which had previously been cathodised at -1.0 mA/cm.^{2} in O_2-free pH = 6.0 ammonium citrate.

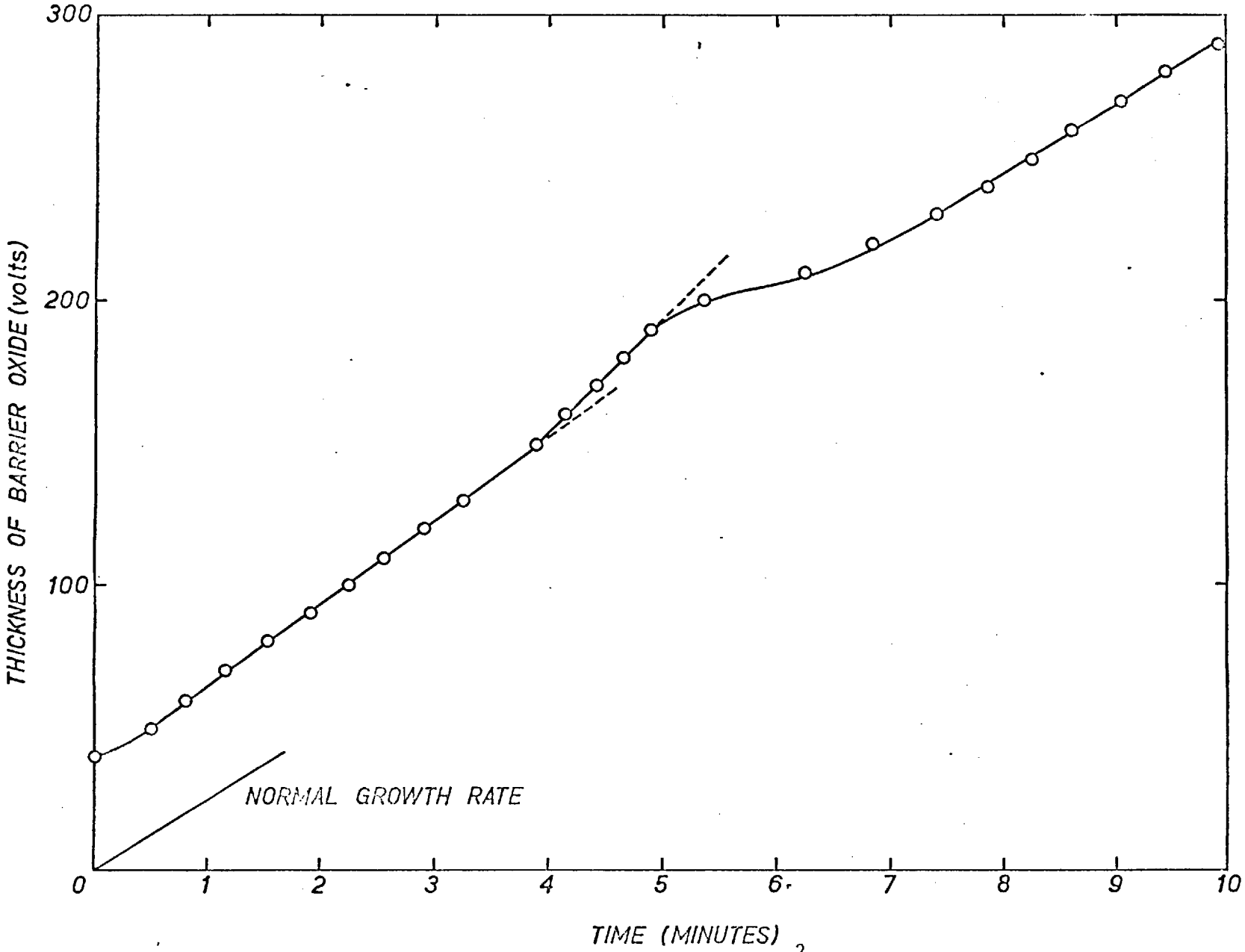

Figure 27. Voltage increase during the application of 1.0 mA/cm.^{2} anodic current to a 40 volt anodic alumina film previously cathodised at -0.25 mA/cm.^{2} for 2 hours and then left exposed to the atmospher

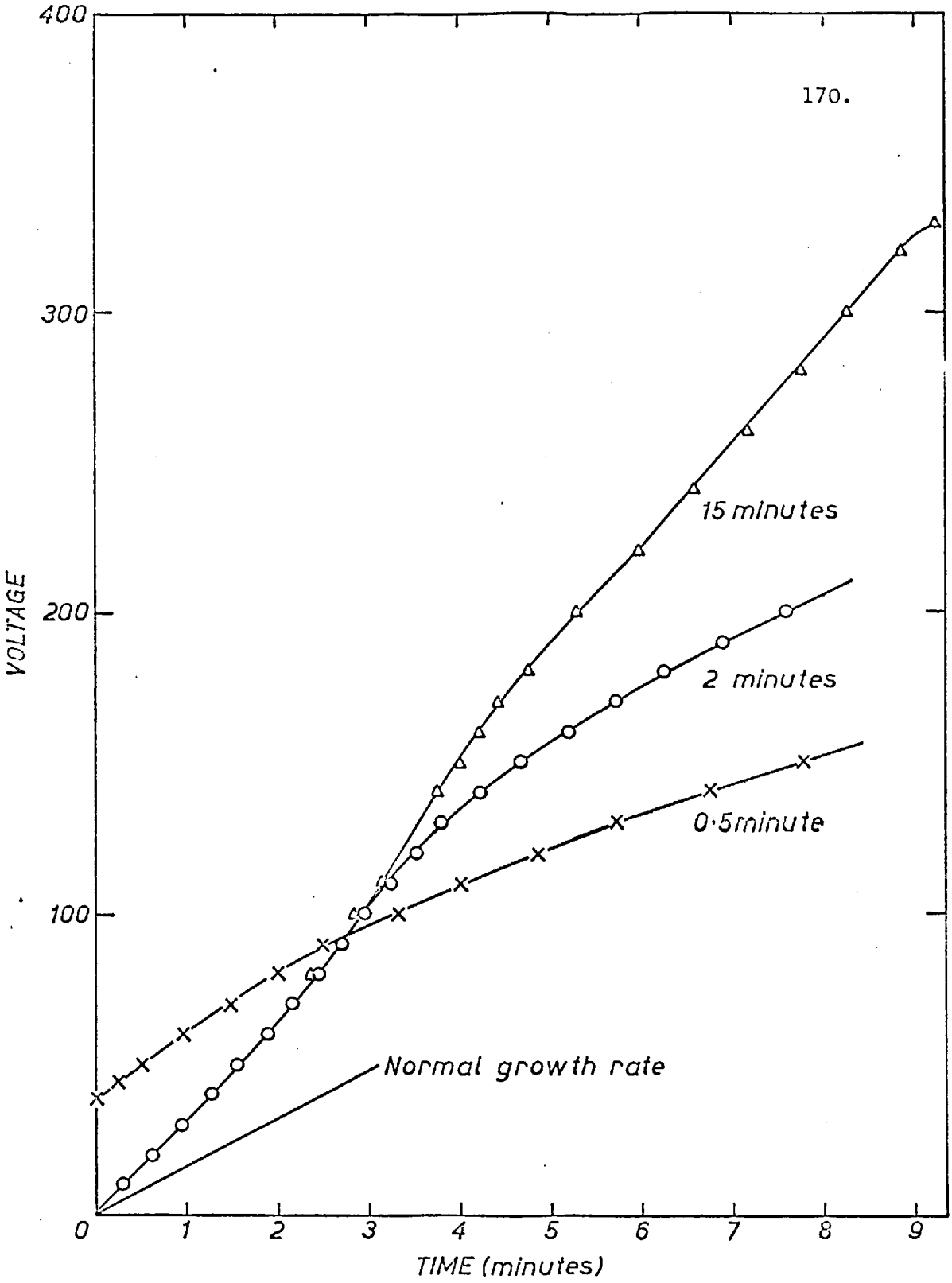

Figure 28. *Voltage increase during the application of 1·0 mA/cm² anodic current to a 50v. anodic alumina film previously hydrated by boiling in pH=8·0 H_2O for various times.*

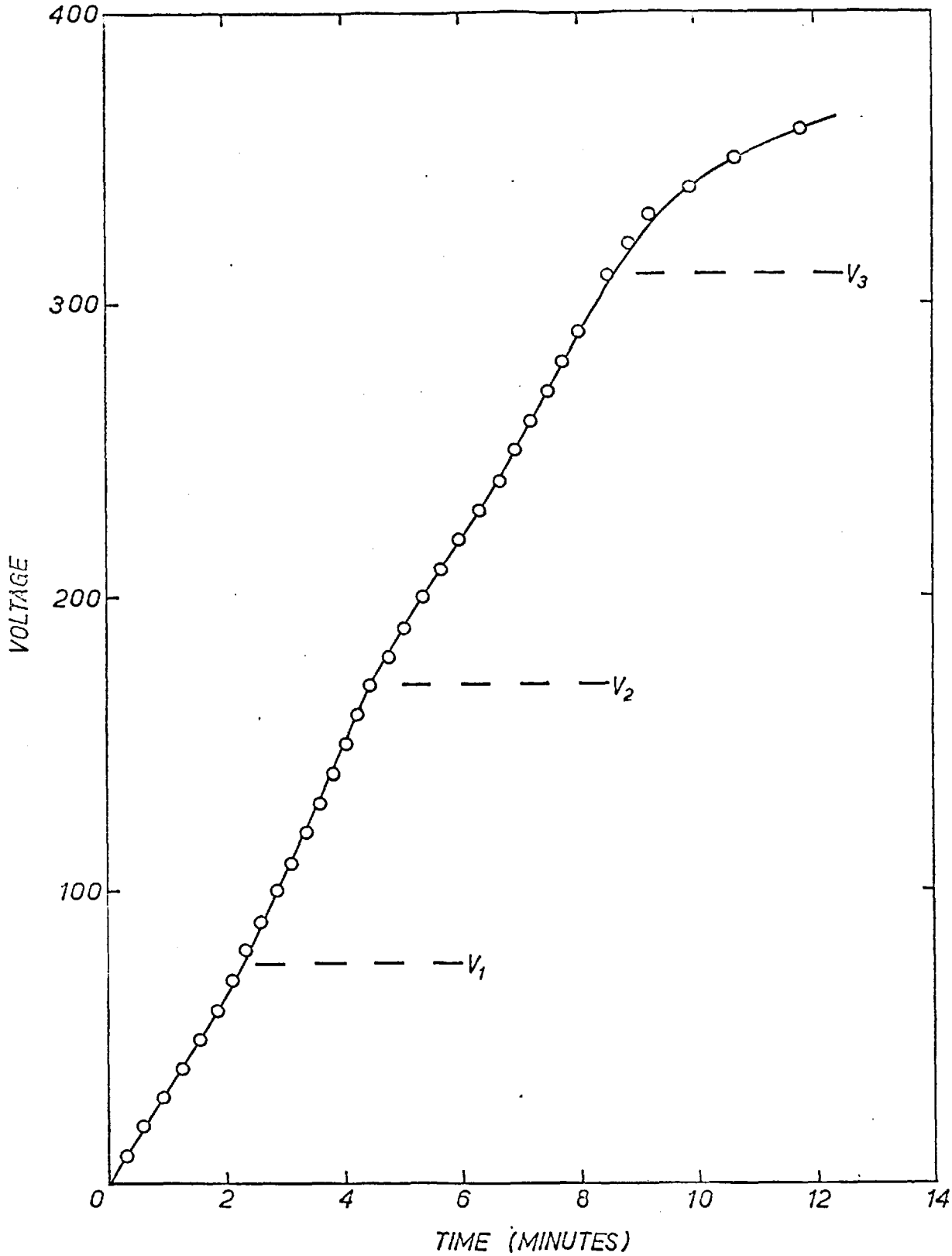

Figure 29. Voltage increase during the application of 1.0 mA/cm.^{2} anodic current to a 50 volt anodic alumina film previously boiled for 1 hour in pH = 8.0 water.

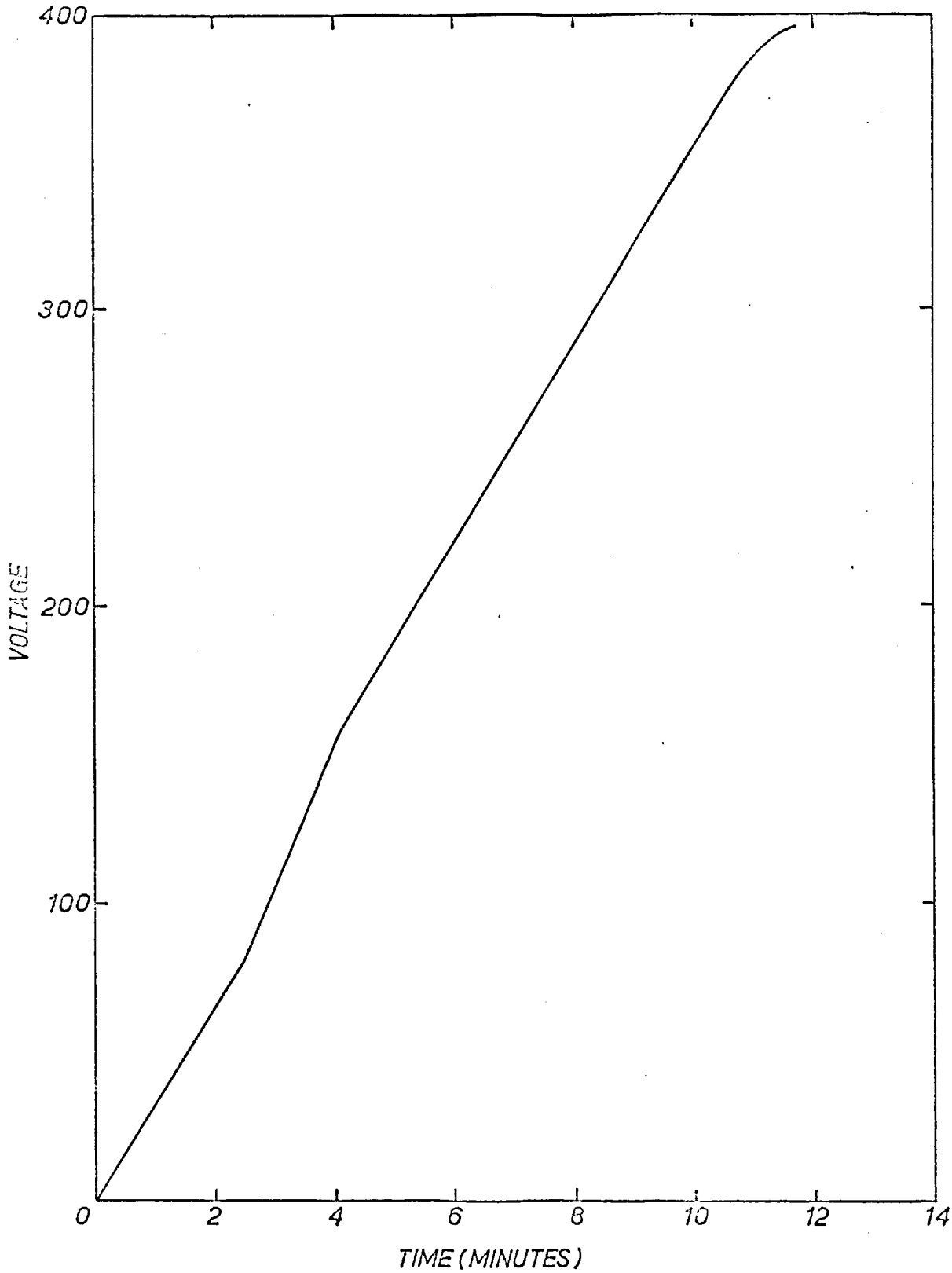

Figure 30. Anodisation at 1.0 mA/cm.^{2} of aluminium after 30 minutes boiling in pH = 9 water.

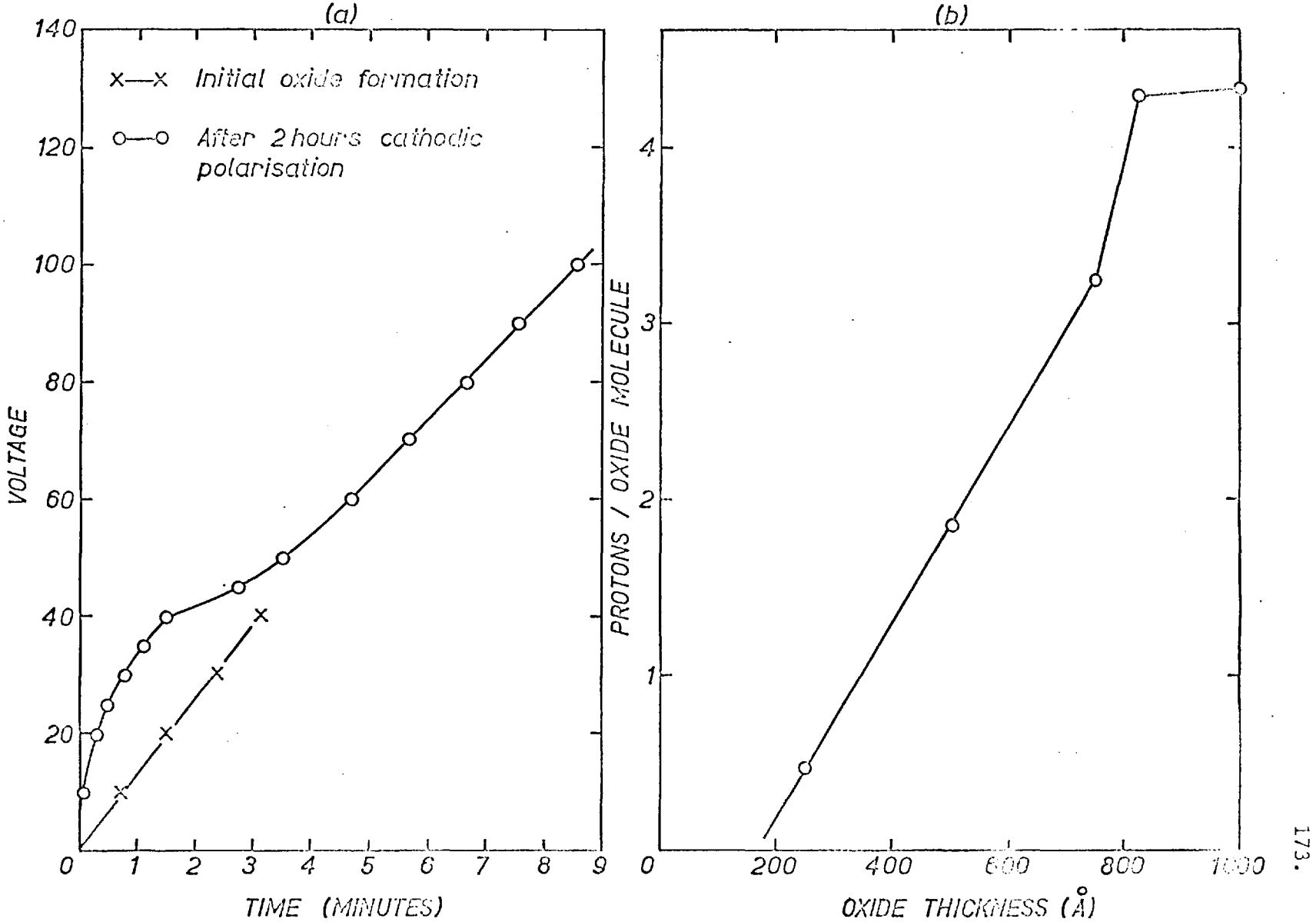

Figure 31. (a) Voltage response during anodisation at 1.0 mA/cm.^{2} of a 40 volt zirconia film, following cathodic polarisation at -0.25 mA/cm.^{2} in O_2-free pH = 5 citrate.

(b) Proton gradient in 40 volt film after 2 hours cathodic polarisation (as 31a).

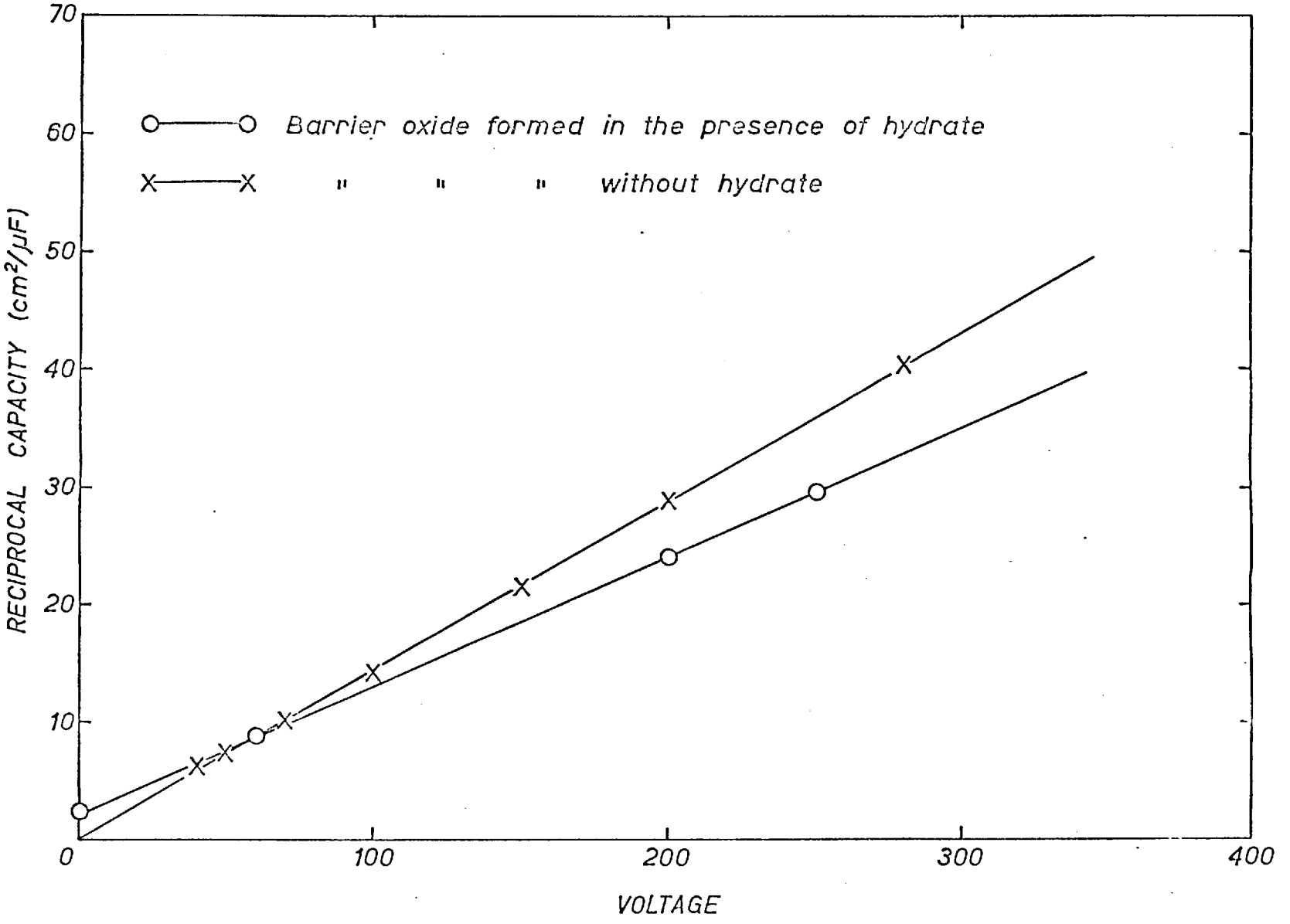

Figure 32. Relationship between reciprocal capacity and barrier voltage during anodising of aluminium at 1.0 mA/cm.^{2}.

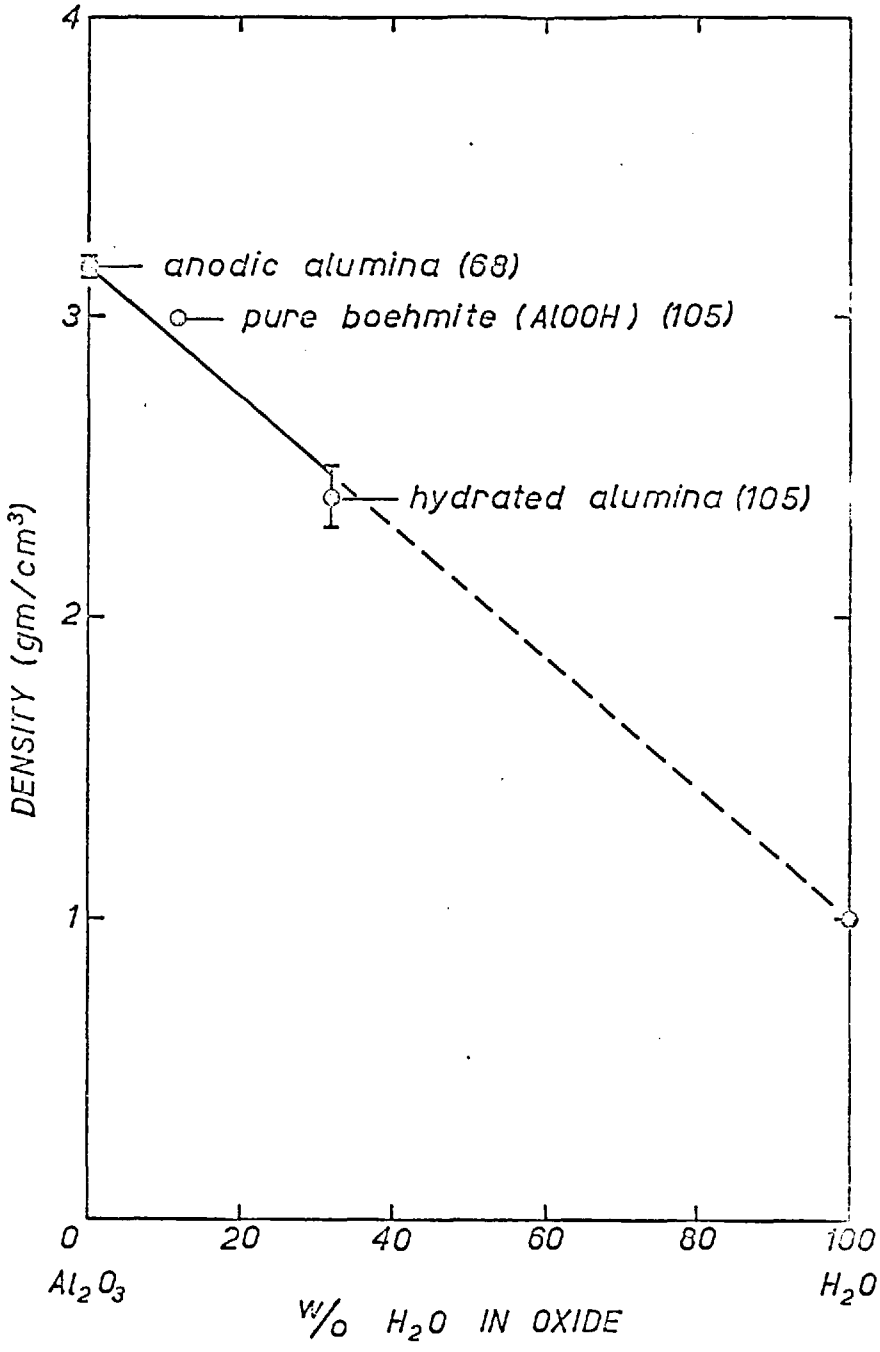

Figure 33. The decrease in density of aluminium oxide with increasing water content.

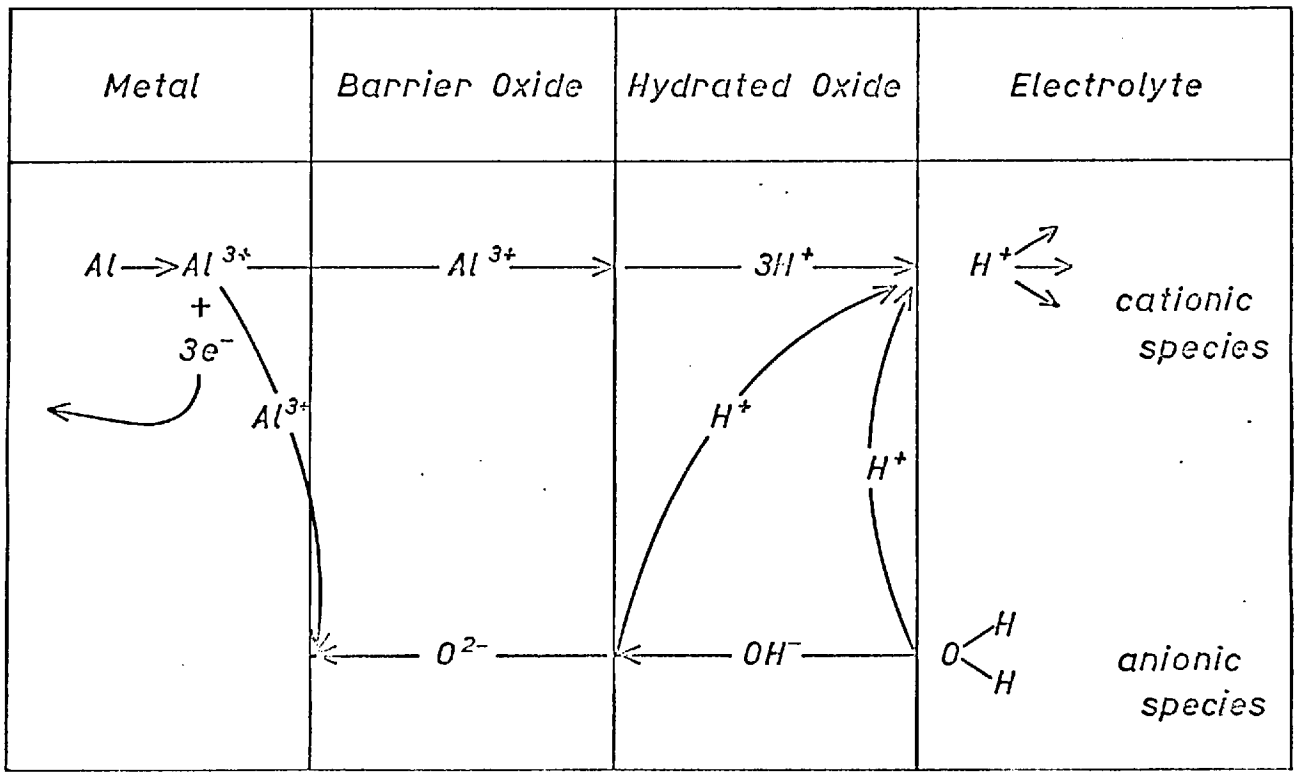

Figure 34. Ionic species mobile during deprotonation.

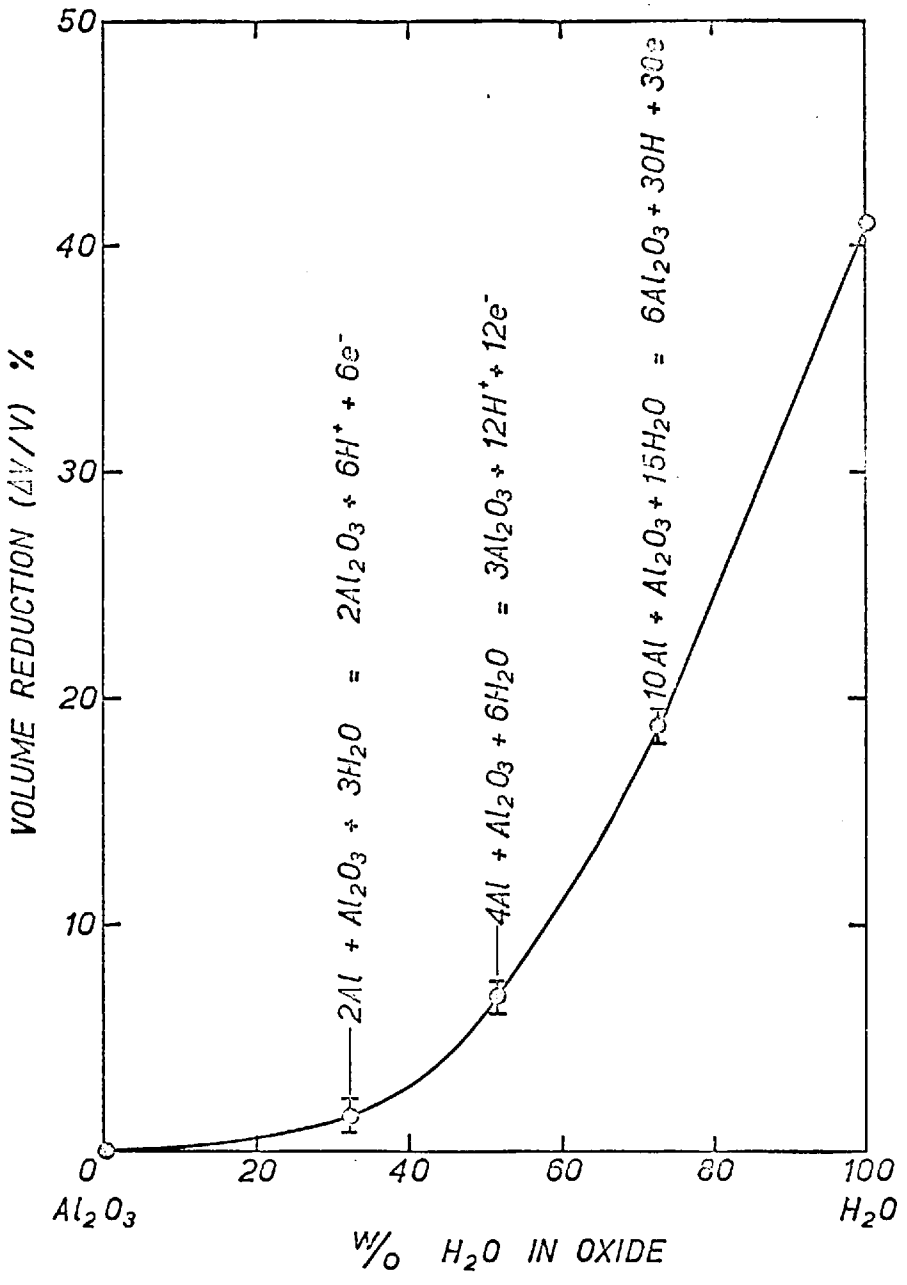

Figure 35. Volume reduction accompanying deprotonation of alumina containing various amounts of water.

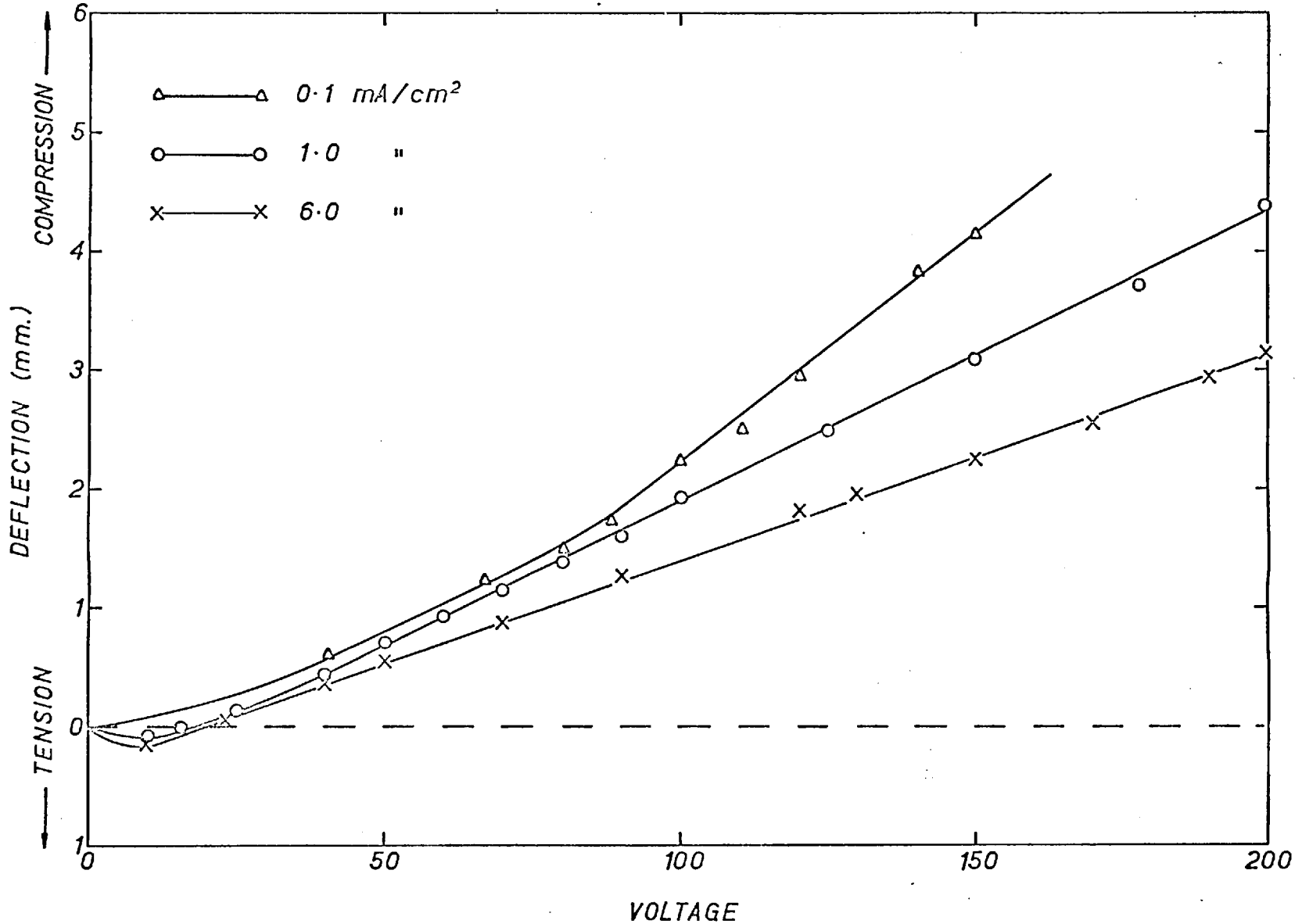

Figure 36. Deflection of zirconium foils during anodising in pH = 9.0 ammonium borate.

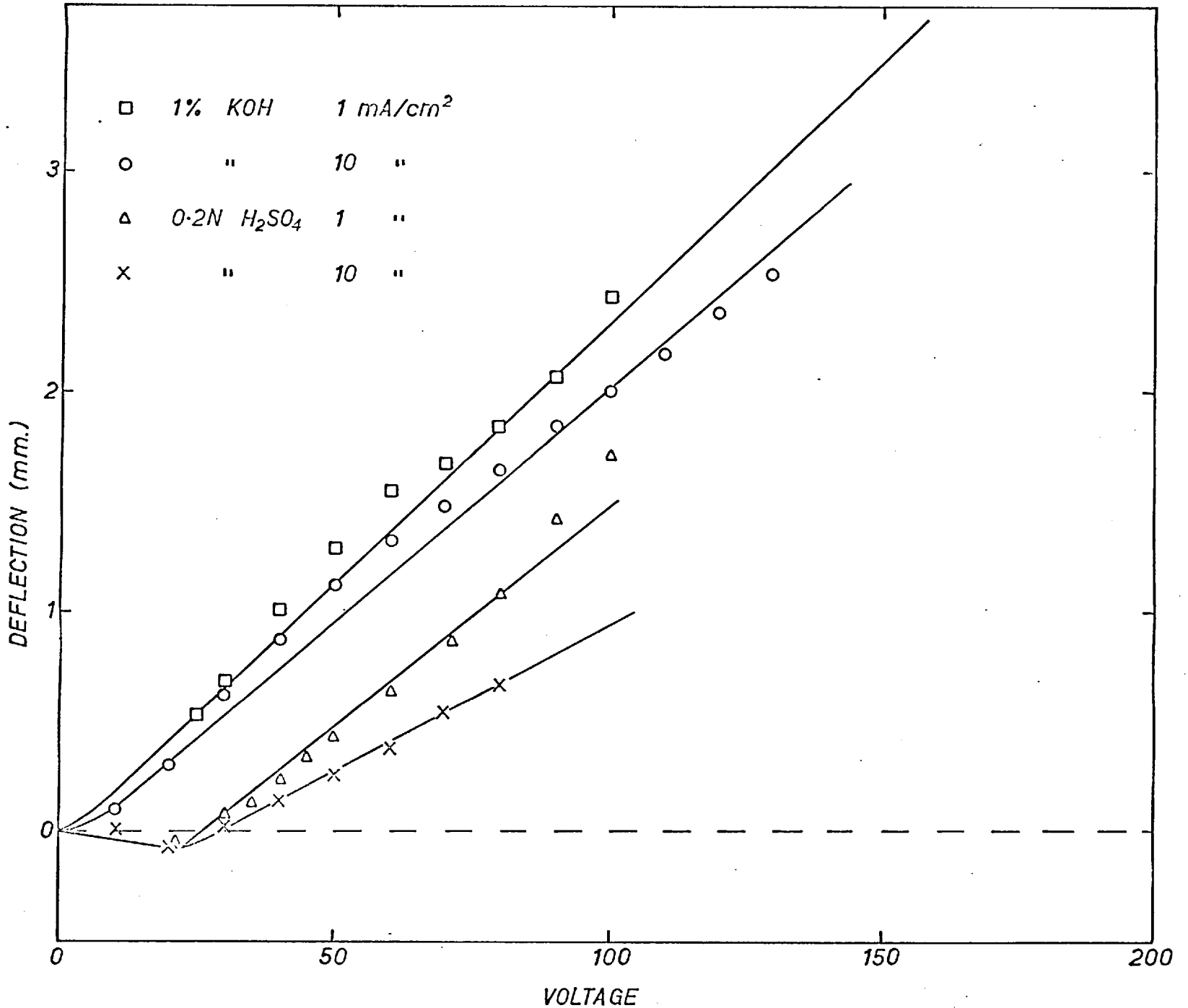

Figure 37. Deflection of zirconium foils during anodising.

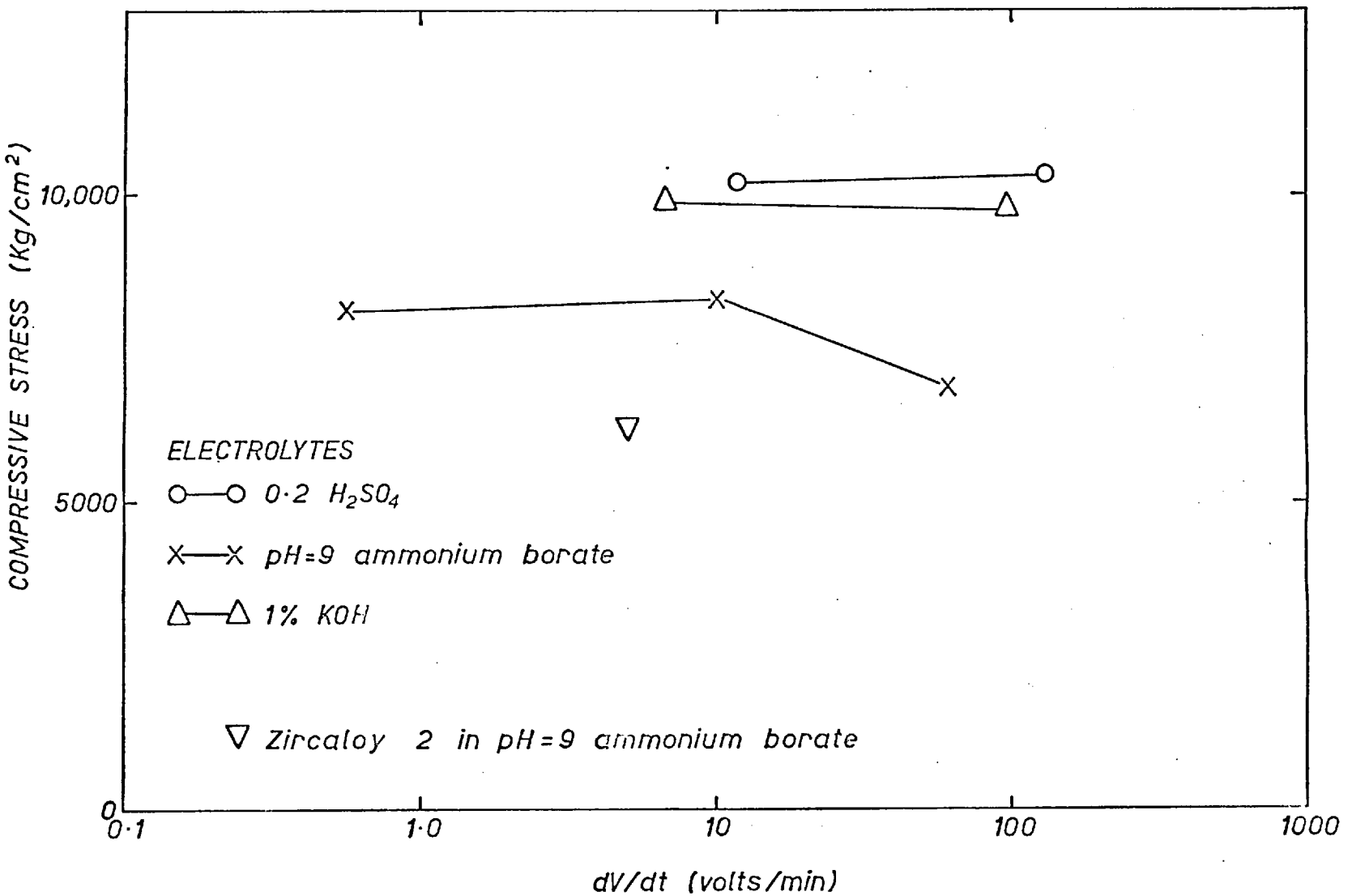

Figure 38. Stress in zirconia plotted vs. growth rate (dV/dt).

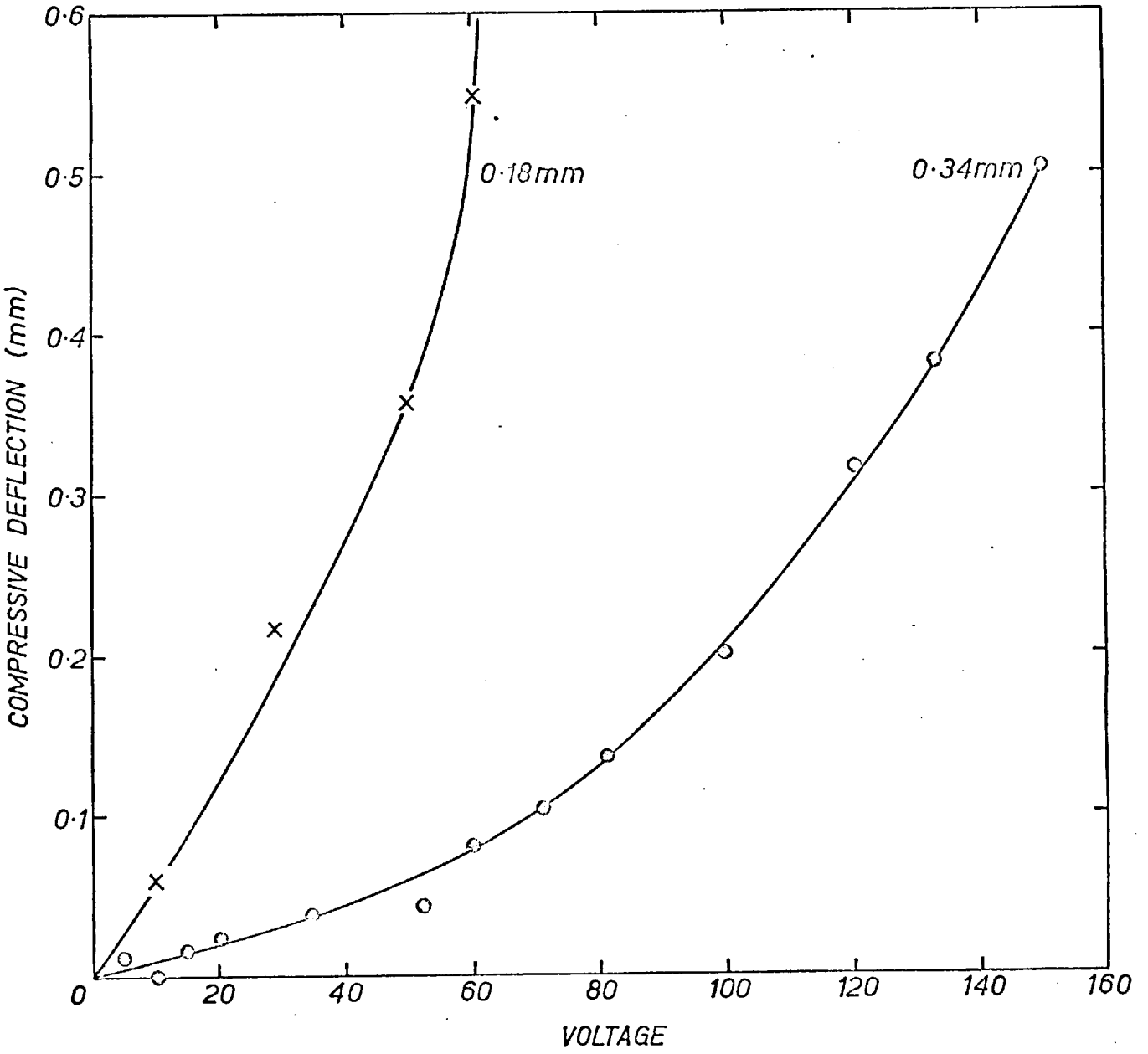

Figure 39. Deflections of Zircaloy 2 foils of different thickness during anodising at 1.0 mA/cm.^{2} in pH = 9.0 ammonium borate.

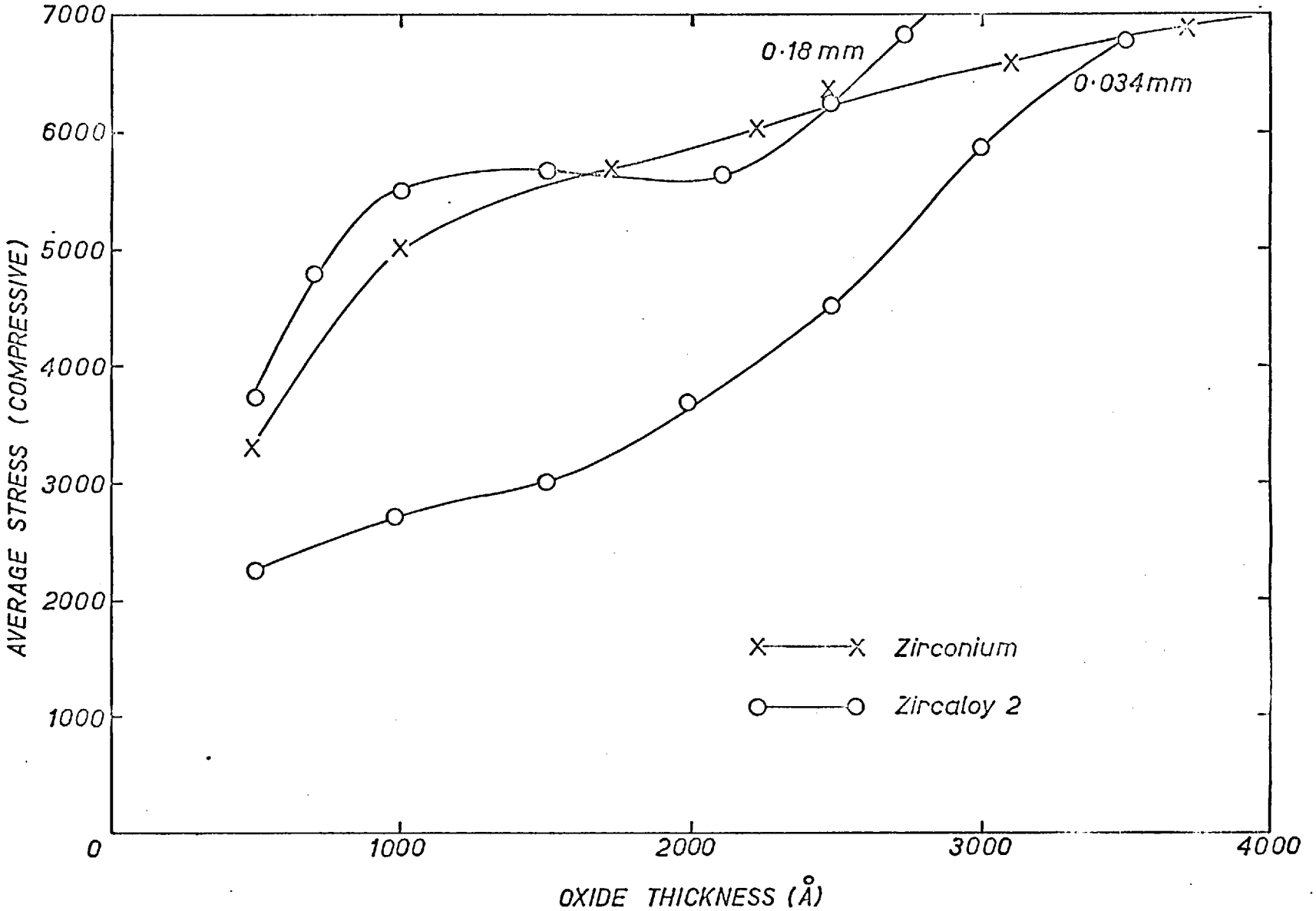

Figure 40. Average stresses generated during anodising of zirconium and Zircaloy 2.

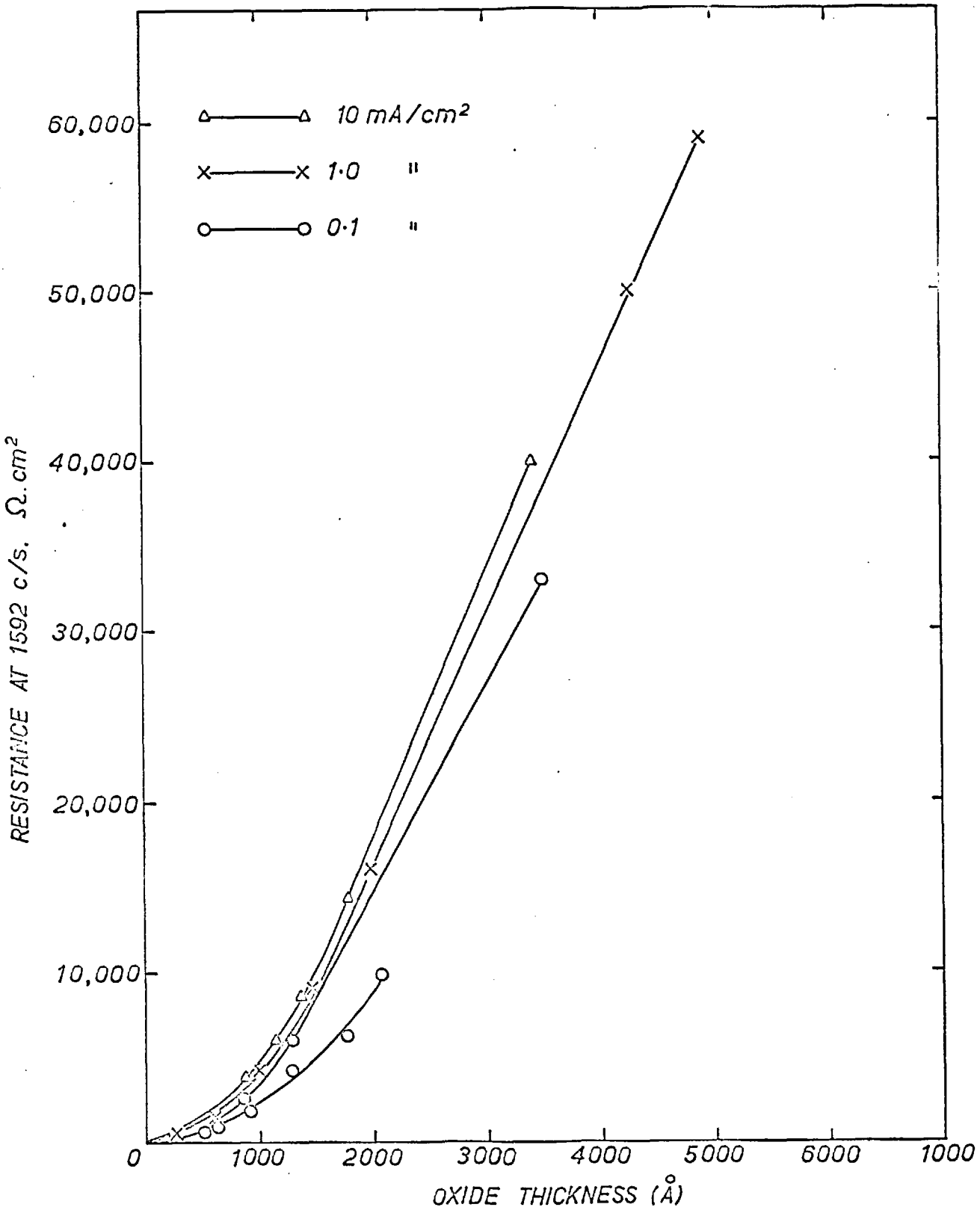

Figure 41. Resistance of anodic films on zirconium grown at different current densities in pH = 9.0 ammonium borate.

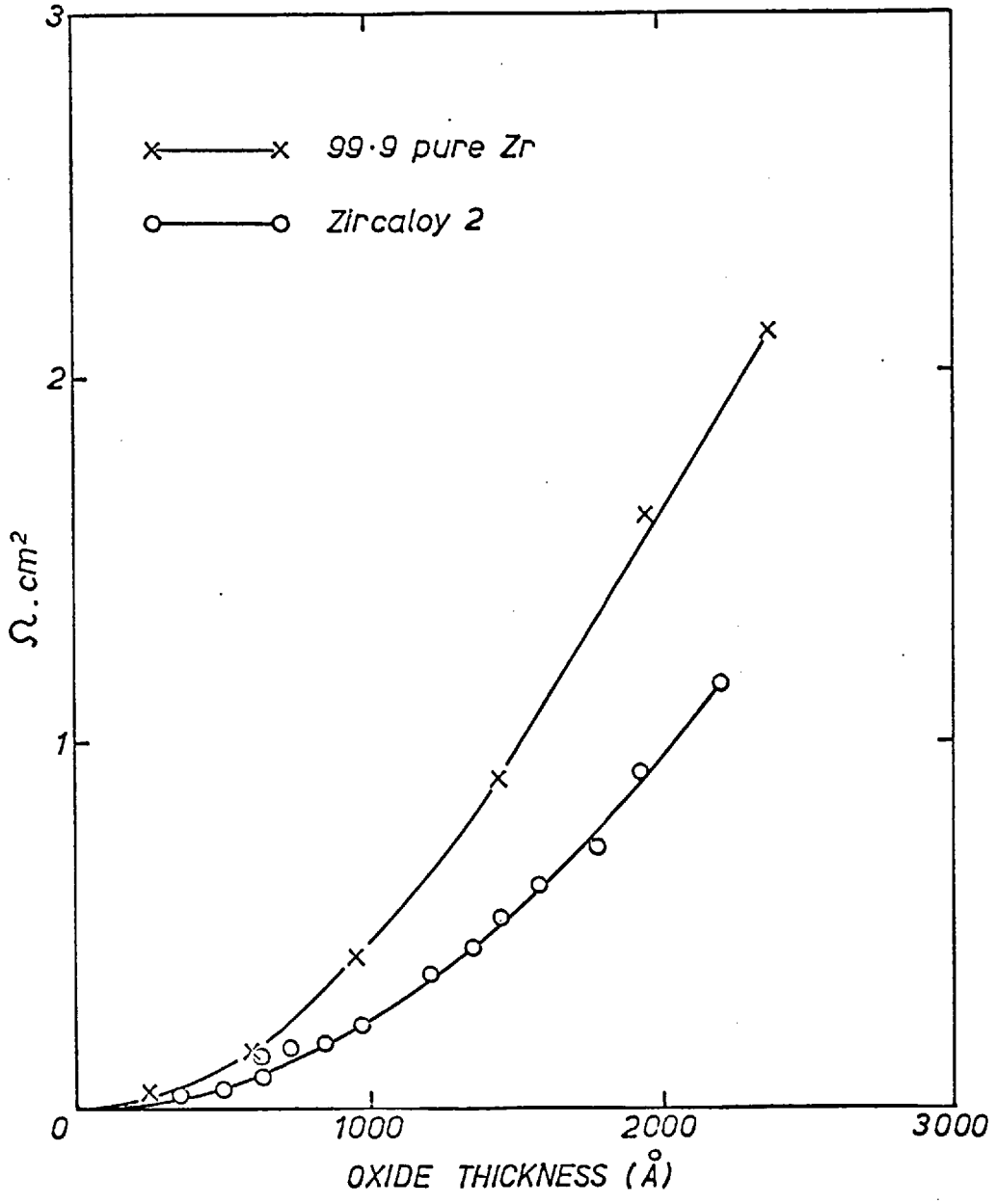

Figure 42. Resistance of anodic film grown at 1.0 mA/cm.^{2} in pH = 9.0 ammonium borate.

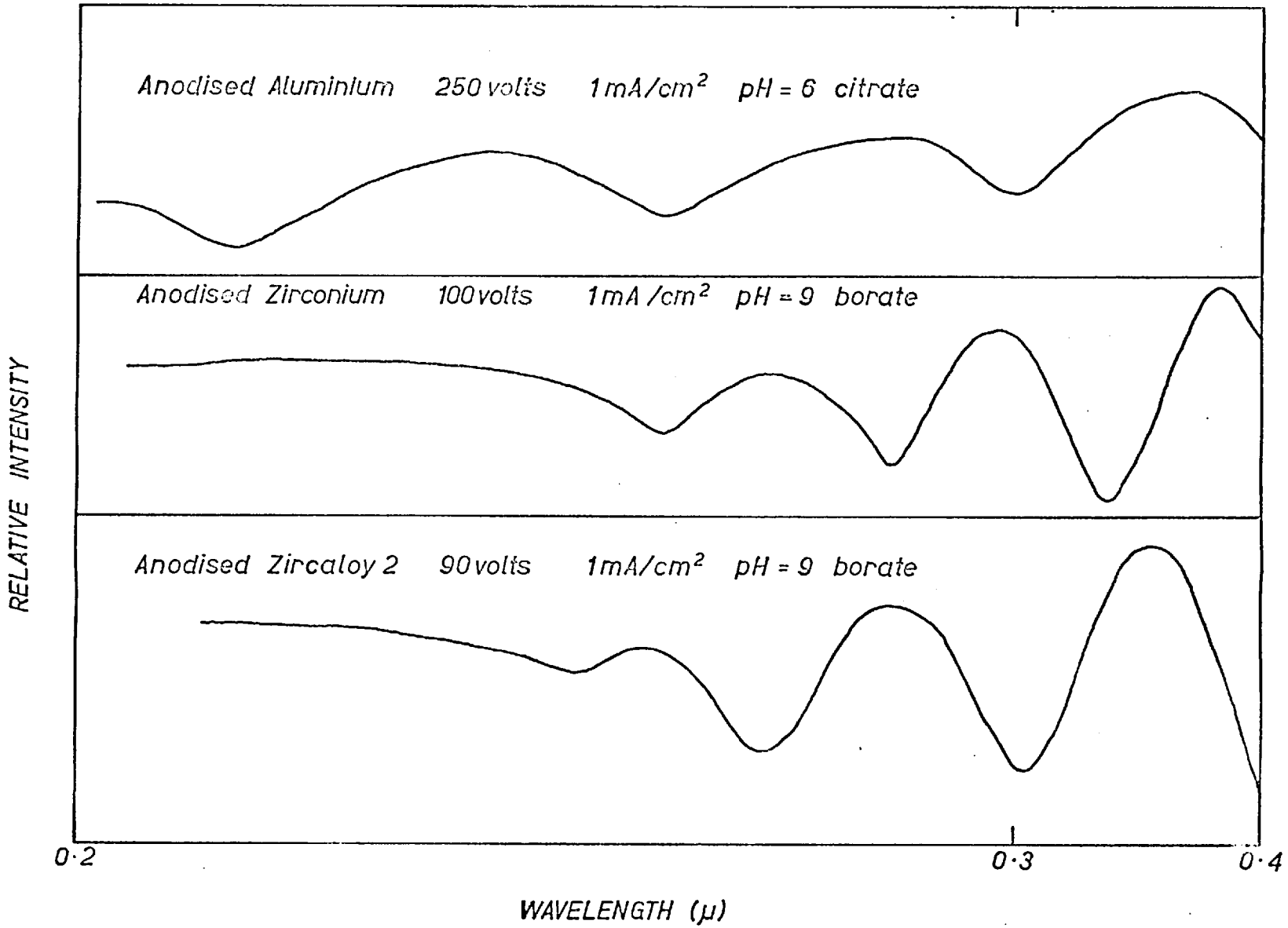

Figure 43. Measurement of oxide thickness by spectrophotometry. Variation in reflected intensity with wavelength.

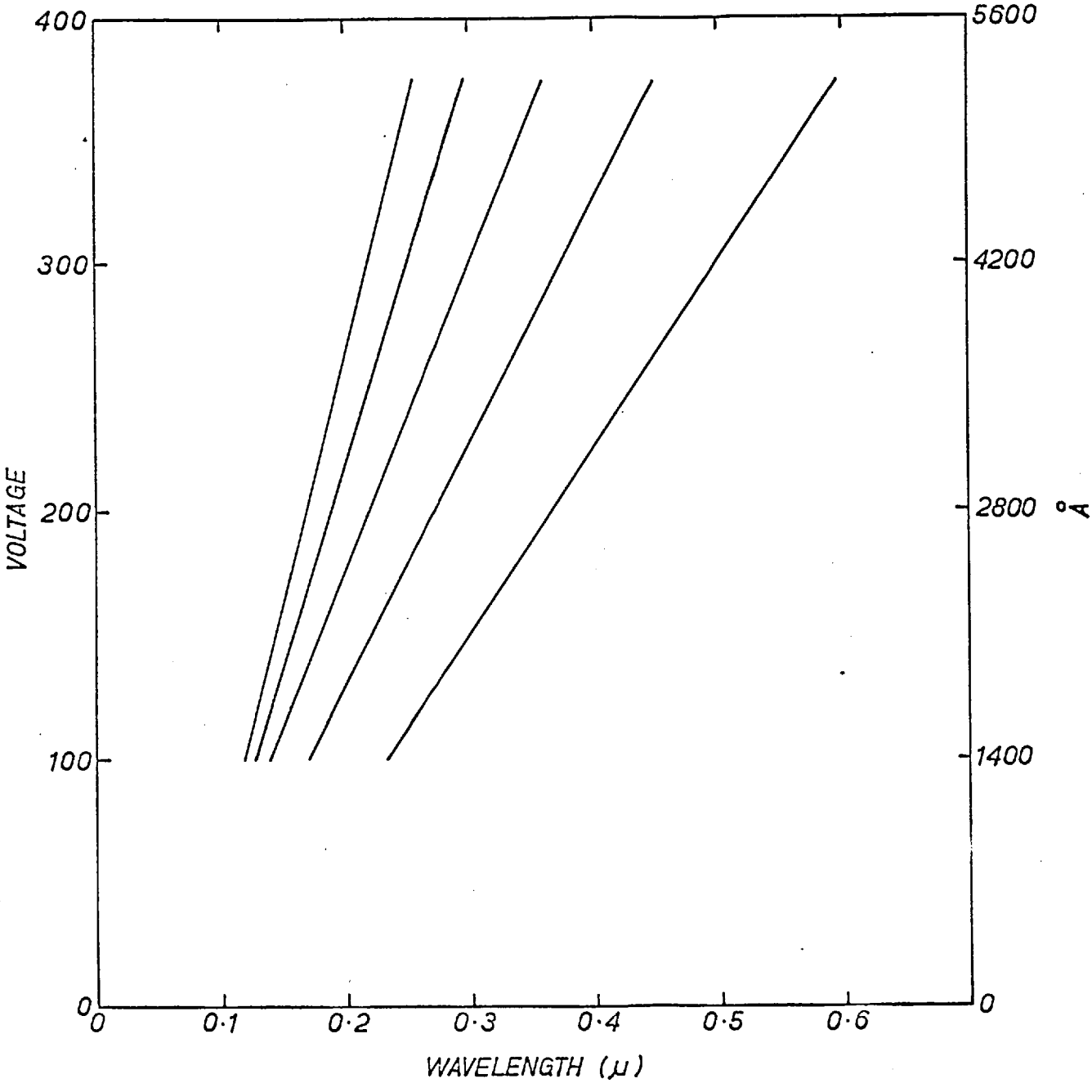

Figure 44. Thickness of alumina vs. reflectivity minima.

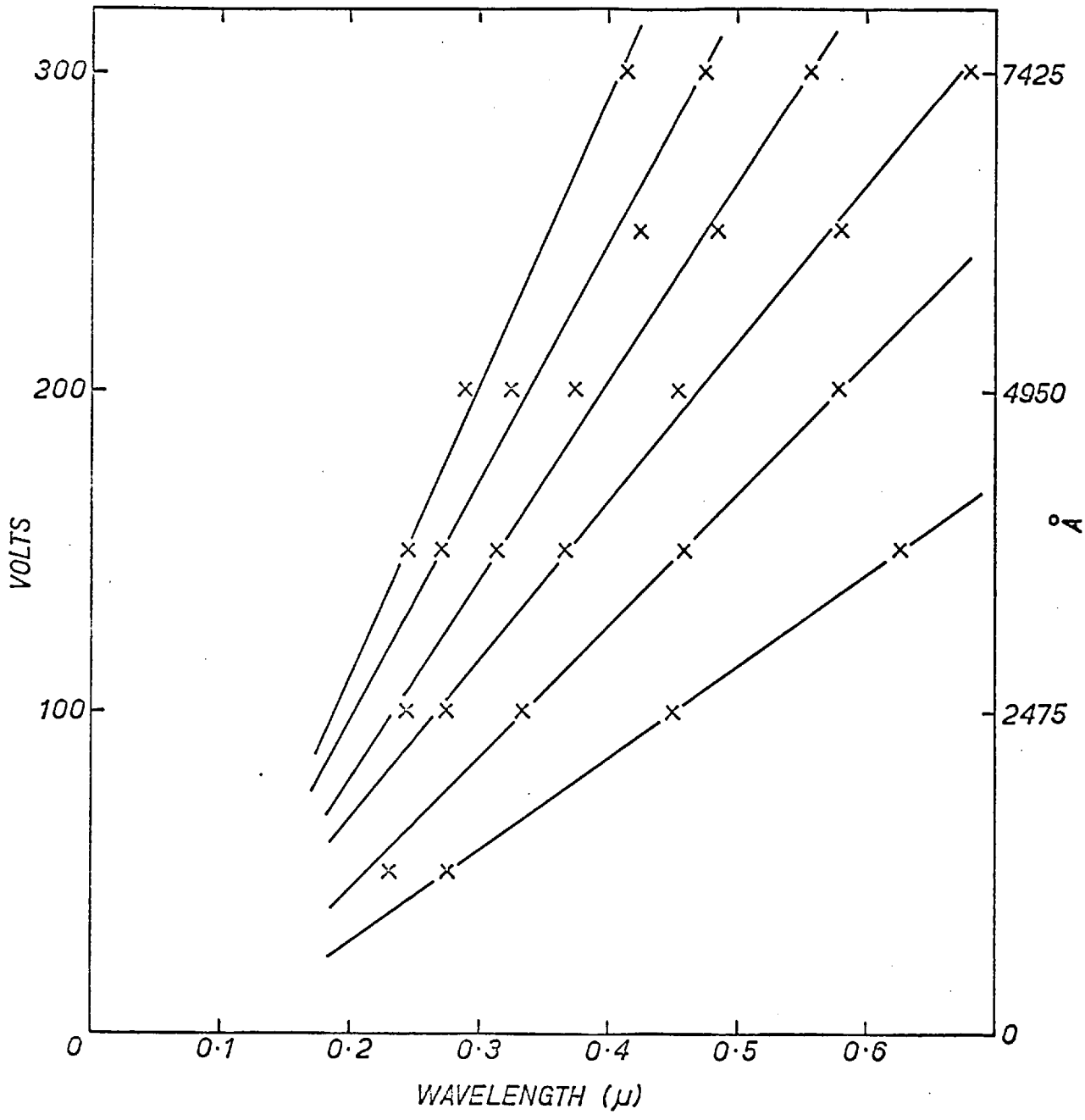

Figure 45. Thickness of zirconia vs. reflectivity minima wavelength.

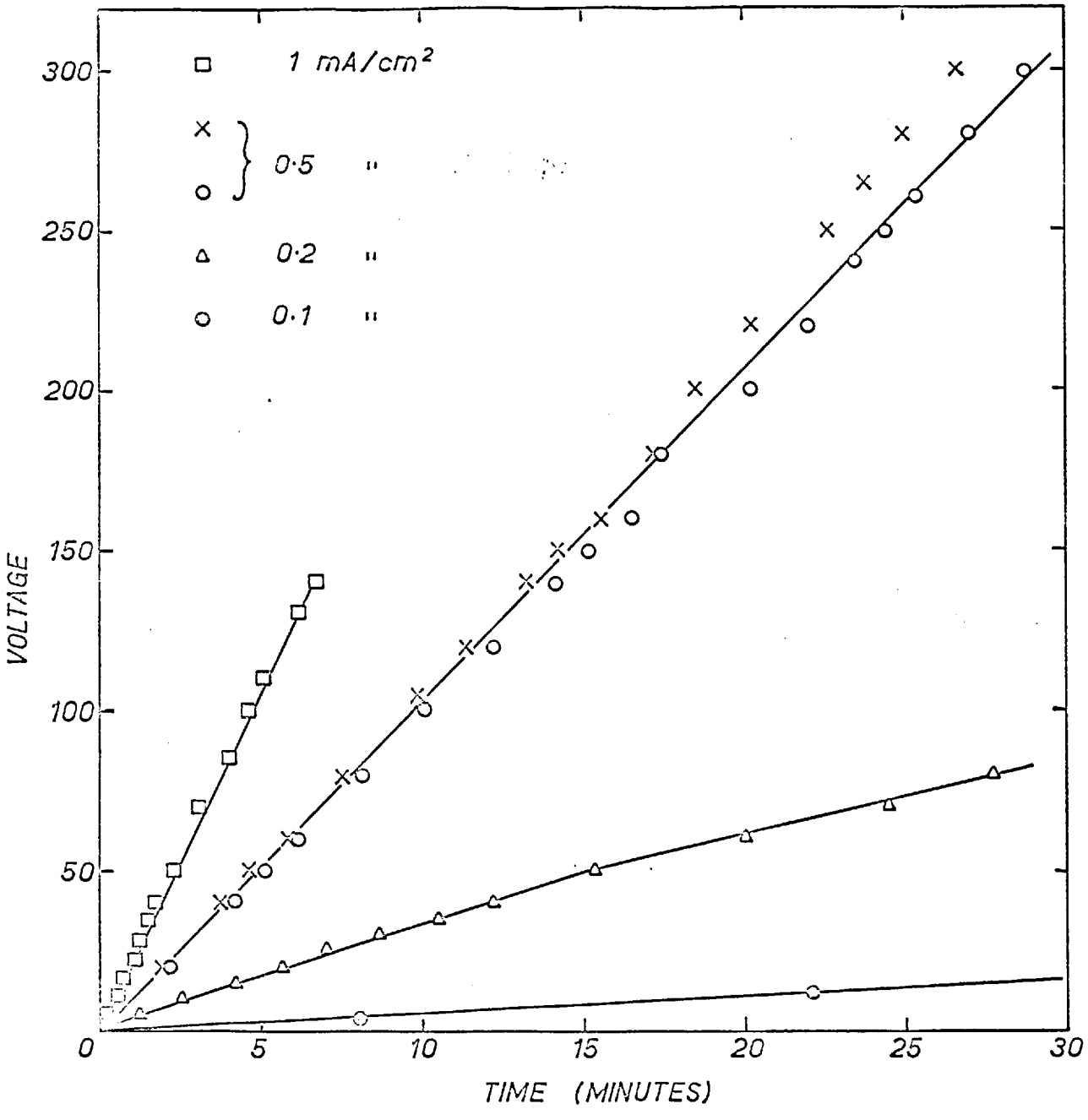

Figure 46. Voltage rise during anodising of aluminium in pH = 9.0 ammonium borate.

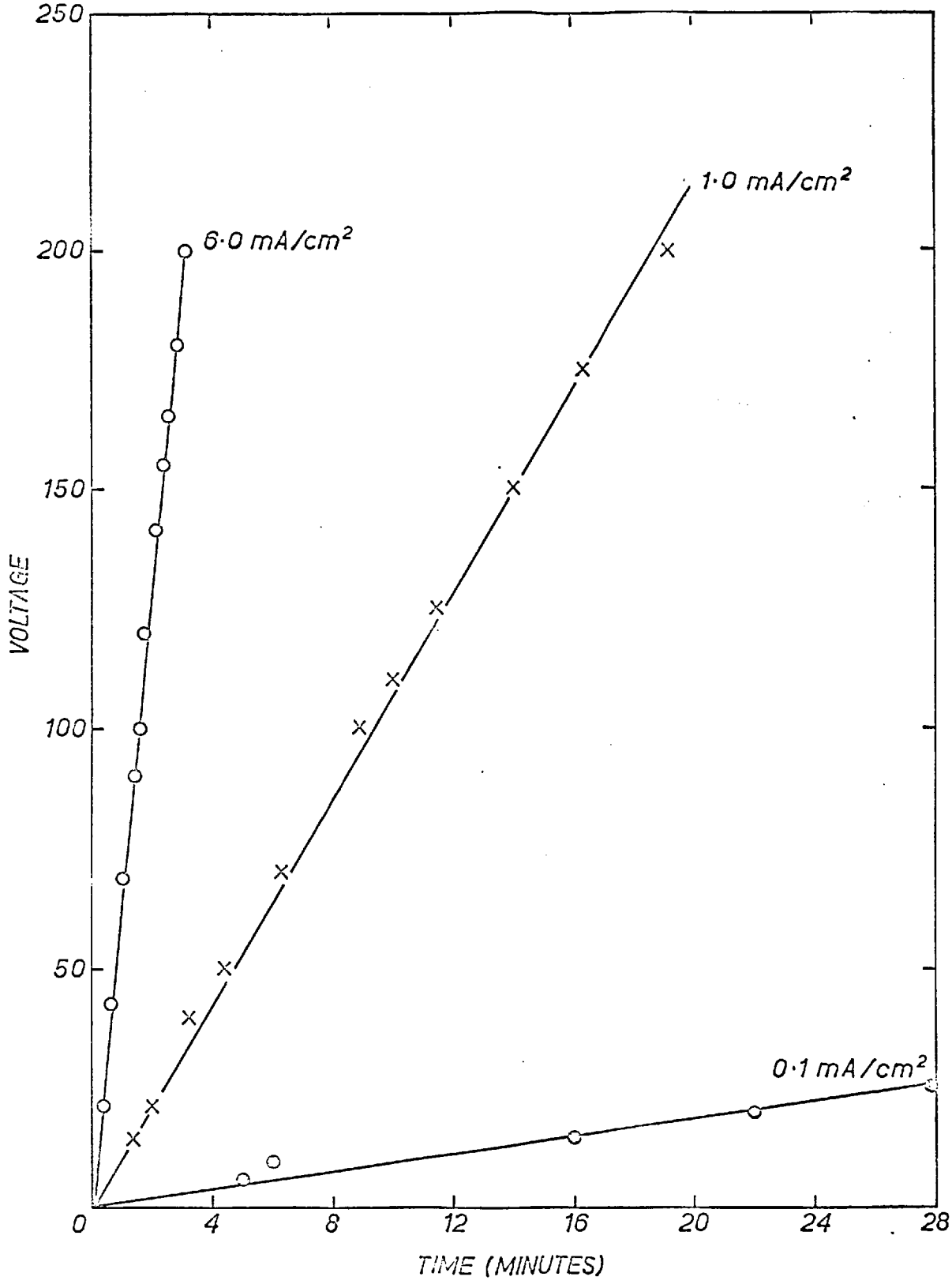

Figure 47. Voltage versus time during the anodising of zirconium in pH = 9.0 ammonium borate.

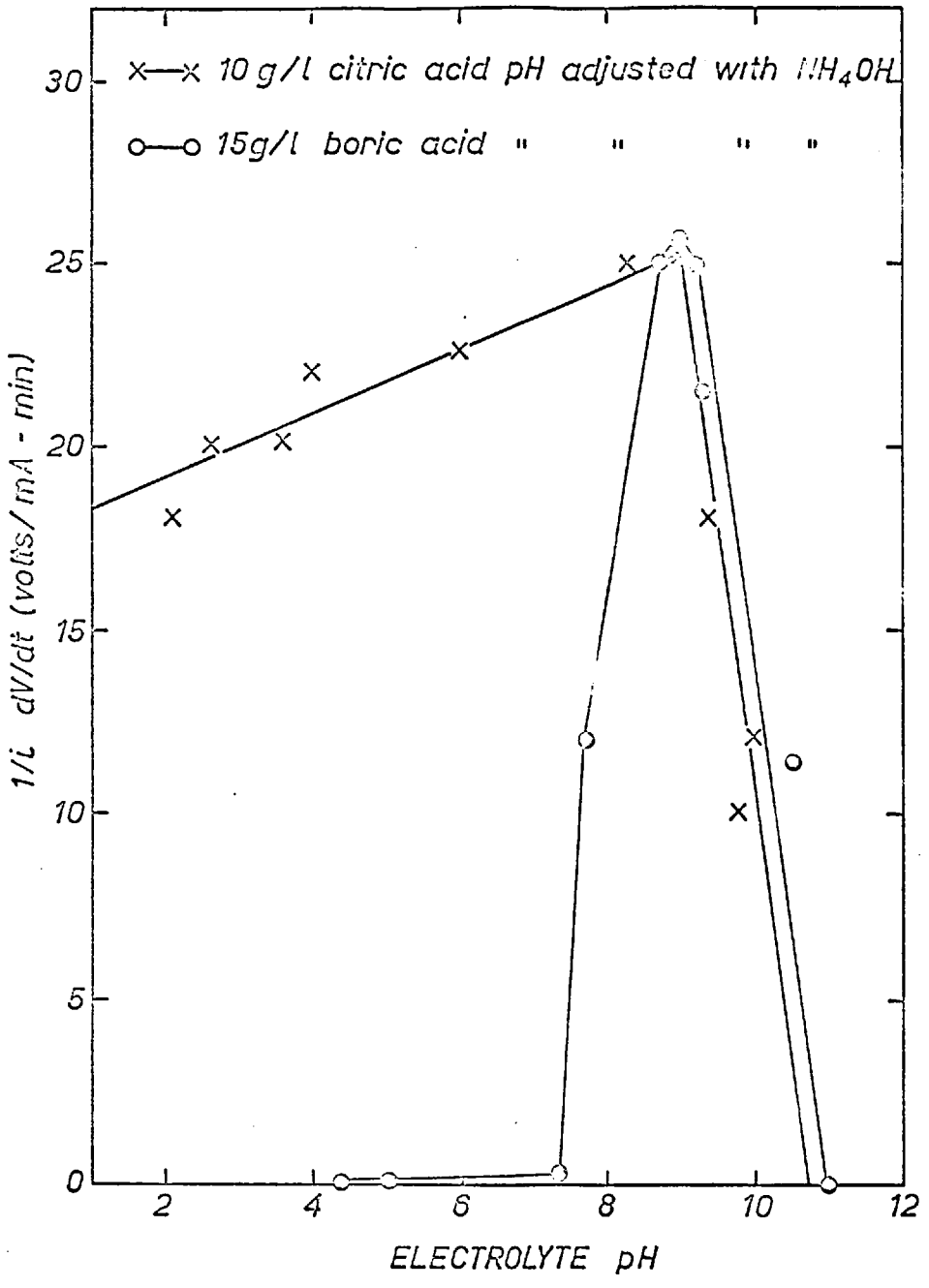

Figure 48. Plots of unitary growth rate $\frac{1}{i}\frac{dV}{dt}$ versus electrolyte pH for growth of anodic films on 99.99% aluminium.

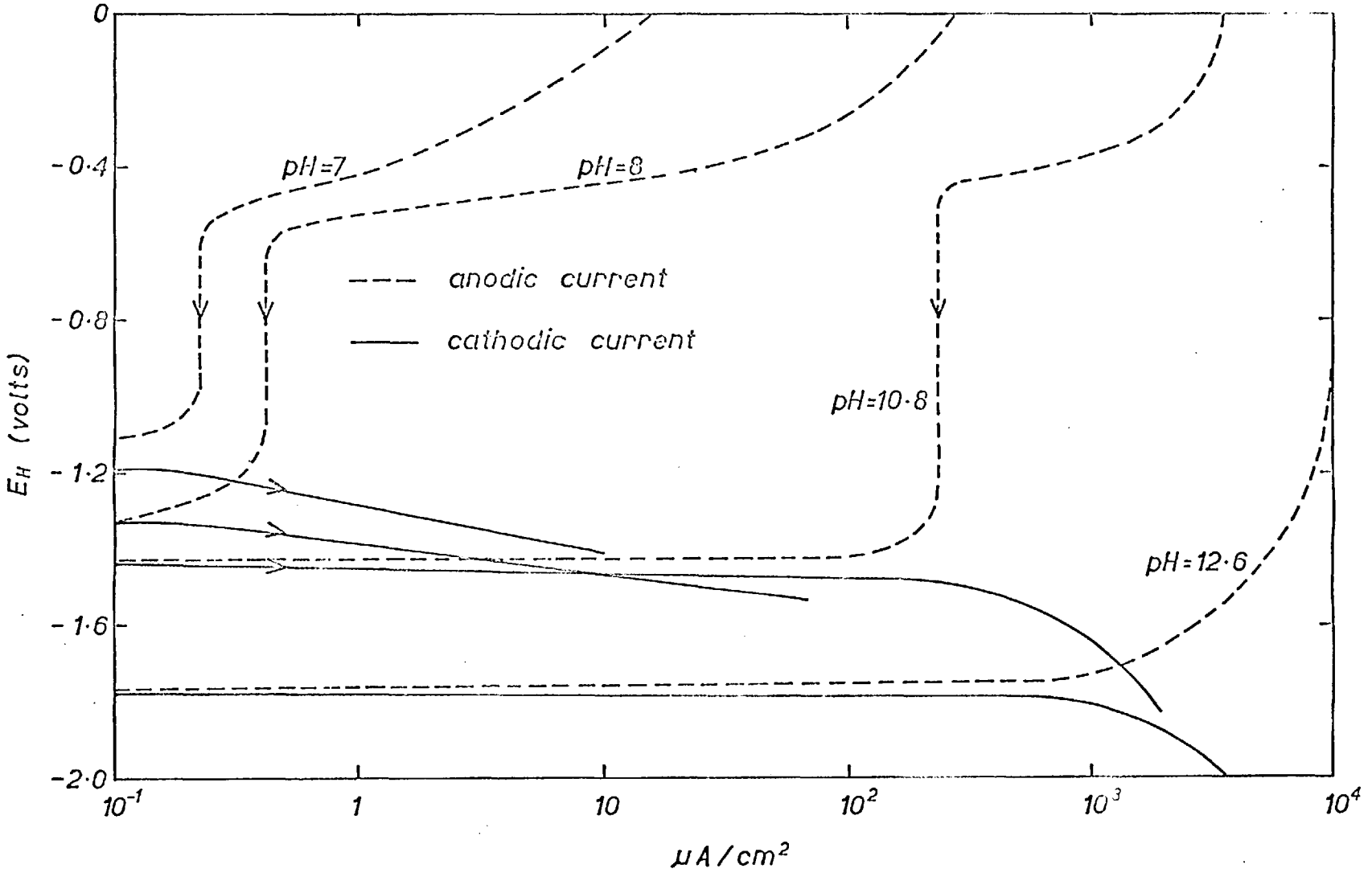

Figure 49. Effect of pH on polarisation characteristics of anodised aluminium electrodes in alkaline Na_2SO_4.

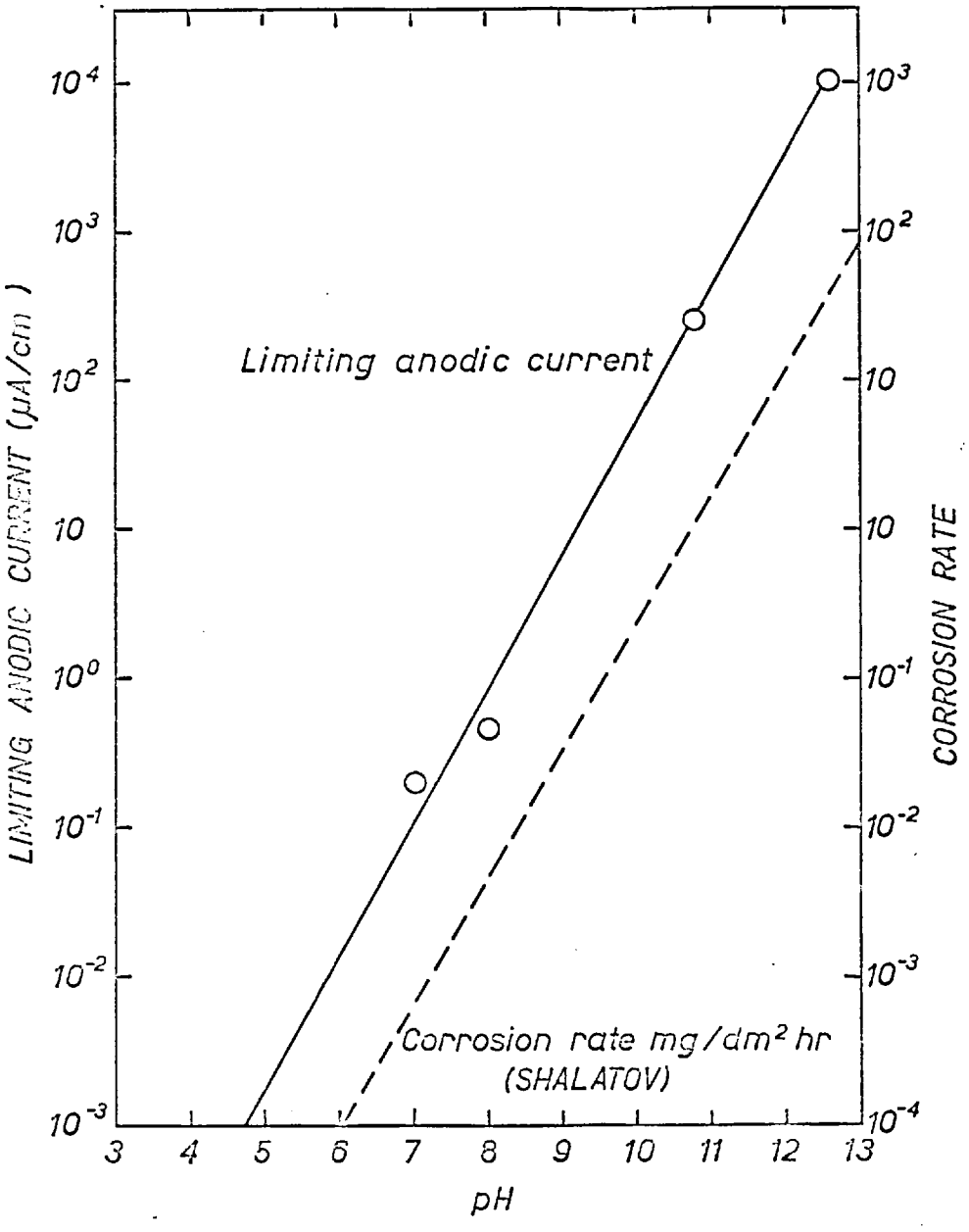

Figure 50. Influence of pH on the corrosion rate of aluminium (after Shalatov) compared with limiting anodic current found during polarisation of anodised aluminium.

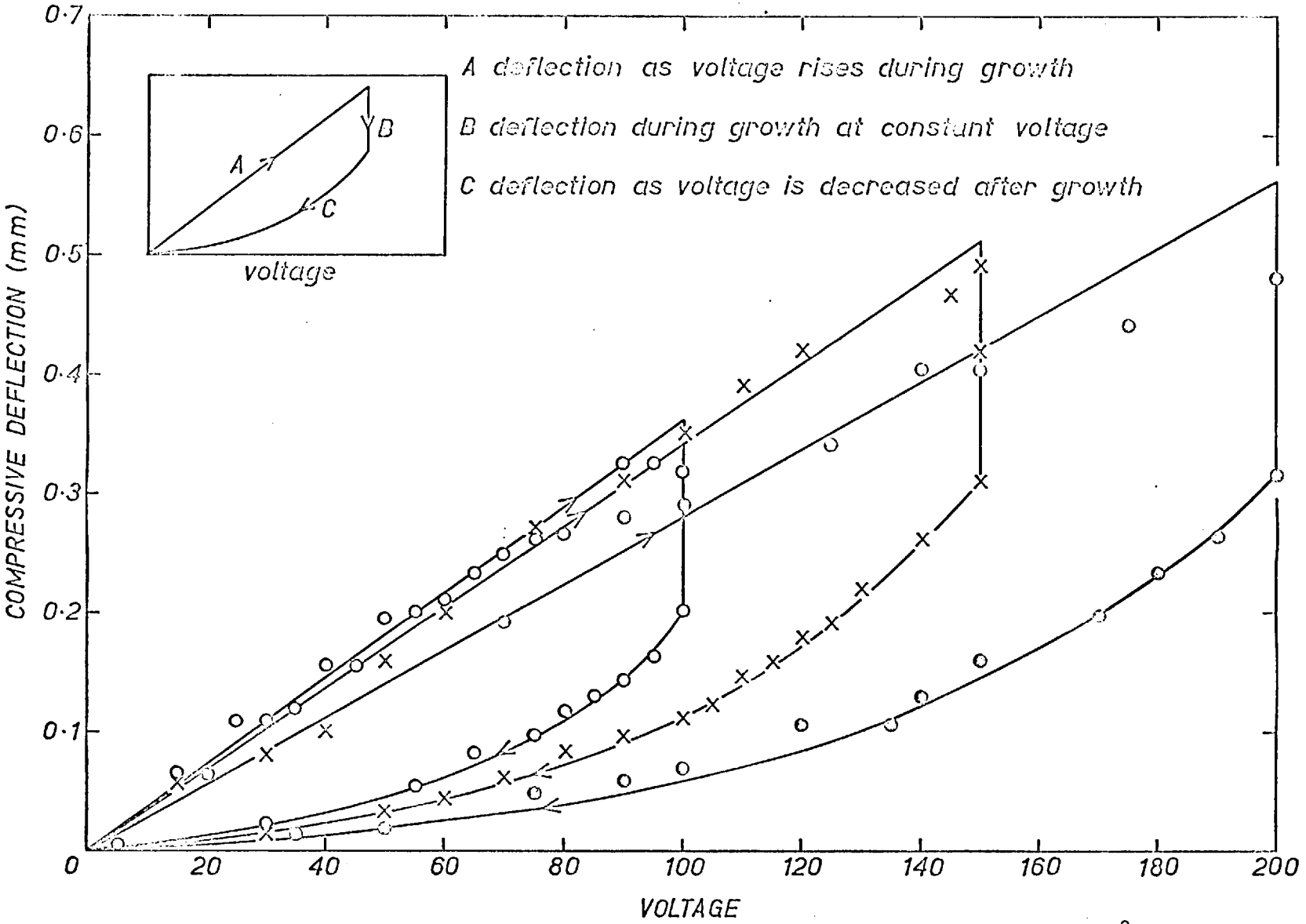

Figure 51. Hysteresis of electrostatic deflection for zirconium anodised at 1.0 mA/cm.^{2} in pH = 9.0 ammonium borate.

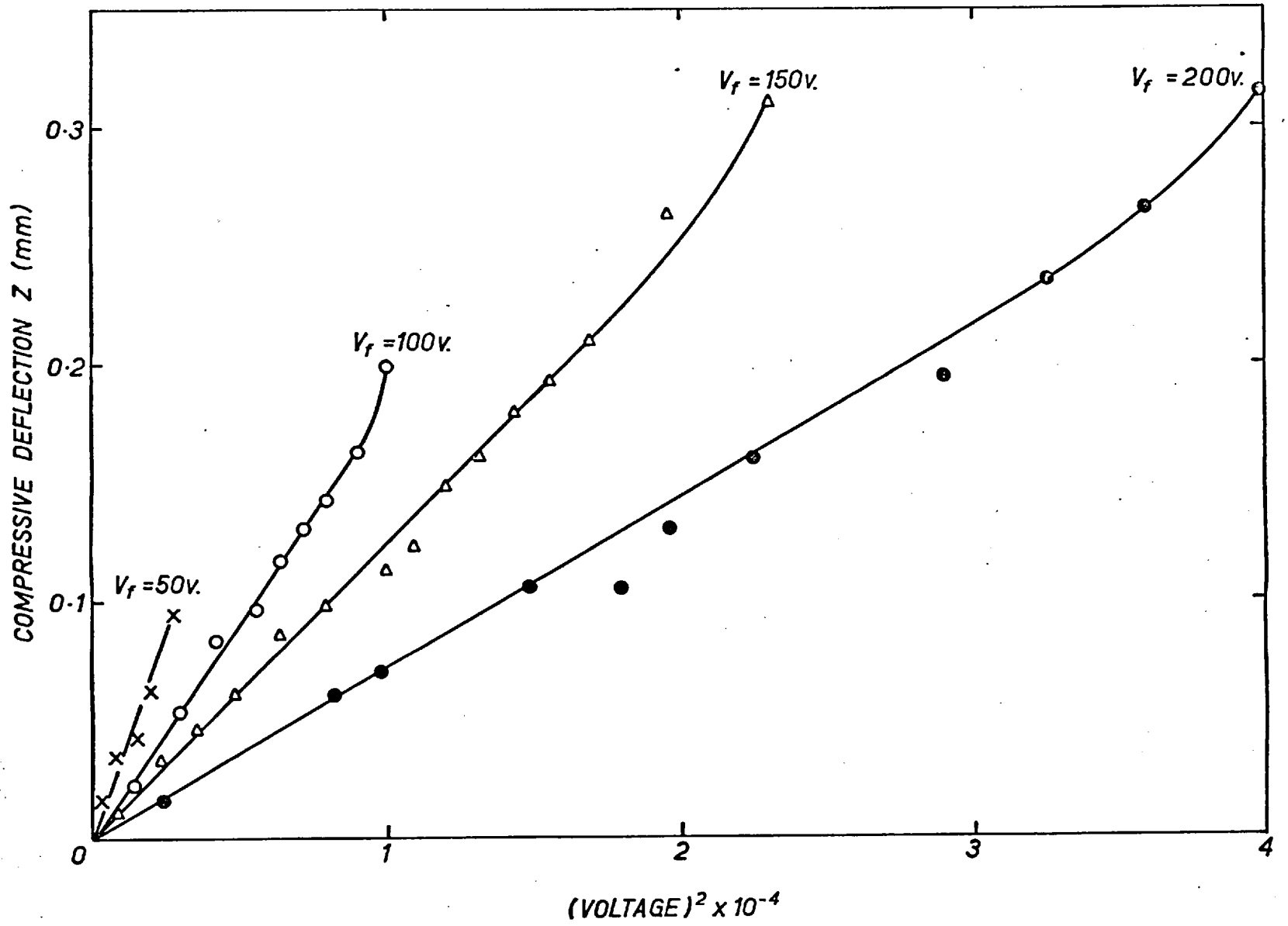

Figure 52. Electrostatic deflection versus the square of the voltage applied to anodic zirconia grown to different formation voltages V_f.

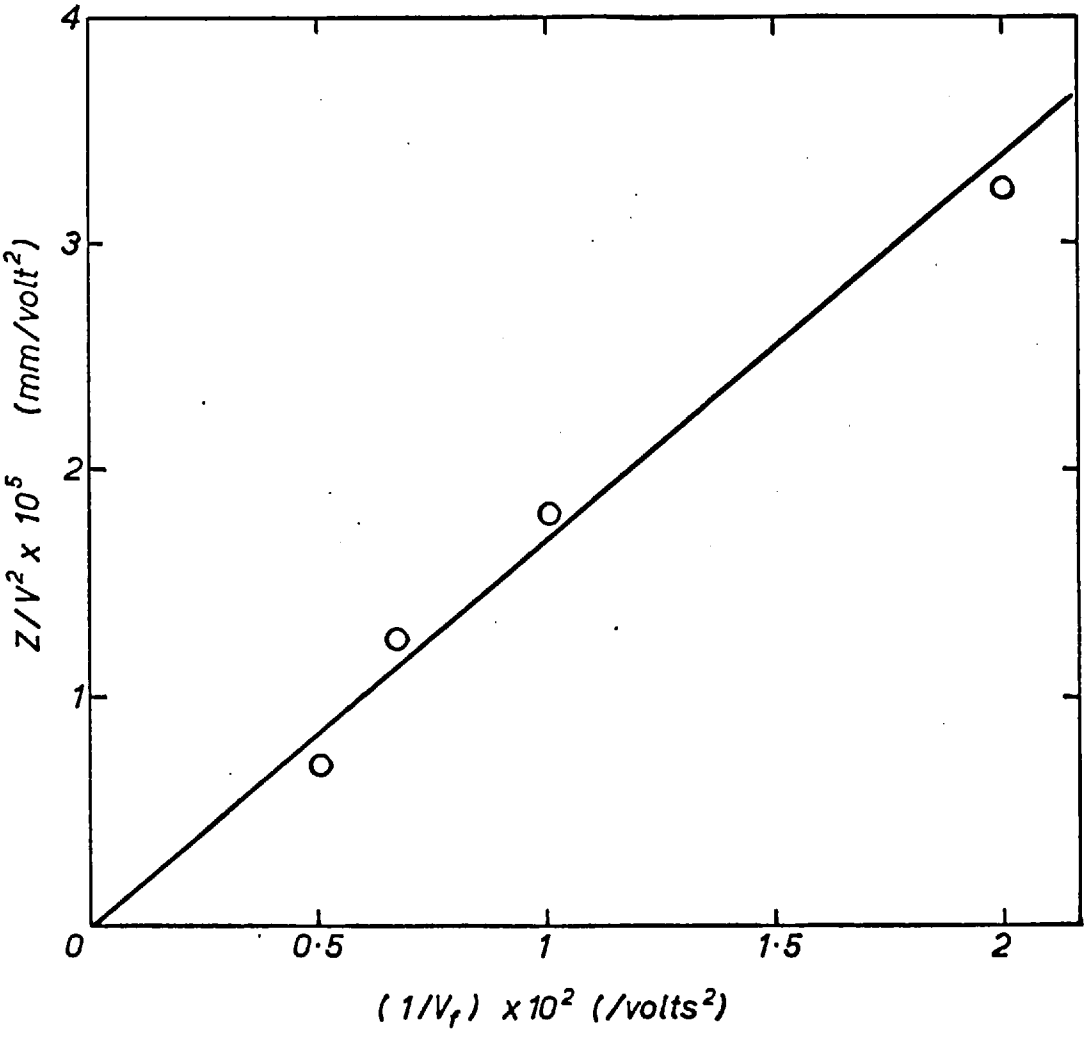

Figure 53. Z/V^2 versus $1/V_f$, the reciprocal of the formation voltage of anodic zirconia.

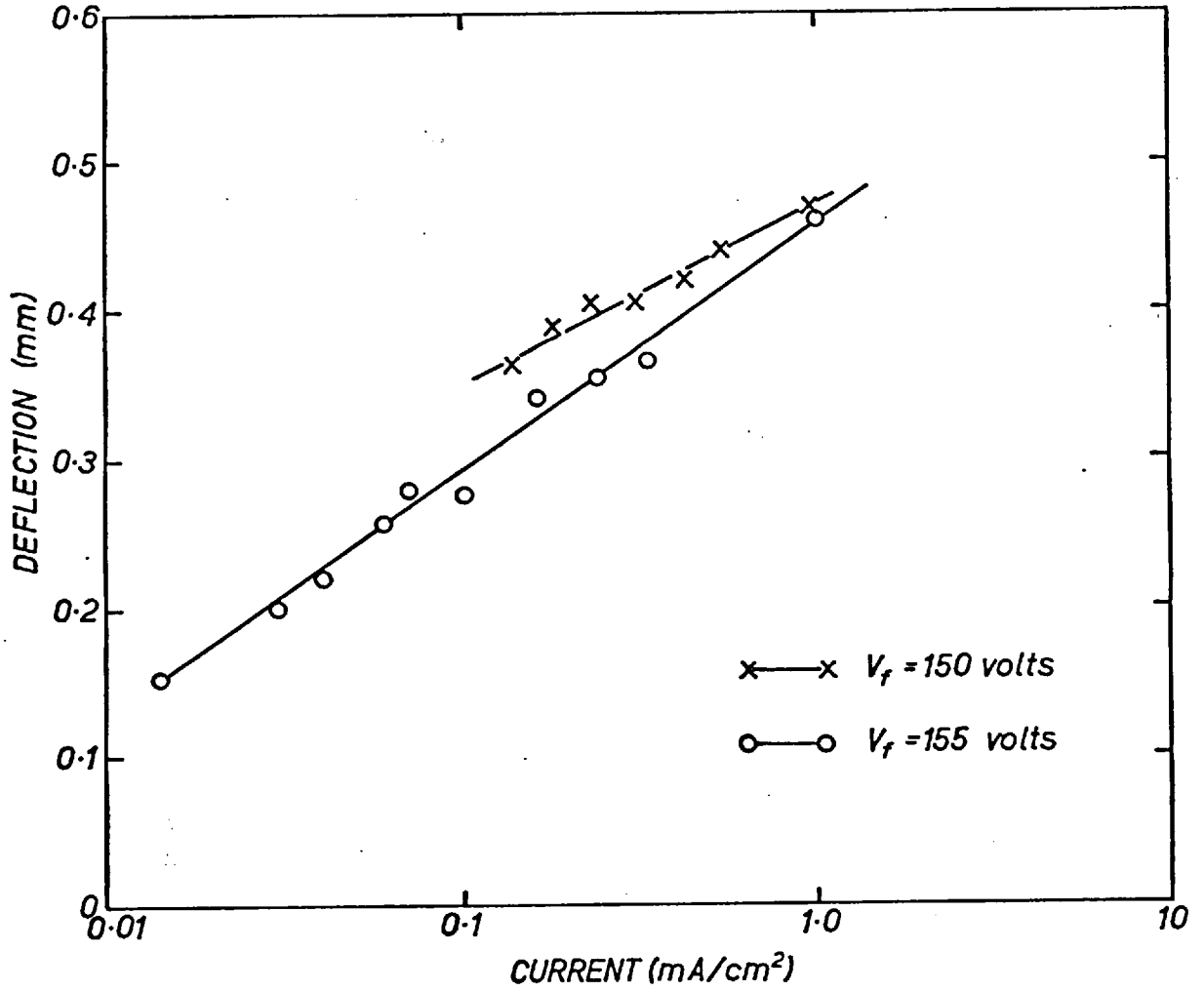

Figure 54. Field on - zero field deflection of foils of zirconium during anodising at constant voltage V_f.

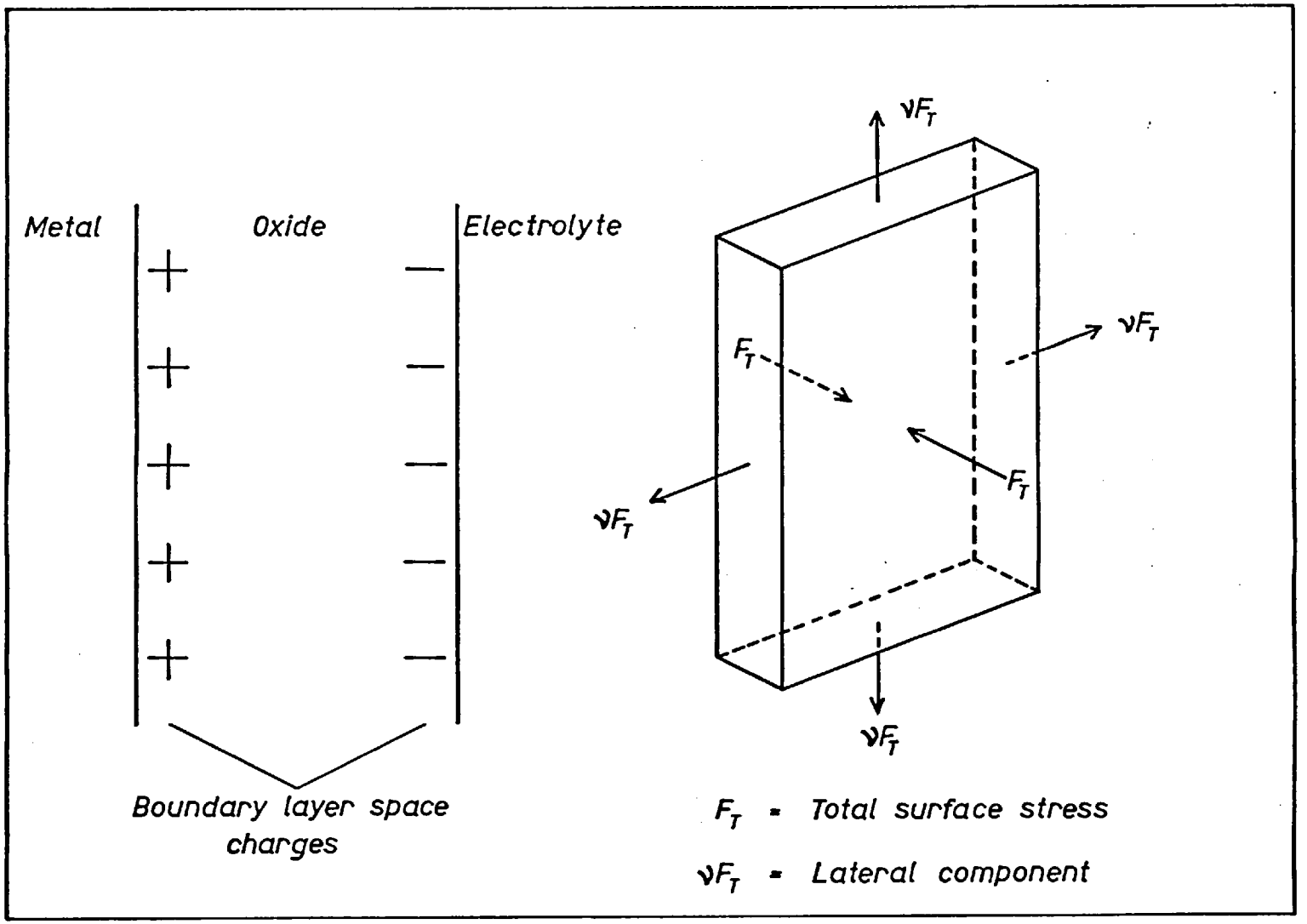

Figure 55. Electrostatic stress due to anodic voltage.

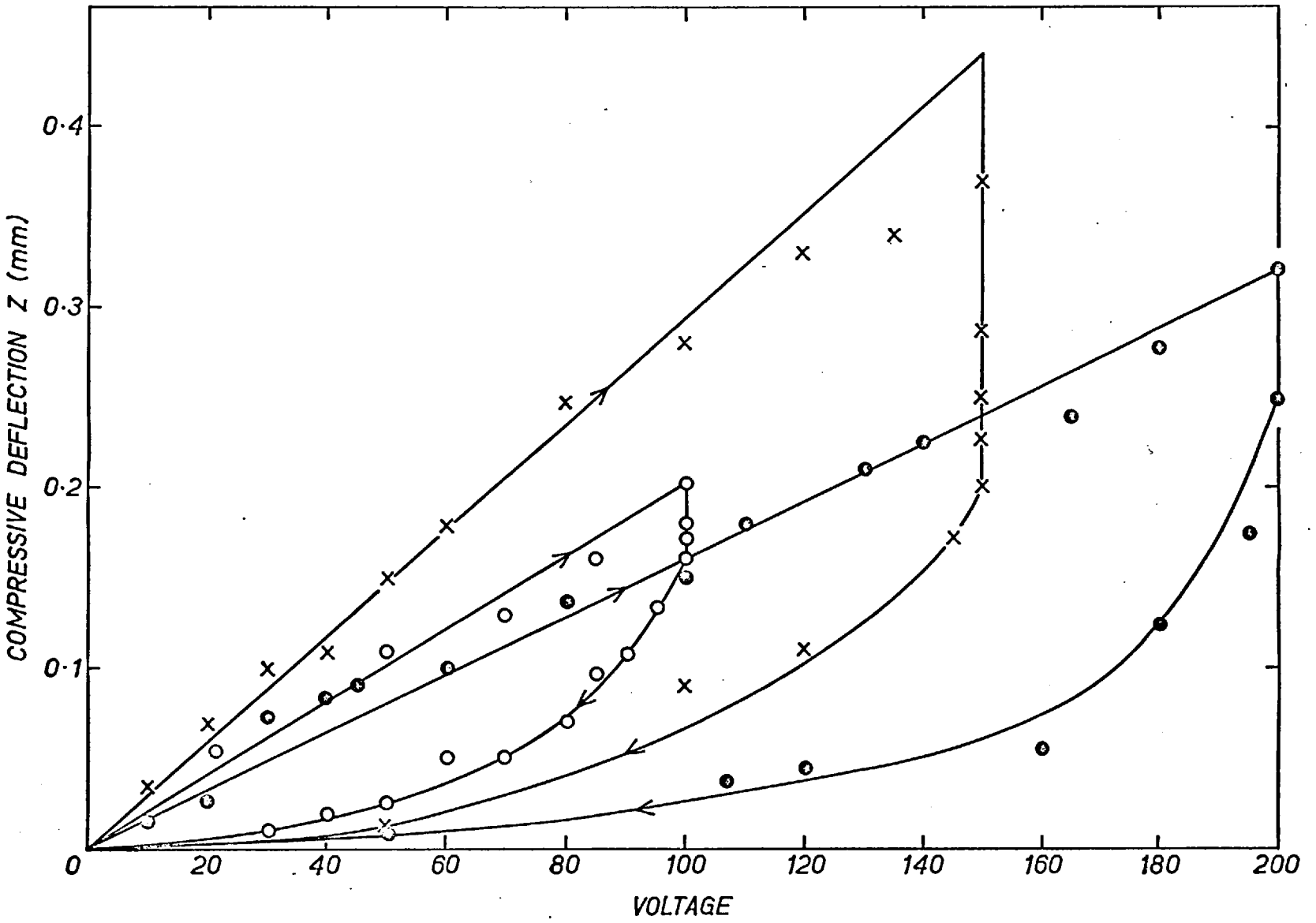

Figure 56. Hysteresis of electrostatic deflection of aluminium foils anodised at 1.0 mA/cm.^{2} in pH = 9.0 ammonium borate.

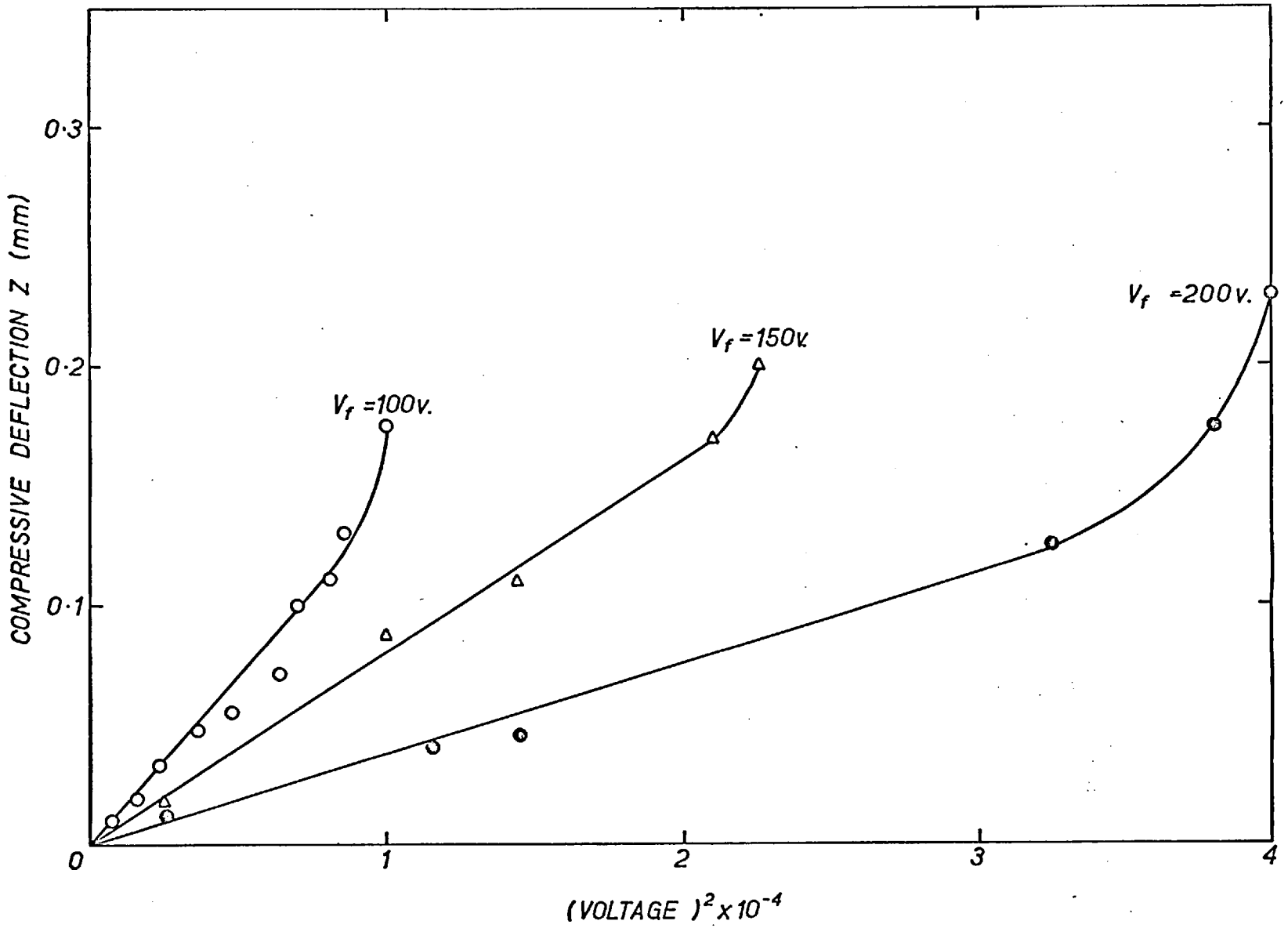

Figure 57. Electrostatic deflection versus the square of the voltage applied to anodic alumina grown to different formation voltages V_f.